Development of genome editing of potato to repress cold-induced sweetening

by
David Alexander Schwegler

Thesis presented in fulfilment of the requirements for the degree of
Master of Science in the Faculty of Sciences at
Stellenbosch University

Supervisor: Prof. James Lloyd

December 2023

Declaration

By submitting this thesis electronically, I declare that the entirety of the work contained therein is my own, original work, that I am the sole author thereof (save to the extent explicitly otherwise stated), that reproduction and publication thereof by Stellenbosch University will not infringe any third-party rights and that I have not previously in its entirety or in part submitted it for obtaining any qualification.

Decmeber 2023

Abstract

In South Africa, the potato (*Solanum tuberosum* L.) has become one of the country's most significant food sources. Its tubers are an abundant source of dietary carbohydrates for human consumption and contain starch, a polymeric carbohydrate composed of amylose and amylopectin that also has numerous industrial uses. Potatoes are often stored at cold temperatures after harvesting, leading to starch being degraded to form the reducing sugars glucose and fructose. When heated to high temperatures, these sugars react with amino acids in the Maillard reaction to produce acrylamide that is neurotoxic and potentially carcinogenic. It is therefore desirable to produce plants with tubers that don't produce reducing sugars when stored at cold temperatures. An enzyme that plays a critical role in starch degradation is α-glucan, water dikinase 1 (GWD1), and plants without GWD1 activity have demonstrated impaired starch degradation including in cold-stored potato tubers. Clustered regularly interspaced palindromic repeats (CRISPR)/Cas9 is a multipurpose technology for genetic engineering and provides new opportunities for developing novel plant characteristics. This system provides a novel method to mutate *StGWD1* to prevent starch degradation. To accomplish this, single guide RNAs were designed to target regions of the gene before a key catalytic phosphohistidine site that is essential for enzyme activity. The guides were transcribed *in vitro* and complexed with Cas9 to assess cleavage of a target-containing sequence. The *in vitro* efficacy assay demonstrated that one of the guides successfully introduced a double-stranded break to the target sequence. Two strategies were used to try to mutate *StGWD1*. The first was a transgene-free method for gene editing that required successful protoplast isolation and regeneration. After successfully isolating viable potato protoplasts, micro-calli were generated from tissue culture of these cells. Unfortunately, regeneration did not proceed further and so a transgenic approach using *Agrobacterium*-mediated transformation was then used to transform leaf explants. This resulted in transgenic calli, although sequencing reactions and Tracking of Indels by Decomposition (TIDE) analysis revealed no editing at the target sequences.

Opsomming

In Suid-Afrika het die aartappel (*Solanum tuberosum* L.) een van die land se belangrikste voedselbronne geword. Sy knolle is 'n oorvloedige bron van dieetkoolhidrate vir menslike gebruik en bevat stysel, 'n polimeriese koolhidraat wat bestaan uit amilose en amilopektien wat ook talle industriële gebruike het. Aartappels word dikwels na oes in koue temperature gestoor, wat veroorsaak dat die stysel afgebreek word om die suikers glukose en fruktose te vorm. Wanneer dit tot hoë temperature verhit word, reageer hierdie suikers met aminosure in die Maillard-reaksie om akrielamied te produseer wat neurotoksies en potensieel kankerverwekkend is. Dit is dus verkieslik om plante te produseer met knolle wat nie suikers produseer wanneer dit in koue temperature gestoor word nie. 'n Ensiem wat 'n kritiese rol in styselafbraaking speel is α-glukaan, water dikinase 1 (GWD1), en plante sonder GWD1-aktiwiteit vertoon verswakte styselafbraaking, insluitend in koudgestoorde aartappelknolle. Gegroepeerde gereelde interspasiëring palindromiese herhalings (CRISPR)/Cas9 is 'n veeldoelige tegnologie vir genetiese ingenieurswese en bied nuwe geleenthede vir die ontwikkeling van nuwe plant eienskappe aan. Hierdie stelsel bied 'n nuwe metode om *StGWD1* te muteer om styselafbraaking te voorkom. Om dit te bereik, is enkelgids-RNA's ontwerp om streke van die geen te teiken voor 'n sleutel katalitiese fosfohistidien-plek wat noodsaaklik is vir ensiemaktiwiteit. Die gidse is *in vitro* getranskribeer en met Cas9 gekomplekseer om splitsing van 'n teikenbevattende volgorde te bepaal. Die *in vitro* doeltreffendheidstoets het getoon dat een van die gidse 'n dubbelstring-breuk suksesvol in die teikenvolgorde ingestel het. Twee strategieë is gebruik om *StGWD1* te probeer muteer. Die eerste was 'n transgeen-vrye metode vir geen redigering wat suksesvolle protoplast isolasie en regenerasie vereis. Nadat lewensvatbare aartappelprotoplaste suksesvol geïsoleer is, is mikro-calli uit weefselkultuur van hierdie selle gegenereer. Ongelukkig het wedergeboorte nie verder voortgegaan nie en dus is 'n transgeniese benadering met behulp van *Agrobacterium*-gemedieerde transformasie gebruik om blaaruitplantings te transformeer. Dit het tot transgeniese calli gelei, alhoewel volgordebepalingsreaksies en '*Tracking of Indels by DEcomposition (TIDE)*' analise geen redigering by die teikenvolgordes aan die lig gebring het nie.

Acknowledgements

I would like to acknowledge and thank the following members and institutions:

To **Stellenbosch University's Postgraduate Scholarship Program** for their funding.

To **Professor James Lloyd,** who has always been readily available and happy to provide advice and guidance. Your support and counsel gave me the ability to overcome hurdles and setbacks that challenged this project, while also providing encouragement.

To my colleagues at the **Institute of Plant Biotechnology**, who have created a wonderful and supportive working environment that greatly aided me throughout this research period. Thank you for the continuous knowledge, advice and laughs throughout the days both inside and outside the labs. I truly appreciate the support and friendship that has bloomed during this period.

To my **family**, thank you for always being patient and understanding. Your support and encouragement have given me the strength and confidence to pursue my dreams.

To my **girlfriend**, who has always displayed keen interest in my research, patiently listened to my ramblings and supported me. Her patience, encouragement, and belief in me were a source of strength during the challenging moments of this thesis. Thank you for your support, sacrifices and understanding that has constantly fuelled my ambitions and interests and given me encouragement through trying times.

Table of Contents

List of figures

Chapter 2:

Figure 2.3 Mechanism of starch phosphorylation. Research by Mikkelsen and Blennow, 2005 indicated GWD1 contains five domains. It is believed that there are two conformations of GWD1, where the phosphohistidine site shifts its position to alternatingly interact with the nucleotide and glucan substrates. During conformation 1, the catalytic histidine interacts with the nucleotide. Catalysis then creates a phosphohistidine that causes a conformational change and results in conformation 2. The starch/glucan binding domain and the phosphohistidine site then engage, allowing the second round of catalysis to produce the phosphorylated glucan polymer. Following catalysis, GWD1 returns to its original conformation 1, where another nucleotide molecule can bind and the cycle repeats. Image was re-drawn from Mikkelsen and Blennow, 2005. Figure created with BioRender.com

Figure 2.4 A simplified model of the CRISPR/Cas immunity mechanism. **Adaptation**: A protospacer sequence from the invading DNA is incorporated into the host DNA's CRISPR array after phage infection. **Expression:** The CRISPR sequence is transcribed and the long-chain product is then processed to produce mature short-chain crRNA. The CRISPR/Cas complex is created when the crRNA combines with the Cas endonuclease. **Interference:**, A functional crRNA guides Cas9 nucleases to selectively recognize and cleave viral DNA/RNA that is identical to the spacer, in order to trigger a particular immune response. The foreign nucleic acid is then cleaved by the Cas endonuclease and degraded. Consequently, the CRISPR/Cas system can confer acquired and inherited resistance to the host. Figure created with BioRender.com.

Figure 2.5 The two mechanisms used for repair of double-stranded DNA breaks caused by the CRISPR/Cas9 complex. Non-homologous end joining may lead to faulty repairs and the insertion of random indels. Larger insertions are produced by homology-directed repair and are specified by a donor DNA segment that serves as a template for the repair. Figure created using BioRender.com

Figure 2.6 Modifications of the Cas9 endonuclease that have been altered by selectively deactivating the catalytic domains. **(A)** The natural Cas9 endonuclease, that is active in both catalytic domains. **(B)** A Cas9 protein that has both of its catalytic domains inactivated and is linked to an alternate active domain. Figure created using BioRender.com

Chapter 3:

Figure 3.1. A diagrammatic representation demonstrating how the synthesized single guide RNA oligonucleotides were ligated into the vector scaffold. (**A)** *BbsI* was used to cut the pGEM-scaffold plasmid, leaving overhangs that were used for (**B)** the unidirectional insertion of the guide RNA oligonucleotides.

Figure 3.2. Bioinformatic analysis of *StGWD1* and prediction of potential guide sites. (A) A diagrammatic representation of the *StGWD1* gene structure. Single guide RNA locations for each gene are labelled as 'Guide 1' and 'Guide 2', corresponding with StGWD1-1, StGWD1-2, respectively. **(B)** Domain structure within the StGWD1 protein. CBM45 starch-binding domains, active site containing a key catalytic histidine that binds phosphate, and ATP-binding sites are shown at the approximate location where they are found within the protein. The black sphere at the end of the protein indicates the C-terminus. **(C)** Nucleotide sequences of the pGEM-scaffold-sgRNA plasmid were obtained from the Central Analytics Facility. T7 transcription sites, sgRNA sequences and Cas9/sgRNA scaffold sequence are highlighted in blue, green and yellow respectively.

Figure 3.3. *In vitro* CRISPR/Cas9 reactions of the *Solanum tuberosum* single guide RNPs. RNPs targeting **(A)** *GWD1_A* and *GWD1_B* **(B)** *PDS* **(C)** *GWD1_A, PDS* and *eIF4E-1* separated on 1.5 % (w/v) agarose-Tris Borate EDTA gels by electrophoresis. **(A)** Red arrows indicating bands caused by sgRNA and blue arrows indicating shift in target DNA fragment when sgRNA is included in the reaction. **(B + C)** Cleaved DNA fragments are indicated with red arrows. The inclusion or omission of each reaction component is represented by a '+' or '-' and shown above each gel image. MW = 100 bp DNA ladder (GeneDireX).

Figure 3.4. Isolation of potato protoplasts. (A) For the purpose of isolating protoplasts, leaves of tissue culture grown plants grown in tissue culture were harvested. **(B)** In preparation for an overnight enzymatic digestion, leaves were cut into 1-2 mm-wide strips. **(C)** By centrifuging on a sucrose-cushion, protoplasts were extracted from the digested solution. **(D)** Centrifugation on a sucrose-cushion enables for the separation of viable protoplasts from cell detritus.

Figure 3.5. Development of potato callus from protoplasts. (A) Alginate lenses suspended in growth medium and displaying visible micro-calli growth after three weeks.**(B)** Micro-calli in an individual alginate lens.

Chapter 4:

Figure 4.1. **Golden Gate cloning strategy**. PCR reactions required to amplify amplicons used in Golden Gate Cloning. Each 20 bp gRNA sequence was split between two primers that are used to create amplicons containing half the gRNA sequence. The first amplicon (PCR1) includes in the 5'-end the *SapI* restriction site, the *CmYLCV* promoter, *Csy4*, the first 12 nucleotides of the StGWD1-1 guide RNA, and an *Esp3I* restriction site in the 3'-end (Figure 4.1). The second amplicon (PCR2) also includes the *Esp3I* site, *Csy4* repeat, and the first 12 nucleotides of StGWD1-2 guide RNA in addition to the last 12 nucleotides of StGWD1-1 guide RNA. The final amplicon (PCR3) includes an *Esp3I* site, the final 12 nucleotides of StGWD1-2, a *Csy4* repeat and a *SapI* site. A similar set of amplicons were created for the StGWD1-3 and StPDS target sequences, with the exception of a *Csy4* repeat and a second target sequence.

Figure 4.2. Amplification of guide RNAs for Golden Gate assembly into *pDIRECT_22C.* (A) Two products can be amplified in PCR1 (when amplifying the fragment containing the promoter) since the template vector has two Csy4 repeats, and the reverse primer binds to either sequence. **(B)** Three PCR reactions are required to amplify two guide RNA sequences (StGWD1-1 and StGWD1-2), and a control reaction without DNA template was included for each PCR reaction. PCR1 contains the promoter sequence and the first half of the first guide. Due to the presence of two *Csy4* repeats within the template vector, PCR1 amplifies two amplicons containing either one or two *Csy4* repeats, and the shorter band containing one *Csy4* repeat is used in Golden Gate assembly. **(C)** Two PCR reactions are required to amplify the guide RNA fragments, spacers and promoter required for the insertion of one guide RNA into *pDIRECT_22C* (StGWD1-3 and/or StPDS). MW = GeneRuler Express DNA ladder (Thermo Fischer Scientific).

Figure 4.3. Diagram of the Cas9/sgRNA *pDIRECT_22C* vector and target site selection in the *StGWD1* and *StPDS* genes. (A) Guide sequences from exon 8 (StGWD1-1) and 23 (StGWD1-2) in Désirée were combined into one construct. The sequence of the guide RNAs are indicated in red, with the PAM (AGG) sequence indicated in green. The structure of the final

pDIRECT:GWD1-1&2 vector cassette is represented with a *CmYLCV* promoter, the two cloned sgRNAs, Csy4 sequences, the spacer sequences, and a 35S terminator. **(B)** The same structure is indicated for the StGWD1-3 and StPDS guides that were independently cloned into separate pDIRECT_22C vectors.

Figure 4.3. Diagram of the Cas9/sgRNA *pDIRECT_22C* vector and target site selection in the *StGWD1* and *StPDS* genes. (A) Guide sequences from exon 8 (StGWD1-1) and 23 (StGWD1-2) in Désirée were combined into one construct. The sequence of the guide RNAs are indicated in red, with the PAM (AGG) sequence indicated in green. The structure of the final pDIRECT:GWD1-1&2 vector cassette is represented with a *CmYLCV* promoter, the two cloned sgRNAs, Csy4 sequences, the spacer sequences, and a 35S terminator. **(B)** The same structure is indicated for the StGWD1-3 and StPDS guides that were independently cloned into separate pDIRECT_22C vectors.

Figure 4.4. *S. tuberosum* explants after co-cultivation with *A. tumefaciens* containing *pDIRECT*:gRNAs. **(A)** Leaf discs placed on CIM directly after infection with *A. tumefaciens*. **(B)** Antibiotic resistant calli appearing on leaf explants (indicated with red arrows) after 8-9 weeks.

Figure 4.5. **The detection of transgene integration into the genome of Désirée potato calli using PCR**. **(A)** integration of StGWD1-1, StGWD1-2, and StGWD1-3. **(B)** Integration of the StPDS guide in eight tested calli, and integration of StGWD1-1 and StGWD1-2 in an additional two calli. **(C)** Integration of *Cas9*. MW = λ DNA digested with *PstI*, and Neg. ctrl is the same PCR reaction but without DNA template. The full images are in the supplementary information section and labelled Figure S4.1.

List of tables

List of abbreviations

µF	Microfarad
µg	Microgram
µL	Microlitre
µmol	Micromoles
µM	Micromolar
ADP	Adenosine diphosphate
AIM	*Agrobacterium* infection medium
Amy	α-amylase
ATP	Adenosine 5'-triphosphate
BAM	β-amylase
BAP	6-Benzylaminopurine
bp	Base pairs
C-3	Carbon-3
C-6	Carbon-6
CAF	Central Analytical Facilities
Cas	Clustered regularly interspaced short palindromic repeats -associated
cDNA	Complementary DNA
CF	Conditioning factor
CIM	Callus induction medium
CIS	Cold induced sweetening
CmYLCV	Cestrum Yellow Leaf Curling Virus
CPM	Clonal propagation medium
CRISPR	Clustered regularly interspaced short palindromic repeat
crRNA	Clustered regularly interspaced palindromic repeat regions ribonucleic acid
Csy4	Csy-type (CRISPR system yersinia) ribonuclease 4
cv	Cultivar
DPE2	Disproportionating enzyme 2
DSB	Double stranded deoxyribonucleic acid break
DNA	Deoxyribonucleic acid
E. coli	*Escherichia coli*

EDTA	Ethylenediaminetetraacetic acid
g	Gram
GA_3	Gibberellic acid
GBSS	Granule bound starch synthase
gDNA	Genomic deoxyribonucleic acid
GMO	Genetically modified organism
GWD	Glucan, water dikinase
gRNA	Guide ribonucleic acid
HDR	Homology Directed Repair
HDS	4-hydroxy-3-methylbut-2-enyl diphosphate synthase
kg	Kilogram
LB	Lysogeny broth
LBA	Lysogeny broth agar
LSF2	Like Sex Four–2
m	Meter
M	Molar
Mg	Milligram
min	Minute
mL	Millilitre
MLO1	Mildew Locus O
mM	Millimolar
MS	Murashige and Skoog salts with vitamins
NAA	Naphthaleneacetic acid
NBT	New breeding technique
NCBI	National Center for Biotechnology Information
NEB	New England Biolabs
PAM	Protospacer adjacent motif
PCR	Polymerase chain reaction
PDS	Phytoene Desaturase
PWD	Phosphoglucan, water dikinase
REP	Repeat

RIM	Root induction medium
RNA	Ribonucleic acid
RNAi	Ribonucleic acid interference
RNP	Ribonucleoprotein
rpm	Revolutions per minute
RS	Reducing sugars
RT	Room temperature
sec	Seconds
SEX4	Starch excess-4
sgRNA	Single guide ribonucleic acid
SIM	Shoot induction medium
SNP	Single nucleotide polymorphism
St	*Solanum tuberosum*
T-DNA	Transfer deoxyribonucleic acid
TALEN	Transcription-activator like effector nuclease
TB	Terrific broth
TIDE	Tracking of Indels by DEcomposition
tracrRNA	Trans-acting clustered regularly interspaced palindromic repeat regions ribonucleic acid
U	Enzyme units
UDP	Uridine diphosphate
v/v	Volume for volume
Vlnv	Vacuolar invertase
w/v	Weight for volume
WT	Wild type
YEP	yeast extract peptone
ZF	Zinc finger
ZFN	Zinc finger nucleases

Chapter 1: Introduction

Potatoes belong to the Genus *Solanum* and are the third-largest food crop consumed globally after rice and wheat. The international potato industry is heavily impacted by the negative effects of post-harvest sweetening during cold storage conditions that decreases tuber quality. This is known as cold induced sweetening where phosphorylated starch is broken down to reducing sugars. When cooked at high temperatures, these react with amino acids to produce both a brown pigment and acrylamide, a neurotoxin and potential carcinogen. Prevention of cold induced sweetening has been successfully achieved using a transgenic approach by repressing transcript accumulation of a gene called α-glucan, water dikinase 1 (*GWD1*) that phosphorylates starch (Lorberth et al., 1998; Ritte et al., 2006). Genome-editing technologies allow the possibility to engineer reduced cold induced sweetening in potatoes through mutation of this gene. Gene editing by CRISPR/Cas9 can be facilitated using either traditional transgenic approaches (such as *Agrobacterium*-mediated transformation of leaf discs; Zhang et al., 2019) or non-transgenic approaches where protoplasts are edited by a CRISPR/Cas9 ribonucleoproteins and regenerated into plants. This second method does not produce plants containing trans DNA and in some geographical regions this means that they are not governed by regulations imposed on transgenic organisms making it the preferred method for genome editing.

1.1 Aims and objectives

This study had three aims that are outlined below, along with the objective steps taken to achieve them.

1. Establish a protocol for potato protoplast culture.
    a. The creation and isolation of potato protoplasts was established and optimised.
    b. Regeneration of protoplasts into plants.
2. To design and assess CRISPR/Cas9-mediated *StGWD1* gene editing *in vitro* in preparation for future non-transgenic *in vivo* experiments.
    a. Design and ligate two *StGWD1* guide RNAs into a vector suitable for non-transgenic transformations.
    b. CRISPR/Cas9 ribonucleoproteins were assembled and assays screening their efficacy were conducted *in vitro.*

3. To design and assess CRISPR/Cas9-mediated *StGWD1* gene editing using a transgenic approach.
    a. Design and ligate *StGWD1* guide RNAs into a vector using Golden Gate Cloning.
    b. Transform leaf explants using *Agrobacterium* containing the vector, and sequence resulting plantlets for gene-editing.

1.2 Overview of Chapters

Chapter 2 of this thesis aimed to explore and review the literature associated with the topics of this study. It includes the agricultural significance of potatoes and the challenges associated with traditional breeding methods. This review also highlights the role of GWD1 in phosphorylating starch and its involvement in starch breakdown. Both new and traditional breeding techniques are discussed, with emphasis on *Agrobacterium*-facilitated gene-editing and CRISPR/Cas9 ribonucleoprotein delivery into protoplasts for genome editing of potato.

Chapter 3 is the first research chapter. It describes the procedures taken to establish the foundations for non-transgenic CRISPR/Cas9 genome editing of *StGWD1*. The process of designing single guide RNAs for the gene targets is described, as well as the screening of these guides *in vitro* for efficacy in DNA cleavage. It also outlines the establishment of a potato protoplast isolation procedure, and culturing these protoplasts to attain the micro-calli stage of development.

Chapter 4 comprises the second research chapter of this thesis. It describes a transgenic approach to engineer potatoes and prevent cold induced sweetening by targeting *StGWD1* using *Agrobacterium tumefaciens*. Plant transformation binary vectors were constructed by Golden gate cloning to contain sequences encoding Cas9 and several guides targeting *StGWD1.* The procedure to transform leaf explants and test regenerated calli is also outlined.

Chapter 5 provides a summary of the findings, highlights future research prospects and concludes this thesis.

References:

Lorberth R, Ritte G, Willmitzer L, Kossmann J (1998) Inhibition of a starch-granule-bound protein leads to modified starch and repression of cold sweetening. Nat Biotechnol **16**: 473–477

Ritte G, Heydenreich M, Mahlow S, Haebel S, Kötting O, Steup M (2006) Phosphorylation of C6- and C3-positions of glucosyl residues in starch is catalysed by distinct dikinases. FEBS Letters **580**: 4872–4876

Zhang Z, Hua L, Gupta A, Tricoli D, Edwards KJ, Yang B, Li W (2019) Development of an *Agrobacterium*-delivered CRISPR/Cas9 system for wheat genome editing. Plant Biotechnol J **17**: 1623–1635

Chapter 2: Literature Review

2.1 Origin and history of cultivated potato

The *Solanaceae* family contains 98 genera and 3,000–4,000 species, one of which is the cultivated potato (*Solanum tuberosum* L.). Other commercially grown crops in the Solanaceae family include tomato (*Solanum lycopersicum* L.), husk tomato (*Physalis* sp.), aubergine (*Solanum melongena* L.), tobacco (*Nicotiana tabacum* L.) and chili pepper (*Capsicum* sp.; Machida-Hirano, 2015; Rabara et al., 2015). Potatoes are native to the Peruvian-Bolivian Andes and are one of the world's main food crops. It is believed that they were domesticated on multiple occasions before being grown in substantial amounts in South America by the Incas in the 16th century (Ortiz and Mares, 2017). During the second half of that century, potatoes were discovered by Spanish explorers and brought to Europe. The plant became a significant crop in Ireland by the end of the 17th century, and in continental Europe by the end of the 18th century (Pitrat and Michel, 2003), but it was only during famines caused by the Napoleonic Wars in the 1800s that continental Europeans actively start eating potatoes. Due to its relatively high vitamin C concentration, potatoes may have helped prevent scurvy among early consumers, notably sailors (Buckenhüskes, 2005). The potato was introduced to Africa in the 18th century by German and English settlers and missionaries who initially brought it to East Africa (Messer, 2008).

2.2 Agricultural significance of potatoes

After rice and wheat, potatoes are the third-most important food crop in the world in terms of human consumption (Birch et al., 2012) and more than one billion people consume them. Currently 378 million tons of potato tubers are produced worldwide on an estimated 19 million hectares of farmland (Devaux et al., 2019). When compared to crops such as rice and wheat, potatoes produce nearly four times the yield per hectare, while also being more water-efficient (https://cipotato.org/potato/potato-facts-and-figures/), high in amino acids and both vitamins C and B6 (Górska-Warsewicz et al., 2021). For all these reasons they provide an excellent source of food to support human populations (Compos et al. 2020).

Potatoes account for 45% of all vegetable crops produced in South Africa, with 2.6 million tonnes produced in 2020 (https://regenz.co.za/resources/farming-potatoes-in-south-

africa/). The annual value of potato production in South Africa is approximately R8 billion, and 8–10 % of all agricultural jobs in South Africa are tied to its cultivation (Potato South Africa, 2021). Because of the differing climatic conditions and soil types of South Africa's nine provinces, potatoes are grown year-round, assuring a steady supply of tubers. Limpopo, the Free State, and the Western Cape (particularly in the sandveld) are the primary potato-producing regions (Machakaire et al., 2021). With nearly R2 billion of export earnings accumulated over the previous five years, South Africa is the continent's second-largest exporter of both potatoes and seed potatoes. In 2018 alone, South Africa's potato export revenue totalled over R570 million, up 5 % from R540 million in 2017 (Kapuya and Sihlobo, 2015; DAFF, 2019).

The four components of food security are 1. stability, 2. utilization and quality, 3. access and 4. availability of food. From 2017 until 2022, the world's population increased from 7.6 to 8 billion and it is estimated that it will take another 14 years for the population to reach 9 billion and another 34 years to reach 10 billion (https://www.worldometers.info/world-population/). In South Africa, the population grew from 56.4 million to nearly 60 million people between 2016 and 2021 (https://ourworldindata.org/population-growth). It is clear that food production will need to increase to generate more food on the same amount or on reduced areas of arable land. The potato crop can assist in meeting this demand as it has a widely diverse distribution pattern and high current levels of cultivation and demand, particularly in emerging nations with high levels of poverty, hunger, and malnutrition (Devaux et al., 2019). Breeding efforts will be needed, however, to be improve its output. In recent years potato genome sequences have been published which will allow the rational manipulation of the potato to improve yield.

2.3 Potato genome sequence information

The development of fully annotated genome sequences is important for production of biotechnologically improved plants (Visser et al., 2014). The identification of agronomically significant genes as well as the opportunity to create millions of unique genetic markers are both made possible by recent advancements in genome sequencing facilitated by second and third generation DNA sequencing technologies (Edwards and Batley, 2010). These markers

have been used to create genetic and physical maps and to help identify genes or quantitative trait loci responsible for qualities that are economically significant (Varshney et al., 2009).

As potatoes are autotetraploid, it is important that the consensus sequence of the potato genome be obtained from several cultivars in order to accurately represent the species' genetic heterogeneity (Kyriakidou et al., 2020). Recent publications of entire tetraploid genomes of the commercial potato cultivars Otava and Solyntus have increased the tools accessible to researchers studying potatoes (Van Lieshout et al., 2020; Sun et al., 2022). A complete genome sequence for the cultivar Désirée, commonly used in potato research is still lacking, although in 2020, a thorough single nucleotide polymorphism (SNP) map for this cultivar was uploaded to the National Center for Biotechnology Information database (Sevestre et al., 2020).

2.4 Importance of starch

Starch is the largest source of calories within the human diet and is used both in food and non-food industries (Yazid et al., 2018; Carpenter et al., 2015). The main sources of starch include maize, potatoes, tapioca and wheat (Bashir and Aggarwal, 2019). Roughly 52% of globally produced starch is used within the food industry (for example in baking where it is used as a gelling and moisture-retention agent, or in processed foods where it acts as a thickener or stabilising agent) and the remainder is used within non-food industries (for example in pharmaceuticals as a filler, or for production of biofuels or textiles; Bashir and Aggarwal, 2019; Makroo et al., 2021). For non-food industries starch often needs to be altered physically or chemically (such as by the addition of covalently bound phosphate) to alter its physicochemical properties for specific industrial processes (Zia-ud-Din et al., 2017). Starches from some plants – such as potato – contain naturally high levels of covalently bound phosphate, while those from other plants – especially those found in cereal endosperm – contain very low levels (Tabata et al., 1975; Blennow et al., 2000; Pfister and Zeeman, 2016). As the extent of starch phosphorylation is one of the characteristic that determines its physicochemical properties, it influences its economic value (Carpenter et al., 2015; Uitdewilligen et al., 2022).

2.4.1 Starch structure

Starch is a polyglucan that is comprised of two separate fractions with differing structures, amylose and amylopectin. Amylopectin is the major fraction of most starches and is responsible for the crystallinity observed in the starch granule (Seung, 2020). It is composed of α-1,4-D-glucose units with numerous branching points linked by α-1,6-glycosidic bonds (Figure 2.1). Within a starch granule, amylopectin forms alternating crystalline (containing glucan chain double helices) and amorphous (which is composed of the branch point zone linking two clusters; Zeeman et al., 2010) lamellae. Amylose is a mostly linear molecule that consists of α-1,4-linked D-glucose monomers with intermittent α-1,6-linked branchpoints (Figure 2.1), and does not appear to contribute to the structural organization of starch granules (Koroteeva et al., 2007; Kozlov et al., 2007).

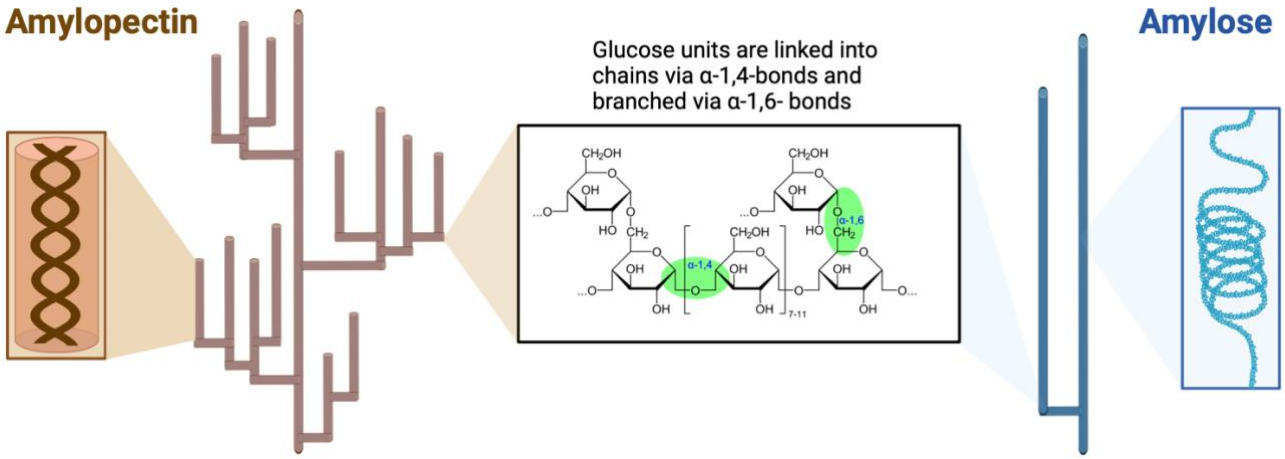

Figure 2.1 **Structural architecture of starch granules**. Amylopectin and amylose are two glucose polymer components found in starch that both contain α-1,4-linked linear chains and α-1,6-linked branch points. Amylose is mostly linear and forms single helices with few branching points. Amylopectin has a branching structure that enables adjacent chains to form double helices that pack into crystalline lamellae, while branch points occupy the amorphous lamellae. Figure created using BioRender.com

The structural properties and functionality of starch are influenced by the ratio of amylose and amylopectin (Alcázar-Alay and Meireles, 2015; Makroo et al., 2021), which is greatly affected by the plants genetic background (Yazid et al., 2018). About 30% of most starch granules are typically amylose, while the remaining portion is amylopectin (Wang et al., 2018).

Glucose moieties within starch naturally contains some covalently bound phosphate and the amylopectin fraction is the only portion that is phosphorylated (Viksø-Nielsen et al., 1998), where 70% of the phosphates are monoesterified at the C-6 position, and 30% are monoesterified at the C-3 position of the glycosyl unit (Takeda and Hizukuri, 1982).

2.4.2 Starch Biosynthesis

Starch accumulates as granules within plastids, and it is known that many plastid-localized enzymes coordinate their actions to synthesise starch from ADP-glucose (Sonnewald and Kossmann, 2013; Lloyd and Kossmann, 2015). The metabolism of starch in leaves and tubers displays many similarities in terms of the classes of enzymes involved; however, there are variations in starch metabolism between the two tissues (Figure 2.2; Van Harsselaar et al., 2017). In leaves, starch is produced directly from photosynthate during the day and is broken down during the night to maintain metabolic processes in the absence of photosynthesis (Pfister and Zeeman, 2016). Plants develop more slowly and suffer carbon starvation if this night-time glucose supply is diminished, as demonstrated by *Arabidopsis thaliana* mutants with defective starch production (Caspar et al., 1985; Niittylä et al., 2004; Stitt and Zeeman, 2012; Paparelli et al., 2013). In potato tubers, starch accumulates throughout tuber growth and is retained for an extended period of time to maintain the energy requirements of the dormant tuber. Stored starch is also used to feed the growth of new shoots after dormancy (Van Harsselaar et al., 2017).

The starch molecule's intricate structure suggests that a coordinated pathway of biosynthesis involving numerous enzyme classes will be necessary for its biosynthesis. These enzymes are thought to perform multiple tasks and depend on one another in order to function. The majority of these enzyme classes consist of multiple isoforms that have distinct functions in the synthesis of the polymers (Nakamura et al., 1995; Patron et al., 2002; Seung et al., 2015). They can influence the amounts of the two polyglucan fractions, the arrangement of various chain lengths within amylopectin (Tetlow and Emes, 2011), the phosphorylation of glucosyl residues (Ritte et al., 2002; Baunsgaard et al., 2005; Kötting et al., 2005; Lütken et al., 2010) and the development of granule morphology (Szydlowski et al., 2009; Crumpton-Taylor et al., 2013). One starch synthase, the granule bound starch synthase (GBSS) is responsible for amylose synthesis (Pfister and Zeeman, 2016), while several soluble

starch synthases (SSI, SSII, SSIII and SSIV) synthesise α-1,4 chains before starch branching enzymes (1,4-α-glucan: 1,4-α-glucan 6-glucosyl transferase) introduce branching points (Tetlow and Emes, 2014; Pfister and Zeeman, 2016).

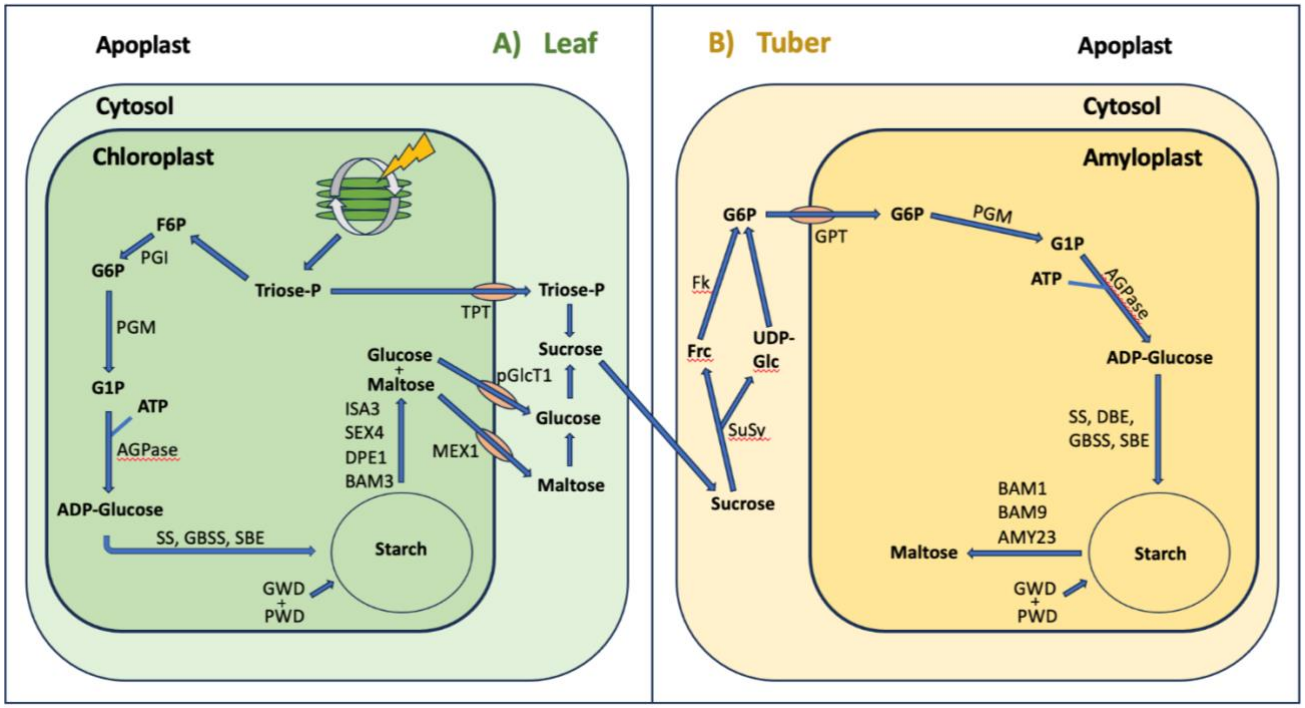

Figure 2.2 **The proposed metabolic pathways of starch synthesis and degradation in leaves and tubers of potato**. **A)** In leaves, photo-assimilates are generated from the Calvin Cycle. Triose phosphates can either be exported into the cytosol or be used to synthesise fructose-6-phosphate in the chloroplast. Phosphoglucoisomerase and phosphoglucomutase synthesise glucose 1-phosphate from fructose 6-phosphate which is used to synthesize ADP-glucose by ADP-glucose pyrophosphorylase. Plastid localised starch synthases use this to synthesise linear glucan chains which are joined by starch branching enzymes to generate the polymer. During starch catabolism, amylopectin is first phosphorylated by glucan, water dikinase that allows access to α- and β-amylases which form soluble glucans which are then further degrades to maltose and glucose. Maltose is then transported into the cytosol where it is degraded into glucose, which is used to synthesise sucrose. This is loaded from the leaf into the phloem where it is transported to the tuber. **B)** After unloading, sucrose is cleaved into UDP-glucose and fructose by sucrose synthase. Both UDP-glucose and fructose are metabolised in several enzymatic steps to produce glucose 6-phosphate, which is transported into the amyloplast by a glucose 6-phosphate translocator and reconverted into glucose 1-phosphate by plastidial phosphoglucomutase. The glucose 1-phosphate is again used as substrate for ADP-glucose biosynthesis, which is then used to synthesise starch using the same enzymes described in leaf tissue.

Little is known about starch degradation in potato tubers (Sergeeva et al., 2022) except that glucan, water dikinase is also essential for starch degradation (Lorberth et al. 1998) to allow access to α- and β-amylases (Sergeeva et al., 2012; Streb and Zeeman 2012; Pfister and Zeeman 2016). Image was re-drawn from Ferreira et al., 2010; Van Harsselaar et al., 2017.

2.4.3 Starch phosphorylation affects starch catabolism

Starch phosphate is important for different reasons ranging from plant growth to the types of industrial processes starch can be used for (Ellis et al., 1998; Zhang et al., 2014; Thuynsma et al., 2016). As stated above, starch phosphorylation is the first step in starch degradation, and without it plants cannot degrade starch as efficiently compared to those with normal starch phosphorylation (Lorberth et al., 1998; Ritte et al., 2004; Mahlow et al., 2014). The enzyme predominantly responsible for starch phosphorylation is glucan water dikinase (GWD) that acts primarily on amylopectin (Ritte et al., 2006). Three GWD isoforms have been identified in plants, GWD1, GWD2 and GWD3 and their roles will be discussed in more detail below.

2.4.4 The glucan, water dikinase family

The glucan, water dikinase family is known to be ancient as plant species from all the major phyla contain *GWD1* like genes (Mdodana et al., 2019). Their actions have been studied in one bryophyte (*Physcomitrella patens*) and several angiosperms, and these studies have demonstrated a conserved role in starch phosphorylation and degradation (Lorberth et al., 1998; Ritte et al., 2004; Zhou et al., 2017; Mdodana et al., 2019). Glucan water dikinase 1 (GWD1) was first identified in potato (Lorberth et al., 1998) and was initially known as the R1 protein before its biochemical function as a α-glucan water dikinase was elucidated (Ritte et al., 2002). The model plant *Arabidopsis thaliana* contains one *GWD1* like gene and two similar paralogs named *GWD2* and *GWD3* (also known as phosphoglucan, water dikinase, *PWD*; Baunsgaard et al., 2005; Kötting et al., 2005). Both GWD1 and GWD3 localise to the plastid and incorporate phosphate into starch. The *gwd1* and *gwd3* mutants both lead to repression of starch degradation, with the effect being more severe in *gwd1* mutants (Yu et al., 2001; Baunsgaard et al., 2005; Kötting et al., 2005) while GWD2 is extra-plastidial and is not involved in starch metabolism (Glaring et al., 2007). *Atgwd2* mutants do, however, demonstrate

reduced growth and a reduced numbers of viable seeds and reduced ability to respond to abiotic stress (Pirone et at., 2017; Gurrieri et al., 2020).

2.4.4.1 Starch phosphate is incorporated by redox controlled dikinase reactions

Both GWD1 and GWD3 utilise a dikinase-type reaction mechanism that transfers β-phosphate from ATP to glucosyl residue within amylopectin releasing the γ-phosphate into solution (Ritte et al., 2002). GWD1 phosphorylates amylopectin at the C-6 position and GWD3 incorporates at the C-3 position, but GWD3 only acts once amylopectin has been phosphorylated by GWD1 (Baunsgaard et al., 2005; Kötting et al., 2005). Starch phosphate can be decreased, therefore, at both the C-6 and C-3 positions by down-regulating or mutating only the *GWD1* gene (Yu et al., 2001). At the start of the night, GWD1 displays reversible binding to leaf starch granules (Ritte et al., 2000), and it has been demonstrated that the partitioning of GWD1 between its soluble and granule-bound forms is redox controlled (Mikkelsen et al., 2005). As plants lacking GWD1 or GWD3 isoforms exhibit impaired starch degradation (Lorberth et al., 1998; Baunsgaard et al., 2005; Kötting et al., 2005), it has been proposed that transient starch breakdown is initiated by starch phosphorylation (Mikkelsen et al., 2005). It is thought that phosphorylation of crystalline starch promotes disruption of double helical glucan chains, solubilizing crystalline structures and making them accessible to hydrolytic enzymes (Hejazi et al., 2008; Blennow and Engelsen, 2010).

2.4.4.2 Importance of GWD on plant growth and fertility

Studies on the significance of GWD in various plant species have been conducted. In potato, leaf and tuber starch degradation was reduced in transgenic potatoes that express an antisense *GWD1* transcript (Lorberth et al., 1998), while transgenic lines where the gene was repressed only in tubers produced a decrease in tuber size and an increase in tuber numbers (Viksø-Nielsen et al., 2001). Mutations in *GWD1* in all plant species where this has been examined demonstrate reduced starch phosphate and impairment in starch degradation in photosynthetic tissue (Lorberth et al., 1998; Yu et al., 2001; Edner et al., 2007; Zhou et al., 2017; Mdodana et al., 2019; Wang et al., 2021), but many other effects have also been observed. These include effects on plant fertility (Nashilevitz et al., 2009; Vriet et al., 2010),

development of reproductive structures (Mdodana et al., 2019), plant growth (Bowerman et al., 2016; Zhou et al., 2017) and amounts of storage starch (Ral et al., 2012; Zhou et al., 2017).

2.4.4.3 Key domains affecting GWD1 activity

The C-terminus of potato GWD1 contains a catalytic domain that contains a histidine which undergoes autophosphorylation during catalysis and transfers the phosphoryl group from ATP to starch (Figure 2.3). When this histidine residue was replaced with alanine, the resulting enzyme was catalytically inactive (Mikkelsen et al., 2004). Another study by Mikkelsen et al. (2005) demonstrated that GWD enzymatic activity is almost completely lost upon enzyme oxidation, but can be reversed by reduction. Inactivation by oxidation within potatoes results from a reversible disulfide bridge which forms between the C1004 and C1008 cysteine residues. A C1008S mutation resulted in a permanently active GWD enzyme *in vitro*, validating that C1004 and C1008 bridging is responsible for GWD inactivation (Mikkelsen et al., 2005). However, Skeffington et al., 2014 found that redox regulation of GWD is insignificant for the regulation of starch breakdown in *Arabidopsis* leaves at night.

2.4.5 The pathway of starch degradation

Although GWD1 is involved in starch synthesis through the incorporation of phosphate groups, it is clear that it is also involved in starch degradation (Lorberth et al., 1998). As described above, many *gwd1* mutants exist, which all demonstrate reduced rates of starch degradation in their leaves (Yu et al., 2001; Edner et al., 2007; Zhou et al., 2017). Over the past 20 years, many of the other enzymes involved in leaf starch degradation have been identified, often after the isolation of *Arabidopsis* mutants (Caspar et al., 1991; Zeeman et al., 1998; Stettler et al., 2009). After phosphorylation of the starch granule by GWD1 and GWD3, it is accessed by amylolytic enzymes which release phosphorylated malto-oligosaccharides into the stroma (Streb and Zeeman, 2012). The phosphate is removed by two glucan phosphatases (SEX4 and LIKE SEX FOUR-2; Kötting et al., 2009; Samodien et al., 2018) before the malto-oligosaccharides are metabolised by isoamylases, α-amylases and β-amylases (Fulton et al., 2008; Streb et al., 2012). This leads to the production of maltose and linear malto-oligosaccharides within the stroma (Kötting et al., 2009). The malto-oligosaccharides are degraded to maltose and glucose by β-amylases and disproportionating

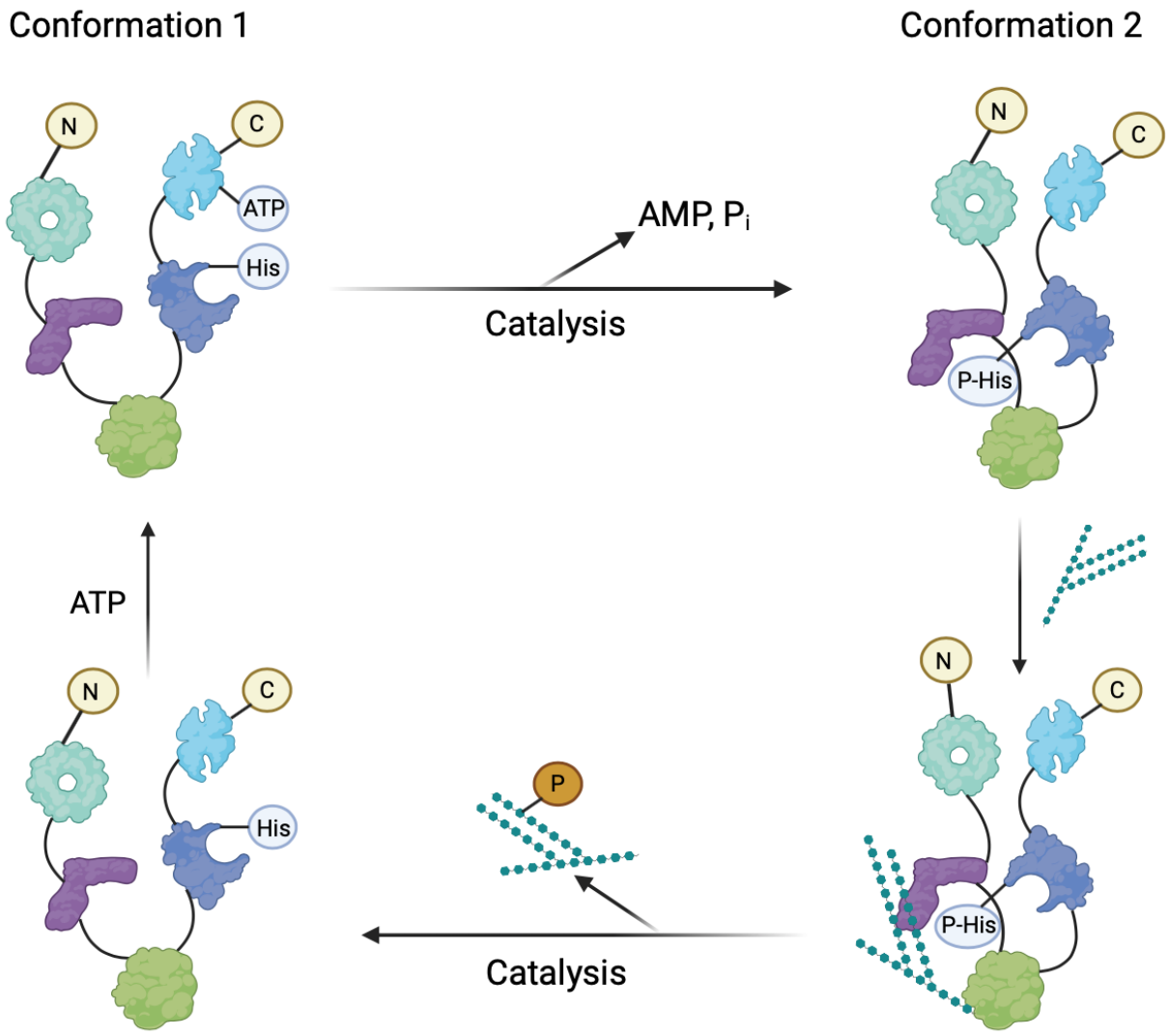

Figure 2.3 **Mechanism of starch phosphorylation**. Research by Mikkelsen and Blennow, 2005 indicated GWD1 contains five domains. It is believed that there are two conformations of GWD1, where the phosphohistidine site shifts its position to alternatingly interact with the nucleotide and glucan substrates. During conformation 1, the catalytic histidine interacts with the nucleotide. Catalysis then creates a phosphohistidine that causes a conformational change and results in conformation 2. The starch/glucan binding domain and the phosphohistidine site then engage, allowing the second round of catalysis to produce the phosphorylated glucan polymer. Following catalysis, GWD1 returns to its original conformation 1, where another nucleotide molecule can bind and the cycle repeats. Image was re-drawn from Mikkelsen and Blennow, 2005. Figure created with BioRender.com

enzyme 1 (Critchley et al., 2001; Hou et al., 2017). The remaining maltose and glucose are exported into the cytosol by two separate transporters specific for each sugar (Niittylä et al.,

2004; Cho et al., 2011), and within the cytosol maltose is degraded to glucose by disproportionating enzyme 2 (Chia et al., 2004; Lloyd et al., 2004; Lütken et al., 2010; George et al., 2012). This pathway has been established mainly in leaves of *Arabidopsis,* but many of the steps have been examined in other Angiosperms and have been demonstrated to play similar roles in those plants (Edner et al., 2007; Nardozza et al., 2013; Wang et al., 2018; Sergeeva et al., 2022). It is unclear if similar pathways of starch degradation exist in other plant organs.

Starch degradation is also involved in several important industrial processes. One example of this occurs in potato tubers that are kept at temperatures below 6 °C in order to prolong sprout dormancy (Wu et al., 2011). These cold-stored tubers undergo a process known as cold induced sweetening (Pollock and Rees, 1975), in which starch is broken down and reducing sugars accumulate (Schippers, 1975; Ewing et al., 1981). When tuber material is fried, the reducing sugars react with amino acids resulting in a dark pigmentation that is not accepted by consumers and also produces the toxin acrylamide (Stadler et al., 2002; Mottram et al., 2002; Bhaskar et al., 2010).

Some of the enzymes shown to be involved in *Arabidopsis* leaf starch degradation have also been demonstrated to be involved in cold induced sweetening. These include α- and β-amylase genes (*Amy23, BAM1*, and *BAM9*; Hou et al., 2017), and *GWD1* (Lorberth et al., 1998). However, other enzymes have been demonstrated to also affect potato leaf starch degradation (StSEX4, StLSF2 and StDPE2), but not cold induced sweetening (Lloyd et al., 2004; Samodien et al., 2018). In those studies the enzymes were repressed with RNAi technology that likely did not lead to complete knockout phenotypes and it would be useful to re-examine this pathway using genome editing technology.

2.5 Biotechnological methods for improving potatoes

2.5.1 Breeding challenges

Solanum tuberosum, ssp. *tuberosum* is the parent species of commercial potato varieties. It is a highly heterozygous autotetraploid and its lineage can be traced back to the diploid cultigen *S. tuberosum* Stenotomum Group, which were domesticated from diploid wild species in the mountains of Southern Peru around 8000-10,000 years ago (Spooner et al., 2005; Hardigan et al., 2017). Potato plants are typically replicated asexually through clonal

propagation (Watanabe, 2015) which has some benefits, including robust early development, better yields, and swift fixation of hybrid vigour. However, relying only on asexual reproduction restricts genetic diversity within populations (Fasoula, 2002). Because of this lack of allelic variation, potato populations frequently react poorly to changes in cultivation conditions or to selection pressure. Because potatoes contain a complex, tetraploid genome, crossing cultivars using conventional breeding methods in this species is slow and laborious (Halterman et al., 2016; Hameed et al., 2018). Sexual incompatibility often exists between wild and cultivated potato species (Halterman et al., 2016) and because they have a polyploid genome, more than one allele may need to be successfully mutated for a trait to be incorporated (Nadakuduti et al., 2018). This makes it difficult to introduce advantageous genes into potato species through traditional breeding techniques and new approaches are required (Lindhout et al., 2011).

One way to improve potato cultivars uses trans- or cis-genic techniques, both of which have been employed in research to improve potatoes (Nadakuduti et al., 2018) and some of which have been commercialized in the United States (Martínez-Prada et al., 2021). The Innate® potato for example was developed by J.R. Simplot® and prevents cold induced sweetening by down-regulating vacuolar invertase enzyme encoded by *Vlnv,* while Amflora™ potatoes contain reduced amylose content (Martínez-Prada et al., 2021).

2.5.2 New breeding techniques

A wide range of methodologies have recently been created that enable targeted mutations in the genome of plants (Schaart et al., 2015). In many countries they are used in conventional plant breeding efforts because they produce genetic alterations that are indistinguishable from naturally occurring mutations. They have been termed "New breeding techniques" (NBTs), and in recent years substantial attention has been directed to developing these approaches to improve agricultural plants. Crop species that stand to gain the most from the adoption of NBTs are ones, like potato, that do not perform well using conventional breeding methods, although they will also help accelerate breeding efforts in other crops (Dhugga, 2022).

Four promising NBTs have been developed for use in plant breeding. These include meganucleases, zinc finger nucleases (ZFNs), transcription-activator like effector nucleases (TALENs), and Clustered Regularly Interspaced Short Palindromic Repeats/CRISPR-associated

(CRISPR/Cas) (Aglawe at al., 2018). Each of these systems employs nuclease enzymes to introduce double-stranded DNA breaks (DSB), which are then improperly repaired, leading to mutations in that area of the target gene.

Meganucleases are endo-deoxyribonucleases that are present in a variety of eukaryotic organisms (Daboussi et al., 2015). They are distinguished by their broad range of target recognition sites, which can range in length from 20 to 40 base pairs (bp), but are normally between 20 and 30 bp. The DNA binding site, which extends in both directions from the cleavage site, and the catalytic domain of meganucleases overlap each other (Stoddard, 2014). Because meganucleases are small proteins, they can be delivered into target cells more easily than some of the alternative techniques. Additionally, they are very specific, which lowers the possibility of off-target cleavage (Zheng et al., 2020). Because their binding domain and catalytic region cannot be separated they are, however, less adaptable than other NBTs in terms of their target range which limits their usefulness.

Zinc finger (ZF) nucleases consist of chimeric enzymes with a DNA-binding ZF protein domain linked to the nuclease domain of the *FokI* restriction enzyme. One nuclease is connected to a group of ZF recognition sites, each of which recognizes a 3 bp sequence (Certo and Morgan, 2016). Greater numbers of ZF sites increase binding specificity, however three ZF sites are normally joined to form a 9 bp recognition site. Because the *FokI* restriction enzyme can only function as a dimer, two ZF nucleases must unite for a DSB to take place. Therefore, the final DNA recognition sequence is 18 base pairs when using three ZF sites per nuclease (Urnov et al., 2010). Zinc finger nucleases are adaptable, modular systems, and the *FokI* nuclease can compound with many ZF recognition sites. Despite the advantage of ZF nuclease recognition sites being programmable, the endonucleases specificity is poor, which can lead to a large percentage of off-target DSBs (Song et al., 2014).

Another class of chimeric endonucleases are TALENS. The TALEN complex is formed from a restriction enzyme and a DNA-binding domain from TAL effectors, which are proteins released by *Xanthomonas* bacterial species (Cade et al., 2012). A repeat-variable di-residue is present at base pairs 12 and 13 in the 33 to 35 bp repeating region that makes up the TAL DNA binding site. The specificity of the binding is determined by this repeat-variable di-residue, which varies for each repeat. The range of potential DNA targets can be expanded by further engineering this residue to target more areas (Lau et al. 2014). Like ZF nucleases, TALENs are modular systems that allow for greater versatility than meganucleases. However,

a significant drawback of their use is that DNA methylation interferes with endonuclease activity and considerably reduces their efficacy. As a result, they are less effective in methylated parts of the genome (Kaya et al., 2017).

The primary focus of this research study is the use of Clustered Regularly Interspaced Short Palindromic Repeats (CRISPR) and CRISPR-associated (Cas) proteins, which together form the CRISPR/Cas gene-editing technology, and this will be discussed in the following section.

2.6 Genome editing using CRISPR/Cas9

2.6.1 CRISPR/Cas: a prokaryotic system for natural immunity

The CRISPR/Cas system is an adaptive immune system that protects prokaryotic organisms from plasmids and viruses that can invade the host cell (Terns and Terns, 2011). It is capable of identifying and degrading foreign DNA or RNA in a sequence-specific manner. The defence mechanism is composed of three phases: (i) adaptation, or spacer acquisition; (ii) crRNA biogenesis; and (iii) target interference (Figure 2.4; Hille and Charpentier, 2016).

During the adaption stage, the host genome's CRISPR-associated (Cas) genes, which encode Cas ribonucleases, receive a novel spacer referred to as the protospacer (Gebre et al., 2018). This is a DNA sequence that is integrated from a nucleic acid sequence from an invading plasmid or virus. The presence of a protospacer adjacent motif (PAM) recognition sequence flanking the protospacer is required for the recognition and cleavage of viral/plasmid protospacers (Deveau et al., 2008; Horvath et al., 2008). A prokaryote's long-lasting immunity to the same virus is ensured by integration of this DNA segment (Mosterd et al., 2021).

The newly acquired spacers must be transcribed to create pre-CRISPR RNA (pre-crRNA), which is then processed into mature small molecule crRNAs corresponding to each protospacer. A short, non-coding RNA called trans-activating CRISPR (tracr) RNA interacts with repetitive areas of the pre-crRNA (Deltcheva et al., 2011; Briner et al., 2014) and is required to mediate specific immunity (Zhao et al., 2020). An RNase III enzyme then processes the tracrRNA-crRNA duplex to form a small mature guide RNA (gRNA; Hille and Charpentier, 2016). Along with the crRNAs, the Cas endonuclease gene is transcribed and translated. A CRISPR/Cas complex is created when the mature Cas protein combines with a dual gRNA (Hille and Charpentier, 2016; Faure et al., 2019). The inserted new spacer sequence will be

transcribed along with the Cas endonuclease gene when the same virus or plasmid infects the bacterium again (Rath et al., 2015).

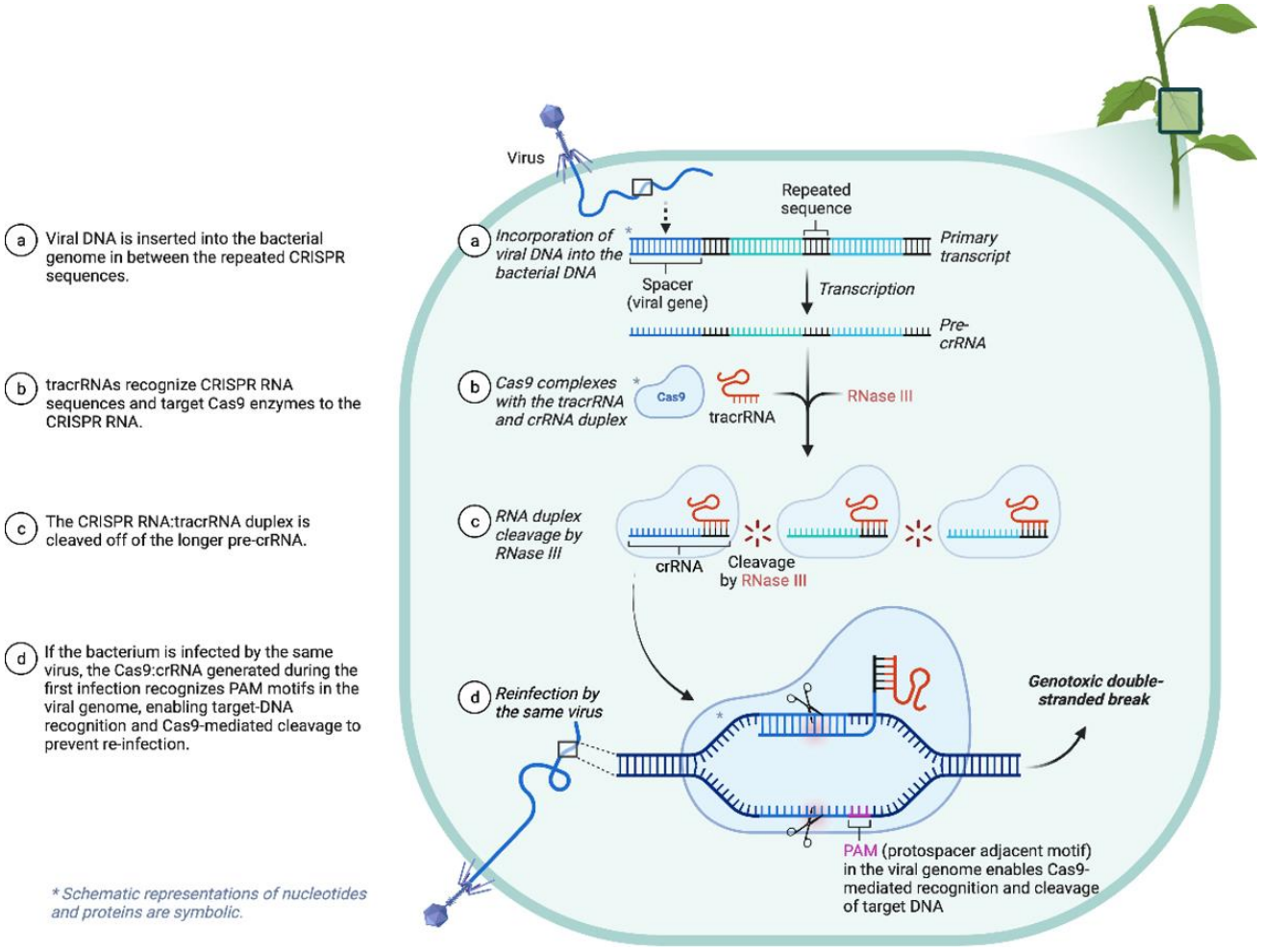

Figure 2.4 **A simplified model of the CRISPR/Cas immunity mechanism**. **Adaptation**: A protospacer sequence from the invading DNA is incorporated into the host DNA's CRISPR array after phage infection. **Expression:** The CRISPR sequence is transcribed and the long-chain product is then processed to produce mature short-chain crRNA. The CRISPR/Cas complex is created when the crRNA combines with the Cas endonuclease. **Interference:**, A functional crRNA guides Cas9 nucleases to selectively recognize and cleave viral DNA/RNA that is identical to the spacer, in order to trigger a particular immune response. The foreign nucleic acid is then cleaved by the Cas endonuclease and degraded. Consequently, the CRISPR/Cas system can confer acquired and inherited resistance to the host. Figure created with BioRender.com.

During the subsequent interference phase of the prokaryotic defence mechanism, the Cas protein causes a double stranded break in the foreign DNA or RNA three base pairs upstream from the PAM site, and the host cell degrades the cleaved nucleic acid (Jore et al.,

2012). The crRNA in the CRISPR/Cas complex directs the endonuclease toward the appropriate location of the invasive nucleic acid. There are two ways that the CRISPR/Cas complex and the invasive nucleic acid can be recognized. These are firstly, through complementary base-pairing of the CRISPR/Cas complex with the crRNA spacer sequence, and secondly by Cas recognition of a PAM site close to the protospacer sequence (Hale et al., 2009; Gleditzsch et al., 2019).

2.6.2 Type II CRISPR/Cas systems

Three main types of CRISPR/Cas systems – Type I, II, and III – are present in prokaryotes. Type II systems are the most commonly used for biotechnological purposes, and these can be further divided into four classes (Makarova et al., 2011). Type II class I CRISPR/Cas systems use a Cas3 enzyme that has two active domains. In this type, a single operon encodes the whole CRISPR/Cas complex. The CRISPR/Cas3 complex must be linked to an effector complex in order to function after it has been assembled, and this system converts pre-crRNA into mature crRNAs (Richter et al., 2012). Type II class II uses the Cas9 protein as its effector (Sapranauskas et al., 2011). The Cas9 protein has two domains, each of which can function individually (Chylinski et al., 2013). Unlike class I systems, class II systems do not require an effector complex to function. The requirement for Cas9 to be guided by an RNA duplex formed from tracrRNA bound to crRNA is another distinctive characteristic of CRISPR/Cas9 systems (Fonfara et al., 2014), which means that they demonstrate a high degree of specificity. Similar to class I systems, class II CRISPR/Cas systems also convert pre-crRNA into mature crRNAs. Type II, Class III CRISPR/Cas systems make use of a Cas10 protein that includes four active domains (Staals et al., 2013). The class III CRISPR/Cas system uses effector complexes and relies on the resultant products of the class I and class II systems rather than processing pre-crRNA itself (Makarova and Koonin, 2015). As a result of its inability to operate autonomously in a cell, this system is less effective compared to class I and II systems (Kolesnik et al., 2021). The least common type II CRISPR/Cas system in nature belongs to class IV. It makes use of the cfs1 protein, also known as Cas12a, which pairs with an effector domain to operate as an endonuclease. This method neither modifies its own pre-crRNA nor incorporates a CRISPR cassette into the host's genome (Makarova and Koonin, 2015).

2.6.3 CRISPR/Cas9 as a preferred engineering tool

The type II class II CRISPR/Cas system has been modified to function as a biotechnological tool that can design precise, site-specific genomic modifications (Jinek et al., 2012). This technique introduces double-stranded DNA breaks into the target genome, which are later repaired by the host (Figure 2.5). Non-homologous end joining (NHEJ) repair, is the most common method used by the host to mend these breaks, but is error-prone and generates alterations to the DNA sequence (Rodgers and McVey, 2016). A second mechanism – Homology Directed Repair (HDR) – can also be used to repair the DNA and the use of HDR can allow more precise genome editing by, for example the introduction of gene knock-in, gene substitution or point mutations (Arnoult et al., 2017; Tang et al., 2019). This repair mechanism enables the creation of more complex insertions and can be applied biotechnologically to introduce insertions or deletions (indels) into a eukaryote genome at targeted sequences in a flexible and effective way.

Due to Cas9's specificity, the type II class II CRISPR/Cas system was the first class chosen for use in genome editing experiments (Knott and Doudna, 2018). Contrary to other endonucleases, Cas9 exclusively interacts with a dual guide RNA that is formed from a mature crRNA complexed with a tracrRNA (trans-acting crRNA). As Cas9 binding to the dual guide RNA is highly specific, there is a very low likelihood of it associating with an incorrect RNA sequence. The dual guide RNA is also highly specific in recognising target sequences, which limits the potential for off-target cleavage. It is only when Cas9 becomes attached to DNA near a PAM site that the enzyme causes dsDNA breaks (Faure et al., 2019). This system was simplified by combining the crRNA-tracrRNA complex into a single guide RNA (sgRNA) by adding a linker loop between the two molecules which is advantageous because the target organism only requires the introduction of one modified RNA molecule (Jinek et al., 2012).

Other Cas endonucleases have also recently been used for gene editing in both plants and mammals (Zhong et al., 2018) which overcome some drawbacks caused by Cas9. These include a limited target range caused by the requirement for a nearby PAM site and the large size (160 kilodaltons) of Cas9. Additionally, the other Cas proteins provide additional features that Cas9 does not (Wada et al., 2022), such as greater specificity and the recognition of different PAM sequences. Recent advancements in CRISPR-Cas systems offer distinctive characteristics that set them apart from well-known Cas proteins like Cas9 and Cas12. For

example, type I CRISPR-Cas10 causes minor indels and bi-directional long-range deletions spanning up to 7.2 kb, while Cas3 can identify and remove substantial portions of a genome using just one guide (Csörgő et al., 2020; Wada et al., 2022). Unlike Cas9 that can edit GC-rich regions upstream from the PAM site, Cas12a can also be used for editing AT-rich regions downstream from the PAM site (Svitashev et al., 2015; Kim et al., 2017a).

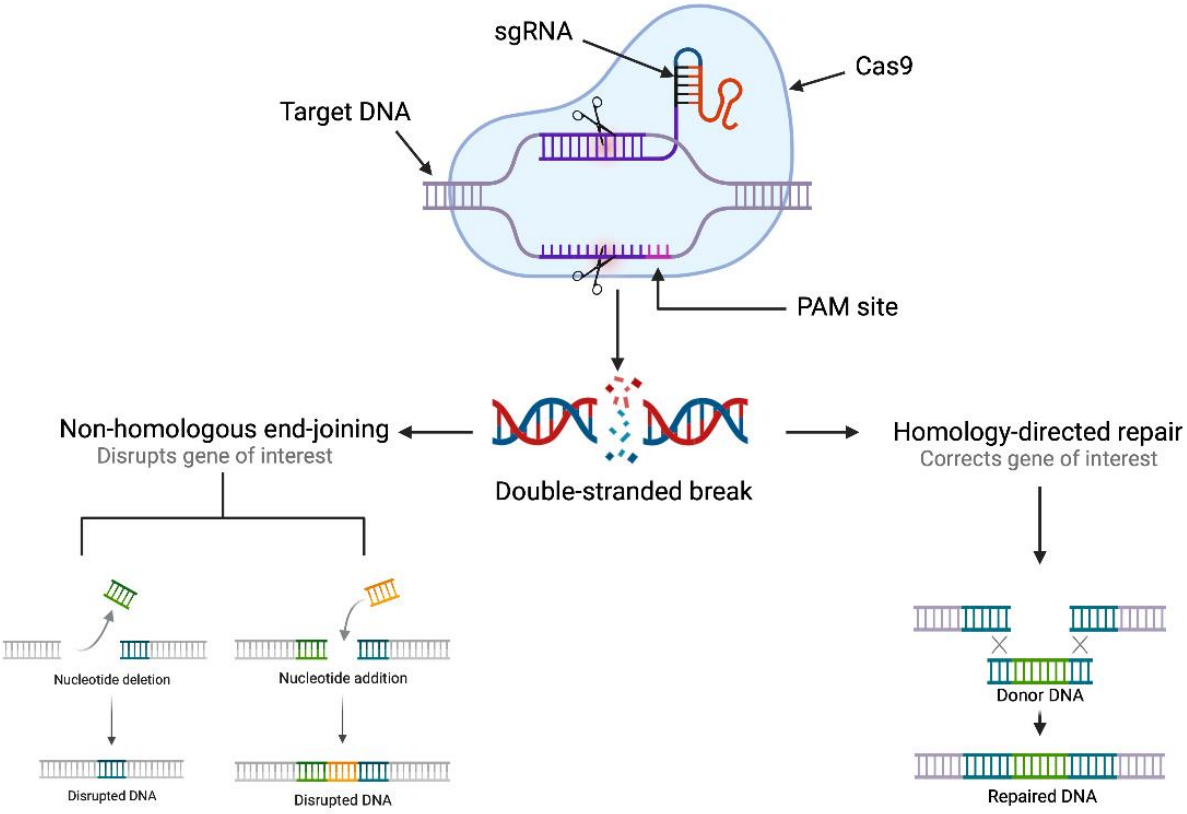

Figure 2.5 **The two mechanisms used for repair of double-stranded DNA breaks caused by the CRISPR/Cas9 complex**. Non-homologous end joining may lead to faulty repairs and the insertion of random indels. Larger insertions are produced by homology-directed repair and are specified by a donor DNA segment that serves as a template for the repair. Figure created using BioRender.com

2.6.4 CRISPR/Cas used beyond gene-editing

Expanded prospects for genome editing in plants have been made possible by the CRISPR/Cas system's capacity to induce DSB in a target genome. The potential of this complex as a biotechnological tool has been further increased by the development of a "dead" Cas9

(dCas9). This lacks endonuclease activity due to point mutations that are introduced into the two nucleolytic domains (RuvC and HNH) present in the Cas9 protein which cleave target DNA strands (Jinek et al., 2012). This method has recently emerged as a potentially effective tool to treat human genetic disorders caused by single base alterations through fusion of dCas9 with catalytic domains able to deaminate cytosine or adenine bases within the host genome (Shalem et al., 2014; Komor et al., 2016; Gaudelli et al., 2017). Shortly after CRISPR/dCas9 technology became available, researchers started coupling regulatory and reporter proteins to dCas9 to take advantage of its targeting capabilities for reversible gene activation or repression (Li et al., 2017; Lowder et al., 2017 a,b), epigenome editing (Hilton et al., 2015; Zezulin and Musunuru, 2018), modulation of chromatin topology (Guo et al., 2015), live-cell chromatin imaging (Dreissig et al., 2017; Xue and Acar, 2018) and DNA-free genetic modifications by fusion to cytidine or adenosine deaminases (Luo et al., 2020; Yu et al., 2020). When combined with sgRNA, dCas9 still moves to a target genomic locus and can direct functionally active domains attached to the CRISPR/dCas9 complex to very specific locations within the host genome (Figure 2.6; Brezgin et al., 2019). Functionally active domains may comprise (a) base editing enzymes, (b) domains used to investigate the chromatin structure, (c) domains for directly altering three-dimensional (3D) chromatin structure to identify gene regulatory elements, and (d) epigenome remodelling factors for activating or suppressing gene expression without introducing a mutation (Brezgin et al., 2019). Regulating gene expression by delivering activator or repressor domains to particular target genes is one of the main features when using dCas9 (Cheng et al., 2013; Gilbert et al., 2013). Site-specific DNA tagging has also been made possible by the coupling of fluorescent proteins to the CRISPR/dCas9 complex to visualise location of genomic loci (Tanenbaum et al., 2014).

Recent advancements in the CRISPR/dCas9 system have made it possible to generate site-specific SNP alterations by joining a base-editing protein to the complex (Kim et al., 2017b). The enzymes cytosine deaminase and adenosine deaminase remove an amino group from cytosine and adenine, converting these nucleotides into respectively thiamine and guanosine (Komor et al., 2016; Gaudelli et al., 2017). This is useful since many features with agricultural significance are controlled by SNPs while gene knockouts or knock-ins can have negative effects on plant phenotypes.

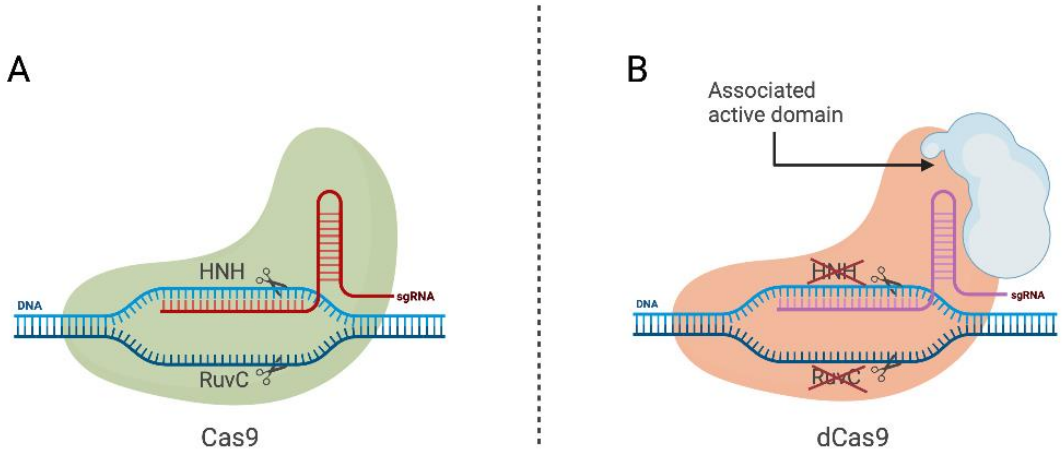

Figure 2.6 Modifications of the Cas9 endonuclease that have been altered by selectively deactivating the catalytic domains. **(A)** The natural Cas9 endonuclease, that is active in both catalytic domains. **(B)** A Cas9 protein that has both of its catalytic domains inactivated and is linked to an alternate active domain. Figure created using BioRender.com

2.6.5 Methods for genome editing with CRISPR/Cas9

CRISPR/Cas components can be delivered into a target organism either as trans DNA that is expressed by the host's transcriptional machinery, or as an already functional and active ribonucleoprotein (RNP; Chen et al., 2019). When introducing trans DNA, the sgRNA sequence and Cas9 coding domain sequence are contained in binary vectors, and integrated into the target cell's genome (Liang et al., 2018; Chen et al., 2019). Before genome editing can take place the expression cassettes must be transcribed and used to produce both sgRNA and Cas9 protein *in vivo*. In seed crops, once targeted mutagenesis has been established, the integrated T-DNA can be eliminated through self-pollination and subsequent genetic segregation (Martínez-Prada et al., 2021). The integration of CRISPR constructs into the genome can, however, result in a greater number of off-target modifications that can be detrimental to plant growth which may restrict the adoption of these technologies for commercial purposes (Chen et al., 2019). Transgenic techniques also lead to the introduction of transgenes into the genome that are problematic for consumers and, while these can be

removed in seed crops by backcrossing, this is not simple in potato. Because of this, non-transgenic techniques would be preferable in this species to avoid these problems.

2.6.5.1 Transgenic method for genome editing

Although many methods of plant transformation have been developed, *Agrobacterium tumefaciens* mediated plant transformation is generally preferred as it demonstrates a high efficiency of transgene integration into the host genome, requires simple equipment, and produces a greater percentage of plants with a single transgene insertion compared to other methods (Gelvin, 2017; Hwang et al., 2017; Asande et al., 2020). The ease of introduction of genes into plants using *Agrobacterium* was greatly improved by the construction of transfer DNA (T-DNA) binary vectors that contain T-DNA borders which become inserted into the plant genomes. Plasmid vectors have been engineered to contain numerous restriction endonuclease sites situated between promoter and terminator sequences within the T-DNA region into which genes of interest are ligated. Key features of T-DNA vectors include specific plant selectable markers, promoters and terminators (Gelvin, 2003). For genome editing, T-DNAs having the ability to encode several gene products can be introduced into plants (Gelvin, 2003; Altpeter et al., 2016). After the modified DNA is integrated into the genome and expressed into the host cell, Cas nuclease activity is high and stable, which increases the likelihood of producing mutations in regenerated plants (Bánfalvi et al., 2020). Stable T-DNA integration of these vectors can also have unfavourable consequences, such as off-target genome modifications are more likely to be found in plant lines with stable Cas and sgRNA integration when compared to transient transformation techniques (Bánfalvi et al., 2020; Chincinska et al., 2023). Regenerated transformants can also be chimeric due to differential editing of the gene within individual calli cells after transformation (Raldugina et al., 2021). Further unfavourable consequences include; (a) the transgene disrupting genes or regulatory components that are crucial for plant development, growth, or productivity; (b) the transgenes integrating into regions of the genome where gene expression is generally low or may exhibit modified or variable expression when plants are placed in the field or are under stress; and (c) the use of a transgenic system is time- and money-consuming and leads to regulatory hurdles inhibiting commercialisation (Gelvin,

2017). Although transgenic systems have been effectively used to transform plants, other techniques can be used to avoid some of these unfavourable consequences.

2.6.5.2 Genome editing without transgene integration

Several non-transgenic methods have been developed that allow plant genome editing. These can be divided into RNA based systems where all components are delivered as RNA and ribonucleoprotein (RNP) based systems where an RNA protein complex is delivered.

For RNA-based delivery the sgRNA and Cas9 are first synthesized *in vitro* and are then either transformed into the plant cell ballistically using particle bombardment, or through PEG-mediated protoplast transformation (Yue et al., 2021). Plasmids (or RNA) that encode a selectable marker gene can be co-transformed into plants with the sgRNA and Cas9 to allow selection of transformed cells. Alternatively selection can be achieved through the use of gRNAs can be designed to create single amino acid changes in genes that result in herbicide resistance (Svitashev et al., 2016; Banakar et al., 2020). Before DSBs can be introduced to the cell's genome, the Cas9 protein must first be synthesized by the plants translational machinery and then form a complex with the sgRNA. Single cells are then used to regenerate whole plants, of which 2-25% are expected to be mutated in the target gene (Nicolia et al., 2015; Svitashev et al., 2016; Andersson et al., 2018). This approach has the benefit of being DNA free, which is favoured by regulatory bodies and customers, and also displays fewer off-target effects compared to the stable expression of CRISPR/Cas DNA in transgenic plants (Chen et al., 2019). However, because RNA is unstable and quickly degraded, a reduced mutation efficiency compared to stable expression of CRISPR/Cas is observed when this technique is applied (Chen et al., 2019). This technique also does not allow for selection of transformed cells, meaning many of the regenerants may not have been exposed to RNPs, and therefore their targets will need to be sequenced.

2.7 Transgene-free genome editing using RNPs to transform protoplasts

Transformation with an RNP complex is the third way to deliver CRISPR/Cas elements to a cell (Woo et al., 2015). In this method, a fully functioning CRISPR/Cas9 RNP complex is created by isolation of RNA from *in vitro* transcription of sgRNA that is complexed with Cas9

protein before the RNP is introduced into protoplasts that are then regenerated into plants (Reed and Bargmann, 2021).

2.7.1 Advantages of RNP genome-editing

When modifying crop species, CRISPR/Cas9 RNPs can be transformed into protoplasts to enable DNA/transgene-free editing with few off-target mutations. Due to the quick breakdown of RNPs and the capacity to titrate their dosage while maintaining high editing efficiency, it also exhibits low toxicity. Since little *in vitro* work is required to build the CRISPR/Cas9 machinery before transformation, this technique is also quicker from a technical viewpoint. Additionally, no trans DNA is integrated (Lin et al., 2018; Zhang et al., 2021). As this project is designed to develop genome editing in potatoes, which are highly heterozygous (interlocus and intralocus) and have tetrasomic inheritance, the CRISPR/Cas RNP transformation method is very useful because it is challenging to cross potatoes in a sexual manner to remove transgenes post integration (Muthoni et al., 2015). Additionally, compared to DNA- or RNA-based CRISPR/Cas transformations, this system is much more effective, less expensive, and more suited for potato genome editing (Zhang et al., 2020).

2.7.2 Isolation, transformation and regeneration methods for potato protoplasts

In order to be used in genome editing approaches, Nicolia et al. (2015) developed a methodology for the isolation, transformation and culture of potato protoplasts for TALEN-mediated genome editing. As the genome editing process for CRISPR/Cas9 is essentially the same, variations of his method have been successfully employed by various groups for CRISPR/Cas genome editing (Andersson et al., 2017; González et al., 2020; Carlsen et al., 2022; Rather et al., 2022).

Potato protoplasts are produced in a two-step procedure that starts with plasmolysis which is then followed by the enzymatic breakdown of the cell wall. Released protoplasts are transformed with RNP's by polyethyleneglycol mediated transformation and then regenerated in the dark in a nutrient rich media (Reed and Bargmann, 2021). Although it is feasible to culture potato protoplasts in liquid (Tavazza and Ancora, 1986), encasing them in an alginate gel is preferred as it allows the regeneration medium to be refreshed without affecting the concentration of the protoplasts (Eeckhaut et al., 2013). In addition to being

popular for isolating potato protoplasts, this method has also been used to successfully generate protoplasts from other crop species, including cabbage (*Brassica oleracea*), canola (*Brassica napus*) and carrot (*Daucus carota*; Kielkowska and Adamus, 2012; Grzebelus and Skop, 2014; Sahab et al., 2019). Individual protoplasts can be hormonally induced to de-differentiate and multiply to generate callus after the regrowth of their cell walls and a full plant can then be regenerated from a callus by inducing shoots and roots from the callus tissue (Ikeuchi et al., 2013)

2.7.3 Hurdles of using protoplasts

Protoplast culture is a highly specialized tissue culture technique and, while species-specific protoplast culture procedures increase the likelihood of success of this approach, they are still an obstacle to progress for protoplast transformation techniques (Eeckhaut et al., 2013). A frequent problem that hinders cell culture is bacterial or fungal contamination of protoplasts, and many antimicrobial and antifungal chemicals have negative effects on plant growth (Herman, 2017).

Plants grown from protoplasts do not all display the same phenotypes due to somaclonal variation and chimera formation. Somaclonal variation is characterized by unanticipated aneuploidy, chromosomal rearrangements, epigenetic alterations, and SNPs that appear during cell culture. Following protoplast regeneration, a high level of somaclonal variation has been noted in potato plants (Fossi et al., 2019), which have negatively affected agriculturally important qualities, such as plant size and general health (Chincinska et al., 2023). It is costly and time-consuming to perform complex genome sequencing and analysis in order to pinpoint the alterations caused by somaclonal variation (Krishna et al., 2016). In plants that can be backcrossed any somaclonal variation can be eliminated, but in clonally propagated plants, this is more difficult meaning that somaclonal variation will be maintained in later generations. Since the processes leading to somaclonal variations are currently unclear, it is doubtful that this problem can be avoided (Fossi et al., 2019). Another undesirable and unanticipated result of protoplast cultivation is the production of chimeras, although these are expected to occur less frequently compared with plants produced using a transgenic approach (Reed and Bargmann, 2021). It has been noted in numerous cases of potato protoplast culture that protoplast fusion during the early phases of regeneration will produce a chimeric plant (Fossi et al., 2019; Bánfalvi et al., 2020). Because uniform

distribution of the modified genomic state is necessary for the success of genome editing in potatoes, the process is less effective when chimeras frequently appear. Plants can be grown from protoplasts to produce a variety of individuals with varying levels of somaclonal variation. These individuals can be screened, and those that have negligible genomic rearrangements or chimerism can be used for future propagation (Krishna et al., 2016). The ability to generate large numbers of regenerants by protoplasts is essential to this techniques' effectiveness since the more regenerants there are, the better the likelihood of identifying individuals with little somaclonal variation. A key feature of this project is to develop the ability to regenerate large numbers of calli from protoplasts. This will be an essential part of any non-transgenic CRISPR editing methodologies for potato.

2.8 References

Adegbaju MS, Morenikeji OB, Borrego EJ, Hudson AO, Thomas BN (2020) Differential evolution of α-glucan water dikinase (GWD) in plants. Plants **9:** 1–17

Aglawe SB, Barbadikar KM, Mangrauthia SK, Madhav MS (2018) New breeding technique "genome editing" for crop improvement: applications, potentials and challenges. 3 Biotech **8**: 336–356

Alcázar-Alay SC, Meireles MAA (2015) Physicochemical properties, modifications and applications of starches from different botanical sources. Food Sci Technol **35**: 215–236

Altpeter F, Springer NM, Bartley LE, Blechl AE, Brutnell TP, Citovsky V, Conrad LJ, Gelvin SB, Jackson DP, Kausch AP, Lemaux PG, Medford JI, Orozco-Cárdenas ML, Tricoli DM, Van Eck J, Voytas DF, Walbot V, Wang K, Zhang ZJ, Stewart CN Jr (2016) Advancing crop transformation in the era of genome editing. Plant Cell **28**: 1510–1520

Andersson M, Turesson H, Nicolia A, Fält AS, Samuelsson M, Hofvander P (2017) Efficient targeted multiallelic mutagenesis in tetraploid potato (*Solanum tuberosum*) by transient CRISPR-Cas9 expression in protoplasts. Plant Cell Rep **36**: 117–128

Andersson M, Turesson H, Olsson N, Fält AS, Ohlsson P, Gonzalez MN, Samuelsson M, Hofvander P (2018) Genome editing in potato via CRISPR-Cas9 ribonucleoprotein delivery. Physiol Plant **164**: 378–384

Arnoult N, Correia A, Ma J, Merlo A, Garcia-Gomez S, Maric M, Tognetti M, Benner CW, Boulton SJ, Saghatelian A, Karlseder J (2017) Regulation of DNA repair pathway choice in S and G2 phases by the NHEJ inhibitor CYREN. Nature **549**: 548–552

Asande LK, Omwoyo RO, Oduor RO, Nyaboga EN (2020) A simple and fast *Agrobacterium*-mediated transformation system for passion fruit KPF4 (*Passiflora edulis f. edulis* × *Passiflora edulis f. flavicarpa*). Plant Methods **16**: 141

Bashir K, Aggarwal M (2019) Physicochemical, structural and functional properties of native and irradiated starch: a review. Food Sci Technol **56**: 513–523

Banakar R, Schubert M, Collingwood M, Vakulskas C, Eggenberger AL, Wang K (2020) Comparison of CRISPR-Cas9/Cas12a ribonucleoprotein complexes for genome editing efficiency in the rice phytoene desaturase (*OsPDS*) gene. Rice **13**: 4

Bánfalvi Z, Csákvári E, Villányi V, Kondrák M (2020) Generation of transgene-free *PDS* mutants in potato by *Agrobacterium*-mediated transformation. BMC Biotechnol **20:** 25

Baunsgaard L, Lütken H, Mikkelsen R, Glaring MA, Pham TT, Blennow A (2005) A novel isoform of glucan, water dikinase phosphorylates pre-phosphorylated α-glucans and is involved in starch degradation in *Arabidopsis*. Plant J **41**: 595–605

Bhaskar PB, Wu L., Busse JS, Whitty BR, Hamernik AJ, Jansky SH, Buell CR, Bethke PC, Jiang J (2010) Suppression of the vacuolar invertase gene prevents cold-induced sweetening in potato. Plant Physiol **154**: 939–948

Birch PRJ, Bryan G, Fenton B, Gilroy EM, Hein I, Jones JT, Prashar A, Taylor MA, Torrance L, Toth IK (2012) Crops that feed the world 8: Potato: Are the trends of increased global production sustainable? Food Secur **4**: 477–508

Blennow A, Bay-Smidt AM, Olsen CE, Moller BL (2000) The distribution of covalently bound phosphate in the starch granule in relation to starch crystallinity. Int J Biol Macromol **27**: 211–218

Bowerman AF, Newberry M, Dielen AS, Whan A, Larroque O, Pritchard J, Gubler F, Howitt CA, Pogson BJ, Morell MK, Ral JP (2016) Suppression of glucan, water dikinase in the endosperm alters wheat grain properties, germination and coleoptile growth. Plant Biotechnol J **14**: 398–408

Brezgin S, Kostyusheva A, Kostyushev D, Chulanov V (2019) Dead Cas systems: types, principles, and applications. Int J Mol Sci **20**: 6041–6067

Briner AE, Donohoue PD, Gomaa AA, Selle K, Slorach EM, Nye CH, Haurwitz RE, Beisel CL, May AP, Barrangou R (2014) Guide RNA functional modules direct Cas9 activity and orthogonality. Molecular Cell **56**: 333–339

Buckenhüskes HJ (2005) Nutritionally relevant aspects of potatoes and potato constituents. Potato in Progress: Science Meets Practice, Wageningen Academic Publishers **6**: 17–26

Cade L, Reyon D, Hwang WY, Tsai SQ, Patel S, Khayter C, Joung JK, Sander JD, Peterson RT, Yeh JRJ (2012) Highly efficient generation of heritable zebrafish gene mutations using homo- and heterodimeric TALENs. Nucleic Acids Res **40**: 8001–8010

Carlsen FM, Johansen IE, Yang Z, Liu Y, Westberg IN, Kieu NP, Jørgensen B, Lenman M, Andreasson E, Nielsen KL, Blennow A, Petersen BL (2022) Strategies for efficient gene editing in protoplasts of *Solanum tuberosum* theme: determining gRNA efficiency design by utilizing protoplast (Research). Front Genome Ed **3**: 1–12

Carpenter MA, Joyce NI, Genet RA, Cooper RD, Murray SR, Noble AD, Butler RC, Timmerman-Vaughan GM (2015) Starch phosphorylation in potato tubers is influenced by allelic variation in the genes encoding glucan water dikinase, starch branching enzymes I and II, and starch synthase III. Front Plant Sci **6**: 1–12

Caspar T, Huber SC, Somerville C (1985). Alterations in growth, photosynthesis, and respiration in a starchless mutant *of Arabidopsis thaliana* (L.) deficient in chloroplast phosphoglucomutase activity. Plant Physiol **79**: 11–17

Caspar T, Lin TP, Kakefuda G, Benbow L, Preiss J, Somerville C (1991) Mutants of *Arabidopsis* with altered regulation of starch degradation. Plant Physiol **95**: 1181–1188

Certo MT, Morgan RA (2016) Salient features of endonuclease platforms for therapeutic genome editing. Mol Ther Nucleic Acids **24**: 422–429

Chen K, Wang Y, Zhang R, Zhang H, Gao C (2019) CRISPR/Cas genome editing and precision plant breeding in agriculture. Annu Rev Plant Biol **70:** 667–697

Cheng AW, Wang H, Yang H, Shi L, Katz Y, Theunissen TW, Rangarajan S, Shivalia CS, Dadon DB, Jaenisch R (2013) Multiplexed activation of endogenous genes by CRISPR-on, an RNA-guided transcriptional activator system. Cell Res **23:** 1163–1171

Chia T, Thorneycroft D, Chapple A, Messerli G, Chen J, Zeeman SC, Smith SM, Smith AM (2004) A cytosolic glucosyltransferase is required for conversion of starch to sucrose in *Arabidopsis* leaves at night. Plant J **37**: 853–863

Chincinska IA, Miklaszewska M, Sołtys-Kalina D (2023) Recent advances and challenges in potato improvement using CRISPR/Cas genome editing. Planta **257**: 1–27

Cho MH, Lim H, Shin DH, Jeon JS, Bhoo SH, Park YI, Hahn TR (2011) Role of the plastidic glucose translocator in the export of starch degradation products from the chloroplasts in *Arabidopsis thaliana*. New Phytol **190**: 101–112

Chylinski K, Le Rhun A, Charpentier E (2013) The tracrRNA and Cas9 families of type II CRISPR-Cas immunity systems. RNA Biol **10:** 726–737

Critchley JH, Zeeman SC, Takaha T, Smith AM, Smith SM (2001) A critical role for disproportionating enzyme in starch breakdown is revealed by a knock-out mutation in *Arabidopsis*. Plant J **26**: 89–100

Crumpton-Taylor M, Pike M, Lu KJ, Hylton CM, Feil R, Eicke S, Lunn JE, Zeeman SC, Smith AM (2013) Starch synthase 4 is essential for coordination of starch granule formation with chloroplast division during *Arabidopsis* leaf expansion. New Phytol **200**: 1064–1075

Csörgő B, León LM, Chau-Ly II, Vasquez-Rifo A, Berry JD, Mahendra C, Crawford ED, Lewis JD, Bondy- Denomy J (2020) A compact cascade-Cas3 system for targeted genome engineering. Nat Methods **17:** 1183–1190

Current world population (2019) *Worldometer*. https://www.worldometers.info/world-population

Daboussi F, Stoddard TJ, Zhang F (2015) Engineering meganucleases for precise plant genome modification. Advances in new technology for targeted modification of plant genomes. Springer New York: 21–38

Department of Agriculture, Forestry and Fisheries DAFF (2019) A Profile of the South African Potato Market Value Chain. Department of Agriculture, Forestry and Fisheries. http://webapps.daff.gov.za/AmisAdmin/upload/Potato%20Market%20Value%20Chain%20Profile%202019.pdf

Deltcheva E, Chylinski K, Sharma CM, Gonzales K, Chao Y, Pirzada ZA, Eckert MR, Vogel J, Charpentier E (2011) CRISPR RNA maturation by trans-encoded small RNA and host factor RNase III. Nature **471**: 602–607

Deveau H, Barrangou R, Garneau JE, Labonté J, Fremaux C, Boyaval P, Romero DA, Horvath P, Moineau S (2008) Phage response to CRISPR-encoded resistance in *Streptococcus thermophilus*. J Bacteriol **190**: 1390–1400

Devaux A, Goffart JP, Petsakos A, Kromann P, Gatto M, Okello J, Suarez V, Hareau G (2019) Global food security, contributions from sustainable potato agri-food systems. Campos H, Ortiz O, The Potato Crop: Its Agricultural, Nutritional and Social Contribution to Humankind. Springer **1**: 3–35

Dhugga KS (2022) Gene editing to accelerate crop breeding. Front Plant Sci **13:** 1–6

Dreissig S, Schiml S, Schindele P, Weiss O, Rutten T, Schubert V, Gladilin E, Mette MF, Puchta H, Houben A (2017) Live-cell CRISPR imaging in plants reveals dynamic telomere movements. Plant J **91**: 565–573

Edner C, Li J, Albrecht T, Mahlow S, Hejazi M, Hussain H, Kaplan F, Guy C, Smith SM, Steup M, Ritte G (2007) Glucan, water dikinase activity stimulates breakdown of starch granules by plastidial β-amylases. Plant Physiol **145**: 17–28.

Edwards D, Batley J (2010) Plant genome sequencing: Applications for crop improvement. Plant Biotechnol J **8**: 2–9

Eeckhaut T, Lakshmanan PS, Deryckere D, Van Bockstaele E, Van Huylenbroeck J (2013) Progress in plant protoplast research. Planta **238:** 991–1003

Ellis RP, Cochrane MP, Dale MFB, Duþus CM, Lynn A, Morrison IM, Prentice RDM, Swanston JS, Tiller SA (1998) Starch production and industrial use. J Sci Food Agric **77**: 289–311

Ewing EE, Senesac AH, Sieczka JB (1981) Effects of short periods of chilling and warming on potato sugar content and chipping quality. Am Potato J **58**: 633– 647.

Farming Potatoes in South Africa: What You Need to Know – RegenZ. https://regenz.co.za/resources/farming-potatoes-in-south-africa

Fasoula DA (2002) The effects of clonal propagation on the genetic improvement of potato. Acta Hort **579:** 71–75

Faure G, Shmakov SA, Makarova KS, Wolf YI, Crawley AB, Barrangou R, Koonin E (2019) Comparative genomics and evolution of trans-activating RNAs in Class 2 CRISPR-Cas systems. RNA Biol **16**: 435–448

Ferreira S, Sonnewald S, Senning M (2010) Comparative transcriptome analysis coupled to X-ray CT reveals sucrose supply and growth velocity as major determinants of potato tuber starch biosynthesis. BMC Genomics **11**: 93

Fonfara I, Le Rhun A, Chylinski K, Makarova KS, Lecrivain AL, Bzdrenga J, Koonin EV, Charpentier E (2014) Phylogeny of Cas9 determines functional exchangeability of dual-RNA and Cas9 among orthologous type II CRISPR-Cas systems. Nucleic Acids Res **42:** 2577–2590

Fossi M, Amundson K, Kuppu S, Britt A, Comai L (2019) Regeneration of *Solanum tuberosum* plants from protoplasts induces widespread genome instability. Plant Physiol **180:** 78–86

Fulton DC, Stettler M, Mettler T, Vaughan CK, Li J, Francisco P, Gil M, Reinhold H, Eicke S, Messerli G, Dorken G, Halliday K, Smith AM, Smith SM, Zeeman SC (2008) β-AMYLASE4, a noncatalytic protein required for starch breakdown, acts upstream of three active beta-amylases in *Arabidopsis* chloroplasts. Plant Cell **20**: 1040–1058

Gaudelli NM, Komor AC, Rees HA, Packer MS, Badran AH, Bryson DI, Liu DR (2017) Programmable base editing of A*T to G*C in genomic DNA without DNA cleavage. Nature **551**: 464–471

Gebre M, Nomburg JL, Gewurz BE (2018) CRISPR-Cas9 genetic analysis of virus-host interactions. Viruses **10**: 55

Gelvin SB (2003) *Agrobacterium*-mediated plant transformation: the biology behind the "gene-jockeying" tool. Microbiol Mol Biol Rev **67**: 16–37

Gelvin SB (2017) Integration of *Agrobacterium* T-DNA into the plant genome. Annu Rev Genet **51**: 195–217

George GM, Bauer R, Blennow A, Kossmann J, Lloyd JR (2012) Virus-induced multiple gene silencing to study redundant metabolic pathways in plants: Silencing the starch degradation pathway in *Nicotiana benthamiana*. Biotechnol J **7**: 884–890

Gilbert LA, Larson MH, Morsut L, Liu Z, Brar GA, Torres SE, Stern-Ginossar N, Brandman O, Whitehead EH, Doudna JA, Lim WA, Weissman JS, Qi LS (2013) CRISPR-mediated modular RNA-guided regulation of transcription in eukaryotes. Cell **154:** 442–451

Glaring MA, Zygadło A, Thorneycroft D, Schulz A, Smith SM, Blennow A, Baunsgaard L (2007) An extra-plastidal α-glucan, water dikinase from *Arabidopsis* phosphorylates amylopectin *in vitro* and is not necessary for transient starch degradation. J Exp Bot **58**: 3949–3960

Gleditzsch D, Pausch P, Müller-Esparza H, Özcan A, Guo X, Bange G, Randau L (2019) PAM identification by CRISPR-Cas effector complexes: diversified mechanisms and structures. RNA Biol **16**: 504–517

González MN, Massa GA, Andersson M, Turesson H, Olsson N, Fält AS, Storani L, Décima Oneto CA, Hofvander P, Feingold SE (2020) Reduced enzymatic browning in potato tubers by specific editing of a polyphenol oxidase gene via ribonucleoprotein complexes delivery of the CRISPR/Cas9 system. Front Plant Sci **10**: 1–12

Górska-Warsewicz H, Rejman K, Kaczorowska J, Laskowski W (2021) Vegetables, potatoes and their products as sources of energy and nutrients to the average diet in Poland. Int J Environ Res **18**: 3217

Grzebelus E, Skop L (2014) Effect of β-lactam antibiotics on plant regeneration in carrot protoplast cultures. In Vitro Cell Dev Biol **50:** 568–575

Guo Y, Xu Q, Canzio D, Shou J, Li J, Gorkin DU, Jung I, Wu H, Zhai Y, Tang Y, Lu Y, Wu Y, Jia Z, Li W, Zhang MQ, Ren B, Krainer AR, Maniatis T, Wu Q (2015) CRISPR inversion of CTCF sites alters genome topology and enhancer/promoter function. Cell **162**: 900–910

Gurrieri L, Merico M, Trost P, Forlani G, Sparla F (2020) Impact of drought on soluble sugars and free proline content in selected *Arabidopsis* mutants. Biology **9**: 1–14

Hale CR, Zhao P, Olson S, Duff MO, Graveley BR, Wells L, Terns RM, Terns MP (2009) RNA-guided RNA cleavage by a CRISPR RNA-Cas protein complex. Cell **139**: 945–956

Halterman D, Guenthner J, Collinge S, Butler N, Douches D (2016) Biotech potatoes in the 21st century: 20 years since the first biotech potato. Am J Potato Res **93**: 1–20

Hameed A, Zaidi SS, Shakir S, Mansoor S (2018) Applications of new breeding technologies for potato improvement. Front Plant Sci **9**: 1–15

Hardigan MA, Laimbeer FPE, Newton L, Crisovan E, Hamilton JP, Vaillancourt B, Wiegert-Rininger K, Wood JC, Douches DS, Farré EM, Veilleux RE, Buell CR (2017) Genome diversity of tuber-bearing *Solanum* uncovers complex evolutionary history and targets of domestication in the cultivated potato. Proc Natl Acad Sci **114**: E9999–E10008

Hejazi M, Fettke J, Haebel S, Edner C, Paris O, Frohberg C, Steup M, Ritte G (2008) Glucan, water dikinase phosphorylates crystalline maltodextrins and thereby initiates solubilization. Plant J **55**: 323–334

Herman EB (2017) Plant tissue culture contamination: challenges and opportunities. Acta Hortic **1155:** 33

Hille F, Charpentier E (2016) CRISPR-Cas: biology, mechanisms and relevance. Philos Trans R Soc Lond B Biol Sci **371**: 1–12

Hilton IB, D'Ippolito AM, Vockley CM, Thakore PI, Crawford GE, Reddy TE, Gersbach CA (2015) Epigenome editing by a CRISPR-Cas9-based acetyltransferase activates genes from promoters and enhancers. Nat Biotechnol **33**: 510–517

Horvath P, Romero DA, Coûté-Monvoisin AC, Richards M, Deveau H, Moineau S, Boyaval P, Fremaux C, Barrangou R (2008) Diversity, activity, and evolution of CRISPR loci in *Streptococcus thermophilus*. J Bacteriol **190**: 1401–1412

Hou J, Zhang H, Liu J, Reid S, Liu T, Xu S, Tian Z, Sonnewald U, Song B, Xie C (2017) Amylases StAmy23, StBAM1 and StBAM9 regulate cold-induced sweetening of potato tubers in distinct ways. J Exp Bot **68**: 2317–2331

Hwang HH, Yu M, Lai EM (2017) *Agrobacterium*-mediated plant transformation: biology and applications. Arabidopsis Book **15**: e0186

Ikeuchi M, Sugimoto K, Iwase A (2013) Plant callus: mechanisms of induction and repression. Plant Cell **25**: 3159–3173

Jinek M, Chylinski K, Fonfara I, Hauer M, Doudna JA, Charpentier E (2012) A programmable dual RNA-guided DNA endonuclease in adaptive bacterial immunity. Science **17**: 816–821

Jore MM, Brouns SJJ, van der Oost J (2012) RNA in defense: CRISPRs protect prokaryotes against mobile genetic elements. Cold Spring Harb Perspect **4**: 1–12

Kapuya T, Sihlobo W (2015) South Africa's commercial and seed potato exports: identifying potential market opportunities in Africa. Agriculture Business Chamber https://agbiz.co.za/uploads/AgbizNews/15101Potato.pdf

Kaya H, Numa H, Nishizawa-Yokoi A, Toki S, Habu Y (2017) DNA methylation affects the efficiency of transcription activator-like effector nucleases-mediated genome editing in rice. Front Plant Sci **8**: 302

Kielkowska A, Adamus A (2012) Peptide growth factor phytosulfokine-α stimulates cell divisions and enhances regeneration from *B. oleracea* var. *capitata* L. protoplast culture. J Plant Growth Regul **38:** 931–944

Kim H, Kim ST, Ryu J, Kang BC, Kim JS, Kim SG (2017a) CRISPR/Cpf1-mediated DNA-free plant genome editing. Nat Commun **8**: 14406

Kim YB, Komor AC, Levy JM, Packer MS, Zhao KT, Liu DR (2017b) Increasing the genome-targeting scope and precision of base editing with engineered Cas9-cytidine deaminase fusions. Nature Biotechnol **35:** 371–377

Ellen Messer (2008) The Cambridge world history of food. Cambridge University Press **85: 187-201**

Knott GJ, Doudna JA (2018) CRISPR-Cas guides the future of genetic engineering. Science **361**: 866–869

Kolesnik MV, Fedorova I, Karneyeva KA, Artamonova DN, Severinov KV (2021) Type III CRISPR-Cas systems: deciphering the most complex prokaryotic immune system. Biochemistry **86**: 1301–1314

Komor AC, Kim YB, Packer MS, Zuris JA, Liu DR (2016) Programmable editing of a target base in genomic DNA without double-stranded DNA cleavage. Nature **533:** 420–424

Koroteeva DA, Kiseleva VI, Krivandin AV, Shatalova OV, Błaszczak W, Bertoft E, Piyachomkwan K, Yuryev VP (2007) Structural and thermodynamic properties of rice starches with different genetic background. Part 2. Defectiveness of different supramolecular structures in starch granules. Int J Biol Macromol **41**: 534–547

Kötting O, Pusch K, Tiessen A, Geigenberger P, Steup M, Ritte G (2005) Identification of a novel enzyme required for starch metabolism in *Arabidopsis* leaves. The phosphoglucan, water dikinase. Plant Physiol **137**: 242–252

Kötting O, Santelia D, Edner C, Eicke S, Marthaler T, Gentry MS, Comparot-Moss S, Chen J, Smith AM, Steup M, Ritte G, Zeeman SC (2009) STARCH-EXCESS4 is a laforin-like Phosphoglucan phosphatase required for starch degradation in *Arabidopsis thaliana*. Plant Cell **21**: 334–346

Kozlov SS, Blennow A, Krivandin AV, Yuryev VP (2007) Structural and thermodynamic properties of starches extracted from GBSS and GWD suppressed potato lines. Int J Biol Macromol **40**: 449–460

Krishna H, Alizadeh M, Singh D, Singh U, Chauhan N, Eftekhari M, Sadh RK (2016) Somaclonal variations and their applications in horticultural crops improvement. 3 Biotech **6**: 1–18

Kyriakidou M, Anglin NL, Ellis D, Tai HH, Stomvik MV (2020) Genome assembly of six polyploid potato genomes. Nature Sci Data **7**: 88

Lau CH, Zhu H, Tay JC, Li Z, Tay FC, Chen C, Tan WK, Du S, Sia VK, Phang RZ, Tang SY, Yang C, Chi Z, Liang CC, Ning E, Wang S (2014) Genetic rearrangements of variable di-residue (RVD)-containing repeat arrays in a baculoviral TALEN system. Mol Ther Methods Clin Dev **1**: 14050

Li Z, Zhang D, Xiong X, Yan B, Xie W, Sheen J, Li JF (2017) A potent Cas9-derived gene activator for plant and mammalian cells. Nat Plants **3**: 930

Liang Z, Chen K, Zhang Y, Liu J, Yin K, Qiu JL, Gao C (2018) Genome editing of bread wheat using biolistic delivery of CRISPR/Cas9 *in vitro* transcripts or ribonucleoproteins. Nat Prot **13:** 413–430

Lin S, Staahl BT, Alla RK, Doudna JA (2014) Enhanced homology-directed human genome engineering by controlled timing of CRISPR/Cas9 delivery. ELife **3**: 1–13

Lin CS, Hsu CT, Yang LH, Lee LY, Fu JY, Cheng QW, Wu FH, Hsiao HCW, Zhang Y, Zhang R, Chang WJ, Yu CT, Wang W, Liao LJ, Gelvin SB, Shih MC (2018) Application of protoplast technology to CRISPR/Cas9 mutagenesis: from single-cell mutation detection to mutant plant regeneration. Plant Biotechnol J **16**: 1295–1310

Lindhout P, Meijer D, Schotte T, Hutten RCB, Visser RGF, van Eck HJ (2011) Towards F1 hybrid seed potato breeding. Potato Res **54**: 301–312

Lloyd JR, Blennow A, Burhenne K, Kossmann J (2004) Repression of a novel isoform of disproportionating enzyme (stDPE2) in potato leads to inhibition of starch degradation in leaves but not tubers stored at low temperature. Plant Physiol **134**: 1347–1354

Lloyd JR, Kossmann J (2015) Transitory and storage starch metabolism: Two sides of the same coin? Curr Opin Biotechnol **32**: 143–148

Lorberth R, Ritte G, Willmitzer L, Kossmann J (1998) Inhibition of a starch-granule-bound protein leads to modified starch and repression of cold sweetening. Nat Biotechnol **16**: 473–477

Lowder LG, Zhou J, Zhang Y, Malzahn A, Zhong Z, Hsieh TF, Voytas DF, Zhang Y, Qi Y (2017a) Robust transcriptional activation in plants using multiplexed CRISPR-Act2.0 and mTALE-Act systems. Mol Plant **11**: 245–256

Lowder LG, Paul JW, Qi Y (2017b) Multiplexed transcriptional activation or repression in plants using CRISPR-dCas9-based systems. Plant Gene Regulatory Networks, Methods Mol Biol **1629**: 167–184

Luo Y, Ge M, Wang B, Sun C, Wang J, Dong Y, Xi JJ (2020) CRISPR/Cas9-deaminase enables robust base editing in *Rhodobacter sphaeroides* 2.4.1. Microb Cell Factories **19**: 1–14

Lütken H, Lloyd JR, Glaring MA, Baunsgaard L, Laursen KH, Haldrup A, Kossmann J, Blennow A (2010) Repression of both isoforms of disproportionating enzyme leads to higher malto-oligosaccharide content and reduced growth in potato. Planta **232**: 1127–1139

Machakaire ATB, Steyn JM, Franke AC (2021) Assessing evapotranspiration and crop coefficients of potato in a semi-arid climate using Eddy Covariance techniques. Agric Water Manag **255**: 1–11

Machida-Hirano R (2015) Diversity of potato genetic resources. Breed Sci **65**:26–40

Mahlow S, Hejazi M, Kuhnert F, Garz A, Brust H, Baumann O, Fettke J (2014) Phosphorylation of transitory starch by α-glucan, water dikinase during starch turnover affects the surface properties and morphology of starch granules. New Phytol **203**: 495–507

Makarova KS, Haft DH, Barrangou R, Brouns SJ, Charpentier E, Horvath P, Moineau S, Mojica FJ, Wolf YI, Yakunin AF, van der Oost J, Koonin EV (2011) Evolution and classification of the CRISPR-Cas systems. Nat Rev Microbiol **9**: 467–477

Makarova KS, Koonin EV (2015) Annotation and classification of CRISPR-Cas systems. Methods Mol Biol **1311**: 47–75

Makroo HA, Naqash S, Saxena J, Sharma S, Majid D, Dar BN (2021) Recovery and characteristics of starches from unconventional sources and their potential applications: a review. Appl Food Res **1**: 1–9

Martínez-Prada M, Curtin SJ, Gutiérrez-González JJ (2021) Potato improvement through genetic engineering. GM Crops and Food **12**: 479–496

Martínez-Fortún J, Phillips DW, Jones HD (2022) Natural and artificial sources of genetic variation used in crop breeding: a baseline comparator for genome editing. Front Genome Ed **4**: 1–18

Mdodana NT, Jewell JF, Phiri EE, Smith ML, Oberlander K, Mahmoodi S, Kossmann J, Lloyd JR (2019) Mutations in Glucan, Water Dikinase Affect Starch Degradation and Gametophore Development in the Moss *Physcomitrella patens*. Sci Rep **9**: 15114

Mikkelsen R, Baunsgaard L, Blennow A (2004) Functional characterization of α-glucan,water dikinase, the starch phosphorylating enzyme. Biochem J **377**: 525–532

Mikkelsen R, Mutenda KE, Mant A, Schürmann P, Blennow A (2005) Glucan, water dikinase (GWD): A plastidic enzyme with redox-regulated and coordinated catalytic activity and binding affinity. Proc Natl Acad Sci **102**: 1785–1790

Mikkelsen R, Blennow A (2005) Functional domain organization of the potato α-glucan, water dikinase (GWD): evidence for separate site catalysis as revealed by limited proteolysis and deletion mutants. Biochem J **385**: 355–361

Mosterd C, Rousseau GM, Moineau S (2021) A short overview of the CRISPR-Cas adaptation stage. Can J Microbiol **67**: 1–12

Mottram DS, Wedzicha BL, Dodson AT (2002) Acrylamide is formed in the Maillard reaction. Nature **419**: 448–449

Muthoni J, Kabira J, Shimelis H, Melis R (2015) Tetrasomic inheritance in cultivated potato and implications in conventional breeding. Aust J Crop Sci **9**: 185–190

Nadakuduti SS, Buell CR, Voytas DF, Starker CG, Douches DS (2018) Genome editing for crop improvement – applications in clonally propagated polyploids with a focus on potato (*Solanum tuberosum* L.). Front Plant Sci **871**: 1-11

Nakamura T, Yamamori M, Hirano H, Hidaka S, Nagamine T (1995) Production of waxy (amylose-free) wheats. Mol Genet Genom **248**: 253–259

Nardozza S, Boldingh HL, Osorio S, Höhne M, Wohlers M, Gleave AP, MacRae EA, Richardson AC, Atkinson RG, Sulpice R, Fernie AR, Clearwater MJ (2013) Metabolic analysis of kiwifruit (*Actinidia deliciosa*) berries from extreme genotypes reveals hallmarks for fruit starch metabolism. J Exp Bot **64**: 5049–5063

Nashilevitz S, Melamed-Bessudo C, Aharoni A, Kossmann J, Wolf S, Levy AA (2009) The *Legwd* mutant uncovers the role of starch phosphorylation in pollen development and germination in tomato. Plant J **57**: 1–13

Nicolia A, Proux-Wéra E, Åhman I, Onkokesung N, Andersson M, Andreasson E, Zhu L (2015) Targeted gene mutation in tetraploid potato through transient TALEN expression in protoplasts. J Biotechnol **204:** 17–24

Niittylä T, Messerli G, Trevisan M, Chen J, Smith AM, Zeeman SC (2004) A previously unknown maltose transporter essential for starch degradation in leaves. Science **303**: 87–89

Ortiz O, Mares V. (2017) The historical, social, and economic importance of the potato crop. The Potato Genome. Compendium of Plant Genomes. Springer **1**: 1–10

Paparelli E, Parlanti S, Gonzali S, Novi G, Mariotti L, Ceccarelli N, van Dongen JT, Kölling K, Zeeman SC, Perata P (2013) Night time sugar starvation orchestrates gibberellin biosynthesis and plant growth in *Arabidopsis*. Plant Cell **25**: 3760–3769

Patron NJ, Smith AM, Fahy BF, Hylton CM, Naldrett MJ, Rossnagel BG, Denyer K (2002) The altered pattern of amylose accumulation in the endosperm of low-amylose barley cultivars is attributable to a single mutant allele of granule-bound starch synthase I with a deletion in the 5'-non-coding region. Plant Physiol **130**: 190–198

Pfister B, Zeeman SC (2016) Formation of starch in plant cells. Cell Mol Life Sc **73**: 2781–2807

Pirone C, Gurrieri L, Gaiba I, Adamiano A, Valle F, Trost P, Sparla F (2017) The analysis of the different functions of starch-phosphorylating enzymes during the development of *Arabidopsis thaliana* plants discloses an unexpected role for the cytosolic isoform GWD2. Physiol Plant **160**: 447–457

Pitrat and Michel (2003) Histoires de legumes; des origines à l'orée du XXI . INRA 167 ISBN 978-2759223558

Pollock CJ, Rees T (1975) Cold-induced sweetening of tissue cultures of *Solanum tuberosum* L. Planta **122;** 105–107

Potatoes South Africa, home page – PSA (2021) https://www.potatoes.co.za/wp-content/uploads/2021/06/STATE-OF-THE-POTATO-INDUSTRY-ADDRESS-SOPIA-REPORT-2021-2.pdf

Rabara RC, Tripathi P, Reese RN, Rushton DL, Alexander D, Timko MP, Shen QJ, Rushton PJ (2015) Tobacco drought stress responses reveal new targets for Solanaceae crop improvement. BMC Genomics **16**: 484

Ral JP, Bowerman AF, Li Z, Sirault X, Furbank R, Pritchard JR, Bloemsma M, Cavanagh CR, Howitt CA, Morell MK (2012) Down-regulation of glucan, water-dikinase activity in wheat endosperm increases vegetative biomass and yield. Plant Biotechnol J **10**: 871–882

Raldugina GN, Hoang TZ, Ngoc HB, Karpichev IV (2021) An increased proportion of transgenic plants in the progeny of rapeseed (*Brassica napus* L.) transformants. Vavilovskii Zhurnal Genet Selektsii **25**: 147–156

Rath D, Amlinger L, Rath A, Lundgren M (2015) The CRISPR-Cas immune system: biology, mechanisms and applications. Biochimie **117**: 119–128

Rather GA, Ayzenshtat D, Teper-Bamnolker P, Kumar M, Forotan Z, Eshel D, Bocobza S (2022) Advances in protoplast transfection promote efficient CRISPR/Cas9-mediated genome editing in tetraploid potato. Planta **256**: 1–17

Reed KM, Bargmann BOR (2021) Protoplast regeneration and its use in new plant breeding technologies. Front Genome Ed **3**: 1–26

Richter C, Gristwood T, Clulow JS, Fineran PC (2012) *In vivo* protein interactions and complex formation in the *Pectobacterium* atro-septicum subtype I-F CRISPR/Cas System. PLoS One **7:** e49549

Ritte G, Lorberth R, Steup M (2000) Reversible binding of the starch-related R1 protein to the surface of transitory starch granules. Plant J **21**: 387–391

Ritte G, Lloyd JR, Eckermann N, Rottmann A, Kossmann J, Steup M (2002) The starch-related R1 protein is an alpha-glucan, water dikinase. Proc Natl Acad Sci USA **99**: 7166–7171

Ritte G, Scharf A, Eckermann N, Haebel S, Steup M (2004) Phosphorylation of transitory starch is increased during degradation. Plant Physiol **135**: 2068–2077

Ritte G, Heydenreich M, Mahlow S, Haebel S, Kötting O, Steup M (2006) Phosphorylation of C6- and C3-positions of glucosyl residues in starch is catalysed by distinct dikinases. FEBS Lett **580**: 4872–4876

Rodgers K, Mcvey M (2016) Error-prone repair of dna double-strand breaks. J Cell Physiol **231**: 15–24

Sahab S, Hayden MJ, Mason J, Spangenberg G (2019) Mesophyll protoplasts and PEG-mediated transfections: Transient assays and generation of stale transgenic canola plants. Methods Mol Biol **1864**: 131–152

Samodien E, Jewell JF, Loedolff B, Oberlander K, George GM, Zeeman SC, Damberger FF, van der Vyver C, Kossmann J, Lloyd JR (2018) Repression of *Sex4* and *Like Sex Four2* orthologs in potato increases tuber starch bound phosphate with concomitant alterations in starch physical properties. Front Plant Sci **9**: 1044

Sapranauskas R, Gasiunas G, Fremaux C, Barrangou R, Horvath P, Siksnys V (2011) The *Streptococcus thermophilus* CRISPR/Cas system provides immunity in *Escherichia coli*. Nucleic Acids Res **39**: 9275–9282

Schippers PA (1975) The influence of storage conditions on chip colour of potatoes. Potato Res **18**: 479–494

Schaart JG, van de Wiel CCM, Lotz LAP, Smulders MJM (2015) Opportunities for products of new plant breeding techniques. Trends Plant Sci **21:** 438–449

Sergeeva LI, Claassens MMJ, Jamar DCL, van der Plas LHW, Vreugdenhil D (2012) Starch-related enzymes during potato tuber dormancy and sprouting. Russ J Plant Physiol **59**: 556–564

Sergeeva EM, Larichev KT, Salina EA, Kochetov AV (2022) Starch metabolism in potato *Solanum tuberosum* L. Vavilovskii Zhurnal Genetiki i Selektsii **26**: 250–263

Seung D, Soyk S, Coiro M, Maier BA, Eicke S, Zeeman SC (2015) Protein targeting to starch is required for localising granule-bound starch synthase to starch granules and for normal amylose synthesis in *Arabidopsis*. PLoS Biology **13**: 1–29

Seung D (2020) Amylose in starch: towards an understanding of biosynthesis, structure and function. New Phytol **228**: 1490–1504

Sevestre F, Facon M, Wattebled F, Szydlowski N (2020) Facilitating gene editing in potato: a single- nucleotide polymorphism (SNP) map of the *Solanum tuberosum* L. cv. Desiree genome. Sci Rep **10:** 2045

Shalem O, Sanjana NE, Hartenian E, Shi X, Scott DA, Mikkelsen TS, Heckl D, Ebert BL, Root DE, Doench JG, Zhang F (2014) Genome-scale CRISPR-Cas9 knockout screening in human cells. Science **343**: 84–87

Skeffington AW, Graf A, Duxbury Z, Gruissem W, Smith AM (2014) Glucan, water dikinase exerts little control over starch degradation *in Arabidopsis* leaves at night. Plant Physiol **165**: 866–879

Song M, Kim YH, Kim JS, Kim H (2014) Genome engineering in human cells. Meth Enzymol **546**: 93–118

Sonnewald U, Kossmann J (2013) Starches-from current models to genetic engineering. Plant Biotechnol J **11**: 223–232

Spooner DM, McLean K, Ramsay G, Waugh R, Bryan GJ (2005) A single domestication for potato based on multilocus amplified fragment length polymorphism genotyping. Proc Natl Acad Sci USA **102**: 14694–14699

Staals RH, Agari Y, Maki-Yonekura S, Zhu Y, Taylor DW, van Duijn E, Barendregt A, Vlot M, Koehorst JJ, Sakamoto K, Masuda A, Dohmae N, Schaap PJ, Doudna JA, Heck AJ,

Yonekura K, van der Oost J, Shinkai A (2013) Structure and activity of the RNA-targeting Type III-B CRISPR-Cas complex of *Thermus thermophilus*. Mol Cell **52:** 135–145

Stadler RH, Blank I, Varga N, Robert F, Hau J, Guy PA, Robert MC, Riediker S (2002) Acrylamide from Maillard reaction products. Nature **419**: 449–450

Stettler M, Eicke S, Mettler T, Messerli G, Hörtensteiner S, Zeeman SC (2009) Blocking the metabolism of starch breakdown products in *Arabidopsis* leaves triggers chloroplast degradation. Mol Plant **2**: 1233–1246

Stitt M, Zeeman SC (2012) Starch turnover: pathways, regulation and role in growth. Curr Opin Plant Biol **15**: 282–292

Stoddard BL (2014) Homing endonucleases from mobile group I introns: Discovery to genome engineering. Mobile DNA **5**: 1–16

Streb S, Eicke S, Zeeman SC (2012) The simultaneous abolition of three starch hydrolases blocks transient starch breakdown in *Arabidopsis*. J Biol Chem **287**: 41745–41756

Streb S, Zeeman SC (2012) Starch metabolism in *Arabidopsis*. Arabidopsis Book **10**: e0160

Sun H, Jiao WB, Krause K, Campoy JA, Goel M, Folz-Donahue K, Kukat C, Huettel B, Schneeberger K (2022) Chromosome-scale and haplotype-resolved genome assembly of a tetraploid potato cultivar. Nat Genet **54**: 342–348

Svitashev S, Young JK, Schwartz C, Gao H, Falco SC, Cigan AM (2015) Targeted mutagenesis, precise gene editing, and site-specific gene insertion in maize using Cas9 and guide RNA. Plant Physiol **169**: 931–945

Svitashev S, Schwartz C, Lenderts B, Young JK, Cigan AM (2016) Genome editing in maize directed by CRISPR-Cas9 ribonucleoprotein complexes. Nat Commun **7**: 13274

Szydlowski N, Ragel P, Raynaud S, Mercedes Lucas M, Roldán I, Montero M, Muñoz FJ, Ovecka M, Bahaji A, Planchot V, Romero JP, D'Hulst C, Mérida Á (2009) Starch granule initiation in *Arabidopsis* requires the presence of either class IV or class III starch synthases. Plant Cell **21**: 2443–2457

Tabata S, Nagata K, Hizukuri S (1975) Studies on Starch Phosphates.3. Esterified Phosphates in Some Cereal Starches. Starke **27**: 333–335

Takeda Y, Hizukuri S (1982) Location of phosphate groups in potato amylopectin. Carbohydr Res **102**: 321–327

Tanenbaum ME, Gilbert LA, Qi LS, Weissman JS, Vale RD (2014) A protein-tagging system for signal amplification in gene expression and fluorescence imaging. Cell **159:** 635–646

Tang XD, Gao F, Liu MJ, Fan QL, Chen DK, Ma WT (2019) Methods for enhancing clustered regularly interspaced short palindromic repeats/Cas9-mediated homology-directed repair efficiency. Front Genet **10**: 1–9

Tavazza R, Ancora G (1986) Plant regeneration from mesophyll protoplasts in commercial potato cultivars (Primura, Kennebec, Spunta, Desirée). Plant Cell Rep **5:** 243–246

Terns MP, Terns RN (2011) CRISPR-based adaptive immune systems. Curr Opin Microbiol **14**: 321–327

Tetlow IJ, Emes, MJ (2011) Starch biosynthesis in higher plants: the enzymes of starch synthesis. Murray M-Y, editor: Comprehensive Biotechnology, Second Edition, Elsevier **4**: 47–65

Tetlow IJ, Emes MJ (2014) A review of starch-branching enzymes and their role in amylopectin biosynthesis. IUBMB Life **66**: 546–558

Thuynsma R, Kleinert A, Kossmann J, Valentine AJ, Hills PN (2016) The effects of limiting phosphate on photosynthesis and growth of *Lotus japonicus*. S Afr J Bot **104**: 244–248

Uitdewilligen JGAML, Wolters AMA, van Eck HJ, Visser RGF (2022) Allelic variation for alpha-Glucan Water Dikinase is associated with starch phosphate content in tetraploid potato. Plant Mol Biol **108**: 469-480

Urnov FD, Rebar EJ, Holmes MC, Zhang HS, Gregory PD (2010) Genome editing with engineered zinc finger nucleases. Nat Rev **11:** 636–646

Van Harsselaar JK, Lorenz J, Senning M, Sonnewald U, Sonnewald S (2017) Genome-wide analysis of starch metabolism genes in potato (*Solanum tuberosum* L.). BMC Genomics **18**: 1–18

Van Lieshout N, van der Burgt A, de Vries ME, ter Maat M, Eickholt D, Esselink D, van Kaauwen MP W, Kodde LP, Visser RGF, Lindhout P, Finkers R (2020) Solyntus, the new highly contiguous reference genome for potato (*Solanum tuberosum*). G3 – Genes Genom Genet **10**: 3489–3495

Varshney RK, Nayak SN, May GD, Jackson SA (2009) Next-generation sequencing technologies and their implications for crop genetics and breeding. Trends Biotechnol **27**: 522–530

Viksø-Nielsen A, Blennow A, Hamborg Nielsen T, Lindberg Moller B (1998) Phosphorylated alpha (1→4) glucans as substrate for potato starch-branching enzyme I. Plant Physiol **117**: 869-875

Viksø-Nielsen A, Blennow A, Jørgensen K, Kristensen KH, Jensen A, Møller BL (2001) Structural, physicochemical, and pasting properties of starches from potato plants with repressed r1-gene. Biomacromolecules **2**: 836–843

Visser RGF, Bachem CWB, Borm T, de Boer J, van Eck HJ, Finkers R, van der Linden G, Maliepaard CA, Uitdewilligen JGAML, Voorrips R, Vos P, Wolters AMA (2014) Possibilities and challenges of the potato genome sequence. Potato Res **57**: 327–330

Vriet C, Welham T, Brachmann A, Pike M, Pike J, Perry J, Parniske M, Sato S, Tabata S, Smith AM, Wang TL (2010) A suite of *Lotus japonicus* starch mutants reveals both conserved and novel features of starch metabolism. Plant Physiol **154**: 643–55

Wada N, Osakabe K, Oskabe Y (2022) Expanding the plant genome editing toolbox with recently developed CRISPR–Cas systems. Plant Phys **188:** 1825–1837

Wang W, Hostettler CE, Damberger FF, Kossmann J, Lloyd JR, Zeeman SC (2018) Modification of cassava root starch phosphorylation enhances starch functional properties. Front Plant Sci **871**: 1–16

Wang Z, Wei K, Xiong M, Wang JD, Zhang CQ, Fan XL, Huang LC, Zhao DS, Liu QQ, Li QF (2021) Glucan, Water-Dikinase 1 (GWD1), an ideal biotechnological target for potential improving yield and quality in rice. Plant Biotechnol J **19**: 2606–2618

Watanabe K (2015). Potato genetics, genomics, and applications. Breed Sci **65**: 53–68

Woo JW, Kim J, Kwon SI, Corvalán C, Cho SW, Kim H, Kim SG, Kim ST, Choe S, Kim JS (2015) DNA-free genome editing in plants with preassembled CRISPR-Cas9 ribonucleoproteins. Nat Biotechnol **33:** 1162–1165

Wu L, Bhaskar PB, Busse JS, Zhang R, Bethke PC, Jiang J (2011) Developing cold-chipping potato varieties by silencing the vacuolar invertase gene. Crop Science **51**: 981–990

Xue Y, Acar M (2018) Live-cell imaging of chromatin condensation dynamics by CRISPR. iScience **4**: 216–235

Yazid MNS, Abdullah N, Muhammad N, Matias-Peralta HM (2018) Application of starch and starch-based products in food industry. J Sci Technol **10**: 144–174

Yu TS, Kofler H, Häusler RE, Hille D, Flügge UI, Zeeman SC, Smith AM, Kossmann J, Lloyd J, Ritte G, Steup M, Lue WL, Chen J, Weber A (2001) The *Arabidopsis sex1* mutant is defective in the R1 protein, a general regulator of starch degradation in plants, and not in the chloroplast hexose transporter. Plant Cell **13**: 1907–1918

Yu S, Price MA, Wang Y, Liu Y, Guo Y, Ni X, Rosser SJ, Bi C, Wang M (2020) CRISPR-dCas9 mediated cytosine deaminase base editing in *Bacillus subtilis*. ACS Synth Biol **9**: 1781–1789

Yue JJ, Yuan JL, Wu FH, Yuan YH, Cheng QW, Hsu CT, Lin CS (2021) Protoplasts: from isolation to CRISPR/Cas genome editing application. Front Genome Ed **3:** 717017

Zeeman SC, Umemoto T, Lue WL, Au-Yeung P, Martin C, Smith AM, Chen J (1998) A mutant of *Arabidopsis* lacking a chloroplastic isoamylase accumulates both starch and phytoglycogen. Plant Cell **10**: 1699–1711

Zeeman SC, Kossmann J, Smith AM (2010) Starch: Its metabolism, evolution, and biotechnological modification in plants. Annu Rev Plant Biol **61**: 209–234

Zezulin A, Musunuru K (2018) Turning up the heat with therapeutic epigenome editing. Cell Stem Cell **22**: 10–11

Zhang Y, Rempel C, Liu Q (2014) Thermoplastic starch processing and characteristics—a review. Crit Rev Food Sci Nutr **54**: 1353–1370

Zhang S, Shen J, Li D, Cheng Y (2020) Strategies in the delivery of Cas9 ribonucleoprotein for CRISPR/Cas9 genome editing. Theranostics **11**: 614–648

Zhang Y, Iaffaldano B, Qi Y (2021) CRISPR ribonucleoprotein-mediated genetic engineering in plants. Plant Commun **2**: 1–13

Zhao J, Fang H, Zhang D (2020) Expanding application of CRISPR-Cas9 system in microorganisms. Synth Syst Biotechnol **5**: 269–276

Zheng N, Li L, Wang X (2020) Molecular mechanisms, off-target activities, and clinical potentials of genome editing systems. Clin Transl Med **10**: 412–426

Zhong Z, Zhang Y,You Q, Tang X, RenQ, Liu S, Yang X, Ren Q, Liu S,Yang L, WangY, ZhengX, Le Y,Zhang Y, Qi Y (2018) Plant genome editing using FnCpf1 and LbCpf1 nucleases at redefined and altered PAM sites. Mol Plant **11:** 999–1002

Zhou W, He S, Naconsie M, Ma Q, Zeeman SC, Gruissem W, Zhang P (2017) Alpha-glucan, water dikinase 1 affects starch metabolism and storage root growth in cassava (*Manihot esculenta* Crantz). Sci Rep **7**: 9863

Zia-ud-Din, Xiong H, Fei P (2017) Physical and chemical modification of starches: A review. Crit Rev Food Sci Nutr **57**: 2691–2705

Chapter 3: Development of protoplast isolation and regeneration for non-transgenic genome editing in *Solanum tuberosum*

3.1 Introduction

Potato (*Solanum tuberosum* L.) is a key non-grain staple food crop grown on a global scale. It is not only used for food and feed, but also as a source of starch for industrial processes (Dolničar, 2021). Numerous studies have focused on introducing desired traits into potato, such as increasing the protein content (Chakraborty et al., 2010), producing resistance to bacterial, fungal and viral infection (Rivero et al., 2012, Hameed et al., 2017), insect pest resistance (Green et al., 2012) and enhanced processing qualities (Bhaskar et al., 2010; Hameed et al., 2018).

Fresh potato qualities are influenced by cultivar-specific visual characteristics, such as eye depth, flesh colour, tuber shape and cooking characteristics. The composition of the tuber has an impact on the eating and aesthetic quality of potato products. For example, starch content affects the texture of cooked products (Andrivon, 2017) while reducing sugar (RS) content directly influences the colour of fried products as they react with free amino acids during the frying process, creating darkly coloured products that are unpleasant and unappealing to customers (Amrein et al., 2003). Reducing sugars such as glucose and fructose occur naturally in potato tubers, but increase during storage at low temperatures (below 6 °C) because under these conditions starch becomes degraded to soluble sugars in a process known as cold induced sweetening (CIS; Müller-Thurgau, 1882).

Starch is a storage polyglucan composed of two distinct molecules, amylose and amylopectin. Both of these are composed of α-1,4 linked glucose chains connected together by α-1,6 branchpoints. They differ based on size and degree of branching with amylopectin being much larger and more highly branched than amylose (Pfister and Zeeman, 2016). The first step in starch degradation is catalysed by glucan, water dikinase 1 (GWD1) and glucan, water dikinase 3 (GWD3; also known as phosphoglucan, water dikinase (PWD)). These enzymes phosphorylate starch, which disrupts double helices formed by glucan chains in amylopectin and allows access to amylolytic enzymes that can then degrade starch (Lorberth et al., 1998; Ritte et al., 2002; Kötting et al., 2005). Phosphorylation occurs mainly in the amylopectin fraction where glycosyl residues can be phosphorylated at either the C6 or C3 position (Tabata and Hizukuri, 1971; Ritte et al., 2006). C6 phosphate is introduces by GWD1,

after which GWD3 phosphorylates the C3 position (Baunsgaard et al., 2005; Kötting et al., 2005).

Transgenic potato plants with reduced *StGWD1* expression demonstrate significantly reduced starch breakdown in cold-stored potato tubers, which is accompanied by a decrease in accumulation of the reducing sugars glucose and fructose (Lorbeth et al., 1998). StGWD1 is a 155 kDa protein and contains a series of starch binding domains at the N-terminus, while at the C-terminus the active site contains a catalytic domain and an ATP-binding site. Within the active site is a key catalytic histidine that is essential for its activity (Mikkelsen et al., 2005). The histidine undergoes autophosphorylation during catalysis and transfers a phosphoryl group from ATP to starch (Ritte et al., 2002; Mikkelsen et al., 2005). Previous bioinformatics analysis of *StGWD1* revealed that the gene is composed of 34 exons and 33 introns (Xu et al., 2011; Uitdewilligen et al., 2022), and the sequence encoding the catalytically essential histidine is in exon 25 (Mikkelsen and Blennow, 2005; Carlsen et al., 2022). Exon 25 also contains a sequence that encodes two cysteine residues shown to play a role in redox regulation of StGWD1 activity due to creation of inter- or intra-disulfide bonds (Mikkelsen et al., 2005; Carlsen et al., 2022).

Through the delivery of synthetically created single guide (sg) RNAs to direct Cas9-mediated cleavage at specified gDNA sequences, CRISPR/Cas9 has the potential to induce site-specific genome breaks (Allen et al., 2020). The components necessary for gene-editing can be introduced into plants as plasmid DNA constructs through *Agrobacterium*-mediated transformation or particle bombardment (Sandhya et al., 2020; Ghogare et al., 2021). In both cases, the CRISPR/Cas expression plasmid constructs are likely to integrate into one or more genomic loci in a stable manner and maintain expression in the host genome. Plants that contain these constructs are classified as genetically modified organisms (GMOs) and face regulatory hurdles and public apprehension (Smyth, 2017; Blancke et al., 2017).

Delivery of preassembled CRISPR/Cas9 ribonucleoproteins (RNPs) into protoplasts can lead to non-transgenic genome editing which overcomes these hurdles (Woo et al., 2015). Carlsen et al. (2022) were able to efficiently target *StGWD1* using polyethylene glycol mediated RNP transformation of protoplasts, although plants were not regenerated so no data was reported on phenotypic effects. Numerous research organizations have succeeded in isolating and regenerating adult plants from potato protoplasts, but the process is difficult and necessitates specialized tissue culture techniques (Tavazza and Ancora, 1986; Nicolia et

al., 2015; Clasen et al., 2016). This stage frequently serves as the limiting step in the establishment of this technique due to its complexity. This chapter aimed at developing a protoplast regeneration system in potato and to create guide RNAs that target *StGWD1*.

3.2 Materials and Methods

3.2.1 Suppliers and DNA sequencing facilities

Chemical reagents were sourced from Bio-Rad (California, USA), and Merck (Massachusetts, USA). Enzymes from Duchefa Biochemie (Haarlem, The Netherlands) were used for protoplast isolation. The kits and enzymes for the molecular biological procedures were obtained from Thermo Fischer Scientific (Massachusetts, USA), Promega Corp (Wisconsin, USA), Invitrogen (Massachusetts, USA), Zymo Research (California, USA), and New England Biolabs (NEB; Massachusetts, USA). Oligonucleotides were supplied by Inqaba Biotech (Pretoria, South Africa). The Central Analytical Facilities (CAF) at Stellenbosch University performed DNA sequencing.

3.2.2 Plant propagation and growth conditions

Wild type *Solanum tuberosum* cv. Désirée plant material was sourced from pre-existing tissue culture stocks and grown in plastic magenta vessels with 65 mL of medium A (2.2% [w/v] MS basal medium with vitamins, 4.4 mM sucrose, 0.8% [w/v] agar, pH 5.8 with KOH). Plantlets were placed in a growth room at 25 °C under a 16/8-hour light/dark photoperiod (50 µmol photons m^{-2} sec^{-1} of photosynthetically active radiation) under OrbitX Neptune LED 150W IP65 light emitting diode lights.

3.2.3 Identification of potential targets and primer design for verification

Putative *Solanum tuberosum StGWD1* target sequences were identified by analysing exon sequences (NM_001288123.1) using CRISPR-RGEN, CRISPR P and CRISPOR (Table 3.2). Primers to amplify regions of *StGWD1* from cv Désirée genomic DNA (gDNA) containing putative targets were designed using Primer3 (https://primer3.ut.ee) and gDNA and messenger RNA (mRNA) accessions (NW_006239172.1 and NM_001288123.1) obtained from the National Centre for Biotechnology Information. Two sets of primers were designed for

StGWD1: the first spanning exons 7, 8 and 9, the second spanning exons 20 to 24. The resulting amplicons acquired using polymerase chain reaction (PCR) are labelled as StGWD1_A and StGWD1_B respectively. An additional set of primers previously used in CRISPR/Cas experiments in Désirée that amplify from exon 6 to 8 within the Phytoene Desaturase (*PDS*) gene were obtained from Bánfalvi et al., 2020 (Table 3.1).

Table 3.1 Primer sequences used to amplify genomic DNA fragments from *Solanum tuberosum*.

Gene	Primer Name	Sequence (5' – 3')	Exons	Amplicon length (bp)
GWD1	GWD1_A_F	GGCCCAGATGTTTCAGTTCC	7	1 646
	GWD1_A_R	GTACTTGTACTGCAGGACTGG	9	
	GWD1_B_F	GCCTCCTCCATTTTGTCTTGG	20	1 510
	GWD1_B_R	AGATTTGCAGTTTTCCGAAGC	24	
PDS	PDS_F	TTTCCCCGAAGCTTTACCCG	6	532
	PDS_R	ATCTGTCACCCTATCCGGCA	8	

3.2.4 Extraction of RNA and synthesis of complementary DNA

Leaves from potato plantlets were removed and immediately frozen in liquid nitrogen, before being ground into powder using a mortar and pestle. Approximately 100 mg of powder was used for RNA extraction using the Maxwell 16 LEV Plant RNA kit (Promega, Madison, USA) following the manufacturer's instructions and an automated RNA extraction system (Maxwell® 16 MDx, Promega). Approximately 1 µg of extracted RNA was used for complementary DNA (cDNA) synthesis using the Thermo Scientific RevertAid First Strand cDNA Synthesis kit (Thermo Fischer Scientific) along with oligo dT_{18} primers as specified by the manufacturer.

3.2.5 Amplification of target regions by PCR

3.2.5.1 Extraction of genomic DNA

A modified version of the procedure described in Doyle and Doyle (1987) was used to isolate gDNA. One hundred and fifty microliters of β-mercaptoethanol was added to 1 mL

CTAB buffer (2 % [w/v] cetyl trimethyl ammonium bromide, 2 % [w/v] PVP, 100 mM TRIS-HCl [pH 8 with KOH], 25 mM EDTA [pH 8 with KOH], 2 M NaCl, 3.4 mM Spermidine) pre-warmed to 65 °C in a 2 mL microcentrifuge tube. Finely ground plant material (0.1 g) was added and the tube vortexed for 30 s. The sample was incubated at 65 °C for 30 min with vortexing for 3 s every 10 min. Samples were centrifuged for 10 min at 16000 x g at room temperature before 1 mL of supernatant was transferred to a new 2 mL microcentrifuge tube. One millilitre of chloroform:isoamyl alcohol (24:1) was added and vortexed for 30 s before centrifuging for 15 min at 16000 x g at room temperature. The upper aqueous layer was transferred to a fresh 2 mL microcentrifuge tube and one volume of chloroform:isoamyl alcohol (24:1) was added before samples were vortexed for 30 s. Samples were then centrifuged for 15 min at 16000 x g at room temperature. The aqueous layer was transferred to a fresh 2 mL microcentrifuge tube containing 1 mL of chloroform:isoamyl alcohol (24:1) before vortexing for 30 s and centrifugation for 15 min at 16000 x g at room temperature. The aqueous layer was then transferred to a new 2 mL microcentrifuge tube and 0.5 mL isopropanol was added before DNA was precipitated for 1 h at -20 °C. The sample was centrifuged again for 15 min at 16000 x g. The supernatant was removed and the pellet re-suspended in 500 µL Milli-Q H_2O which was transferred to a new 2 mL microcentrifuge tube. 0.1 volume of 5 M NaCl and 2.5 volumes of ice-cold ethanol were added and the sample was precipitated overnight at 4 °C. After centrifugation at 12000 x g and 4 °C for 10 min the pellet was washed in 1 mL 70 % (v/v) ethanol. After centrifuging the pellet again at 12000 x g and 4 °C for 10 min, it was re-suspended in 20 µL Milli-Q H_2O.

3.2.5.2 Amplification of target-containing gene fragments

Portions of the *StGWD1* and *StPDS* genes were amplified from gDNA by PCR using Q5® High-Fidelity DNA polymerase (NEB) and the primers listed in Table 3.1.

3.2.5.3 DNA separation by agarose gel electrophoresis

Amplicons were separated on a 0.8% (w/v) agarose-Tris borate EDTA gel containing 0.005% (v/v) ethidium bromide and visualized using a GelDoc imaging system (Thermo Fischer Scientific).

3.2.6 Purification of target-containing gene fragments and ligation into pJET/blunt

Amplicons were purified using the Wizard® SV Gel and PCR Clean-Up System (Promega Corp.) according to the manufacturer's instructions and ligated into pJET1.2/blunt (Thermo Fischer Scientific) according to the manufacturer's protocol.

3.2.7 Bacterial growth media

Terrific broth (TB; 11.8 g L^{-1} tryptone, 23.6 g L^{-1} yeast extract, 9.4 g L^{-1} K_2HPO_4, 2.2 g L^{-1} KH_2PO_4, 4 mL L^{-1} glycerol), lysogeny broth agar (LBA; 10 g L^{-1} tryptone, 5 g L^{-1} yeast extract, 10 g L^{-1} NaCl and 15 g L^{-1} bacteriological agar) and liquid lysogeny broth (LB; 10 g L^{-1} tryptone, 5 g L^{-1} yeast extract, 10 g L^{-1} NaCl) were used for bacterial culture.

3.2.8 Preparation of chemically competent *Escherichia coli* cells

A modified version of the procedure described in Inoue et al. (1990) was used to create competent *Escherichia coli* (*E. coli*) DH5α cells. Bacterial cells were cultivated overnight night at 37 °C on LBA plates. A single colony was used to inoculate 3 mL of LB and cultured overnight at 37 °C with shaking at 200 rpm. This culture was then used to inoculate 200 mL of LB, which was grown in the same conditions until an OD_{600} of 0.5 was attained. The culture was incubated on ice for 10 min before cells were pelleted by centrifugation at 1430 x g for 10 min at 4 °C. The pellet was re-suspended in 20 mL of ice-cold TB and incubated for 10 minutes on ice. After centrifugation at 1430 x g for 10 min at 4 °C, the pellet was re-suspended in 10 mL of ice-cold TB containing 70 µL L^{-1} dimethyl sulfoxide. Liquid nitrogen was used to snap-freeze 50 µL aliquots before storage at -80 °C.

3.2.9 Transformation of plasmids into *Escherichia coli*

Approximately 400 ng of plasmid DNA was added to 50 µL of thawed competent cells, and the mixture was then incubated on ice for 30 min. Samples were subjected to a 45-s heat shock at 42 °C before being returned to ice for two min. Two hundred and fifty microlitres of LB medium was then added and cells were incubated for 30 min at 37 °C while being shaken at 200 rpm. Fifty µL of each transformation were plated onto LBA containing appropriate antibiotics and grown overnight at 37 °C.

3.2.10 Isolating and sequencing plasmid DNA

Bacterial colonies were used to inoculate 6 mL of LB media, which was then shaken at 200 rpm and cultured overnight at 37 °C. Plasmid DNA was then isolated using the Wizard® Plus SV Minipreps DNA Purification System (Promega Corp., USA) according to the manufacturer's instructions and sequenced at the Central Analytics Facility (Stellenbosch University) using pJET1.2 forward (5'-CGACTCACTATAGGGAGAGCGGC-3') and reverse (5'-AAGAACATCGATTTTCCATGGCAG-3') sequencing primers.

3.2.11 Design of single guide RNAs

DNA sequences were uploaded to the CLC Sequence Viewer program (Qiagen, Hilden, Germany) and aligned to corresponding coding sequence accessions acquired for *StGWD1* from the NCBI (Accession numbers: NM_001288123.1 and JQ388473.1). The *StPDS* fragment sequence was aligned to the *StPDS* sequence published in Bánfalvi et al. (2020) (NCBI accession number: LOC102577582).

Single guide RNAs (sgRNAs) for *StGWD1* were designed using the platforms CRISPR RGEN (Park et al., 2015), CRISPR-P (Lei et al., 2014) and CRISPOR (Concordet and Haeussler, 2018). These guides were named StGWD1-1 and StGWD1-2. Prospective off-target cleavage of each guide (StGWD1-1 and StGWD1-2) was evaluated with up to three nucleotide mismatches of the target sequence using Cas-OFFinder in the CRISPR RGEN program (Bae et al., 2014).

3.2.12 Construction of pGEM-Scaffold-sgRNA

For each sgRNA, complementary 20 bp oligonucleotide pairs were created with the inclusion of a 5'-CGTC-3' and a 5'-AAAC-3' sequence at the start of the forward and reverse oligonucleotides respectively (Figure 3.1A). A 50 µL reaction containing 3 µM ATP, 3 µM CTP, 3 µM GTP, 3 µM TTP and 5 µL of NEB 2.1 buffer was then used to anneal the oligonucleotide pairs together. After incubating the reactions for 4 min at 95 °C, the reaction tubes were placed into 500 mL of water at 70 °C that was then allowed to cool at room temperature. Mr. Alex Dijkerman (Department of Genetics, Stellenbosch University) generously donated a pGEM®-T Easy plasmid that contained a sgRNA scaffold sequence downstream of the T7 initiation site (pGEM-scaffold; Dijkerman, 2021). After this plasmid was linearized through

digestion with *BbsI*, each oligonucleotide pair was separately ligated into the vector utilising T4 DNA ligase (Promega Corp; Figure 3.1B). Following ligation, each plasmid was transformed into *E. coli* (DH5α) and plated onto LBA plates containing 100 µg mL^{-1} ampicillin before incubating at 37 °C overnight. The pGEM-scaffold-sgRNA plasmid DNA was then isolated using the Wizard® Plus SV Miniprep DNA Purification System (Promega Corp.) before sequencing with an SP6 primer.

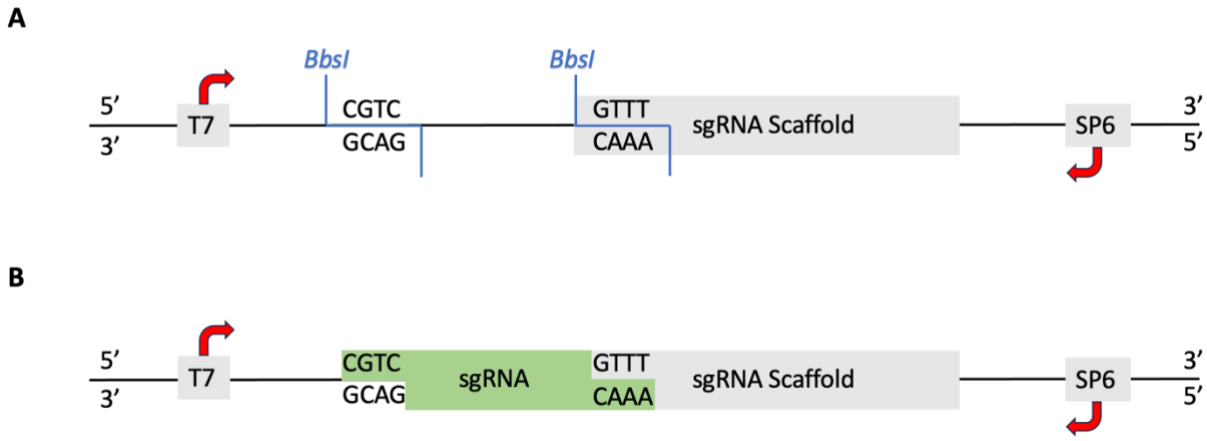

Figure 3.1. **A diagrammatic representation demonstrating how the synthesized single guide RNA oligonucleotides were ligated into the vector scaffold**. (**A)** *BbsI* was used to cut the pGEM-scaffold plasmid, leaving overhangs that were used for (**B)** the guide RNA oligonucleotides' unidirectional insertion.

3.2.13 Transcription of single guide RNAs and *in vitro* analysis

The pGEM-scaffold-sgRNA plasmids were linearized by digestion with *EcoRI* and purified using the Zymoclean Gel DNA Recovery Kit (Zymo Research) according to the manufacturer's instructions. The HiScribe™ T7 High Yield RNA Synthesis Kit (NEB) was then used to transcribe the RNA. The reaction contained 1 µg of linearized plasmid template, 1.5 µL 10X reaction buffer, 7.5 mM ATP, 7.5 mM GTP, 7.5 mM CTP, 7.5 mM UTP and 1000 U T7 RNA polymerase mix, according to manufacturer's instructions. Water was added to a final volume of 20 µL. Following overnight incubation at 37 °C, 5 U of DNase was added to each reaction before purifying the sgRNA transcripts using the RNA Clean and Concentrator kit (Zymo Research) in accordance with the manufacturer's instructions. Agarose gel electrophoresis as previously described was then used to separate the purified sgRNAs.

To verify the *in silico* prediction that each gRNA will bind to Cas9 and cleave their target sequence without the presence of non-specific endonuclease activity, *in vitro* experiments were carried out for each sgRNA. Each reaction contained: 2 µL Cas9 reaction buffer (0.2 M HEPES pH 7.5 with KOH, 0.1 M MgCl, 5 mM dichlorodiphenyltrichloroethane, 1.5 M KCl), 1 µg sgRNA, 1 µg Cas9 protein (Invitrogen TrueCut™ v2), 250 ng purified PCR amplicon, and water to attain a final volume of 20 µL. Included were three negative controls: one without sgRNA, one without sgRNA and Cas9, and one with a non-target DNA fragment. A positive control was also used, which was obtained from a previously synthesised sgRNA designed to target the potato *eIF4E-1* gene (Hurst, 2022). Samples were incubated at 37 °C for 1 h and 10 min, before the enzyme was denatured for 10 min at 65 °C. Agarose gel electrophoresis as previously described was used to separate the reactions.

3.2.14 Protoplast isolation

Protoplasts were isolated and regenerated in accordance with the procedure outlined in Nicolia et al. (2015), with a few minor adjustments. Approximately 30 leaves from the top of 4-6 week old Désirée plants grown in tissue culture were removed and laid abaxial side down on Petri dishes containing 20 mL medium B (Addendum 1; Figure 3.4A). Each dish was incubated for 24 h in the dark at 4 °C. Leaves were cut using a scalpel blade into 1-2 mm-wide slices before removing medium B and adding 25 mL of plasmolysis solution (0.5 M sorbitol). The leaves were then incubated for 30 min in the dark at room temperature. After removing the plasmolysis solution, 30 mL of cell wall digest solution (medium C, Addendum 1) was added (Figure 3.4B). Plates were incubated on a Belly Dancer™ Orbital Platform Shaker (IBI Scientific™) at ten rpm at RT for 14 h in the dark. The solution was then passed through a 100 µM filter (Corning®, USA) that had been pre-wetted with 5 mL of wash solution (Addendum 1). The remaining protoplasts were isolated from the Petri dish by addition of 20 mL wash solution followed by filtration through the 100 µM filter. This solution was centrifuged in a swing bucket rotor (Beckman Coulter; Allegra™ X-22R Centrifuge and SX 4250 rotor) at 50 x g at 24 °C for 5 min with minimum acceleration and deceleration. After removing supernatant, the pellet was re-suspended in 4 mL of wash solution which was layered on top of 6 mL of ice-cold 21% (w/v) sucrose solution. Tubes were centrifuged at 50 x g for 15 min at 24 °C with the lowest acceleration and deceleration settings. Viable protoplasts at the solution's interface

were placed into 3 mL of transformation buffer 1 (0.5 M mannitol, 15 mM $MgCl_2 \cdot 6H_2O$, 0.5% [w/v] MES) for counting using a hemocytometer and a light microscope with 400X magnification.

3.2.15 Suspension of protoplasts in alginate lenses for regeneration

Transformation buffer containing protoplasts was centrifuged for 10 min at 50 x g at 24 °C in a swing bucket rotor (Beckman Coulter; Allegra™ X-22R Centrifuge and SX 4250 rotor). The supernatant was discarded and the pellet was re-suspended in medium E (Addendum 1) to obtain an approximate concentration of 1.6 x 10^6 protoplasts mL^{-1}. The cell suspension was combined with an equivalent amount of sodium alginate solution (0.4 M sorbitol, 2.8% (w/v) sodium alginate), and pipetted as 500 µL drops onto Petri dishes containing 10 mL of solid setting agar (0.4 M sorbitol, 50 mM $CaCl_2 \cdot 2H_2O$, 8 g L^{-1} agar) before being left in the dark at room temperature for 2 h. Each plate then received 3 mL of floating solution (0.4 M sorbitol, 50 mM CaCl2·2H2O) to free the alginate lenses from the surface of the setting agar. After being moved to Petri dishes containing 20 mL of medium E, the lenses were left in the dark at 25 °C.

3.2.16 Regeneration of micro and macro-callus

After 7 d in the dark, the plates were covered with white paper, placed into a light growth room and exposed to cool-white, fluorescent lights (Osram, L58V/740) with a 16/8-h light/dark photoperiod (50 µmol photons m^{-2} sec^{-1} of photosynthetically active radiation). After three weeks, the paper was removed and plates were exposed to full light. Fresh medium E was provided every 2 weeks.

3.3 Results

3.3.1 Bioinformatic analysis of *StGWD1* and identification of targets

Previous analysis of *StGWD1* indicated that it is composed of 34 exons and 33 introns that are located on chromosome 5 (Xu et al., 2011; Uitdewilligen et al., 2022). The largest introns occurred between exons 17 and 18, and exons 28 and 29 (Figure 3.2A). Analysis of the predicted StGWD1 protein (NP_001275052.1) demonstrates it is composed of 1 464 amino

acids. A starch-binding domain (CBM45) is present at location 109-217 and 405-551 and a catalytic domain at location 960-1464 that contains a phosphohistidine and an ATP-binding site (Figure 3.2B; Mikkelsen et al., 2005; Mikkelsen and Blennow, 2005; Glaring et al., 2011).

Exon sequences (NM_001288123.1) were uploaded to CRISPR-RGEN, and analysed for sgRNA sequences containing an out-of-frame score of above 66 (Li et al., 2023) and a GC content above 50 (Konstantakos et al., 2022). Following this screening process, only two exon sequences (exon 8 and 23) met these criteria and these were further analysed using CRISPRP and CRISPOR. All three platforms identified 20 guide sequences in exon 8, and 16 guide sequences in exon 23. The quality scores for putative sgRNAs were then assessed across all three programs (Table 3.2).

Table 3.2 Summary of all results obtained from three single guide RNA prediction programs for the *StGWD1* gene. The GWD1_A and GWD1_B gene targets indicate genomic fragments containing exon 8 and 23 respectively.

Program	**Gene target**	**Total number of guides identified**	**Quality score range (%)**
CRISPR-RGEN	Exon 8	20	49.6 – 85.0
	Exon 23	16	30.4 – 78.0
CRISPR P	Exon 8	20	3.9 – 72.6
	Exon 23	16	1.1 – 73.8
CRISPOR	Exon 8	20	25 – 65
	Exon 23	16	21 – 65

Putative guides were assessed for off-target matches in the *S. tuberosum* genome using the Cas-OFFinder function in CRISPR-RGEN. Guides that would lead Cas9 to an unintended DNA location were removed from consideration, leaving four potential guide sequences– one in exon 8 and three in exon 23. Of these four potential guides, the two guides with the best mean quality ratings across all three programs were chosen for *in vitro* transcription and analysis (Table 3.3).

Table 3.3 Single guide RNAs designed to target *GWD1* in *S. tuberosum* and their quality control scores (%) from the programs CRISPR-RGEN, CRISPR P and CRISPOR.

Gene target	sgRNA name	sgRNA sequence (5'-3')	Quality score (%)		
			CRISPR-RGEN	CRISPR P	CRISPOR
Exon 8	GWD1-1	CCATACAGGACATTCGAGCAAGG	74.8	4.22	42
Exon 23	GWD1-2	CCGTCTTGCACTTGCAAGCAAGG	78	8.14	44

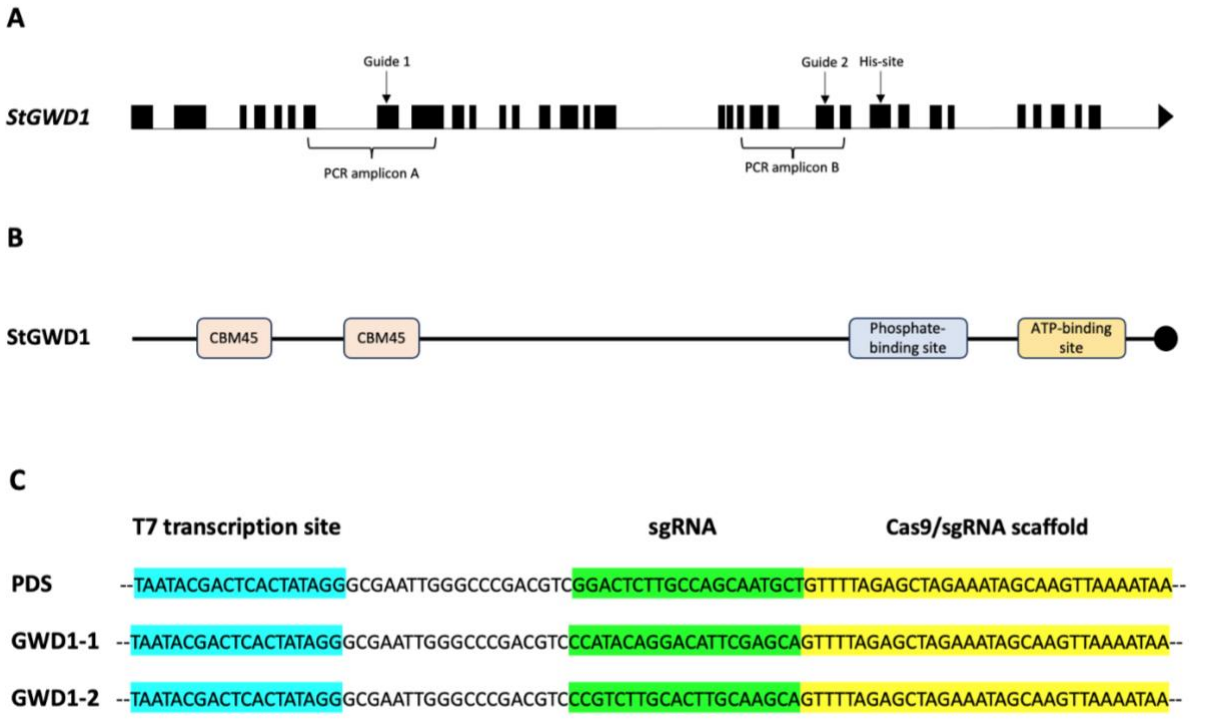

Figure 3.2. **Bioinformatic analysis of *StGWD1* and prediction of potential guide sites.** **(A)** A diagrammatic representation of the *StGWD1* gene structure. Single guide RNA locations for each gene are labelled as 'Guide 1' and 'Guide 2', corresponding with StGWD1-1, StGWD1-2, respectively. **(B)** Domain structure within the StGWD1 protein. CBM45 starch-binding domains, active site containing a key catalytic histidine that binds phosphate, and ATP-binding sites are shown at the approximate location where they are found within the protein. The black sphere at the end of the protein indicates the C-terminus. **(C)** Nucleotide sequences of the pGEM-scaffold-sgRNA plasmid were obtained from the Central Analytics Facility. T7 transcription sites, sgRNA sequences and Cas9/sgRNA scaffold sequence are highlighted in blue, green and yellow respectively.

The chosen guides were aligned to the corresponding coding and gene sequences acquired from the NCBI as well as sequence data obtained from PCR amplicons of the target regions. Alignments were assessed for similarity and the amplicons were demonstrated to be identical to the published guide sequences. A guide sequence known to bind to the *StPDS* gene (Bánfalvi et al. 2020) was also used to act as a potential positive control. Oligonucleotide pairs were synthesized for each guide RNA sequence and cloned into the pGEM-scaffold plasmid (Figure 3.2C).

3.3.2 Single guide RNA transcription and *in vitro* analysis

An *in vitro* cleavage experiment was conducted to evaluate the efficacy of the *in silico* predictions of cleavage of off target regions by RNP's consisting of sgRNAs complexed with Cas9. After the sgRNAs had been synthesised *in vitro* and complexed with Cas9, the resulting RNPs were incubated with PCR amplicons containing the target sequences. The anticipated sizes for each amplicon before and after cleavage are displayed in Table 3.4.

Table 3.4 Expected DNA fragment sizes after cleavage by Cas9 for each DNA target and single guide RNA pair.

Gene target	**Guide**	**Expected DNA fragment size after Cas9 cleavage (bp)**	
St*GWD1_A*	StGWD1-1	Uncut	538
		Cut	164 and 374
StGWD1_B	StGWD1-2	Uncut	574
		Cut	386 and 188
StPDS	Bánfalvi _2020-PDS	Uncut	535
		Cut	286 and 249

To examine if the sgRNA's cleaved in a non-specific manner, each sgRNA was tested using DNA containing either its target sequence or a non-target DNA fragment. The guide sequence that exhibited the greatest similarity to the target was used as non-target DNA, as this was the most likely sequence to be incorrectly cleaved. StGWD1-1 and StGWD1-2 guides were used as controls for each other. For StPDS, the StGWD1_A amplicon containing StGWD1-1 guide sequence was used as a non-target control, along with a control (eIF4E-1) that had

been previously confirmed to cleave a target-containing sequence in *S. tuberosum* (Hurst, 2022). Negative controls without the sgRNA and without both the sgRNA and Cas9 were also conducted. Following incubation with Cas9, DNA fragments were separated by agarose gel electrophoresis (Figure 3.3). Target DNA was successfully cleaved by the StGWD1-1 Cas9 RNP, as was the positive control (Figure 3.3C); no cleavage was observed in the non-target DNA control samples.

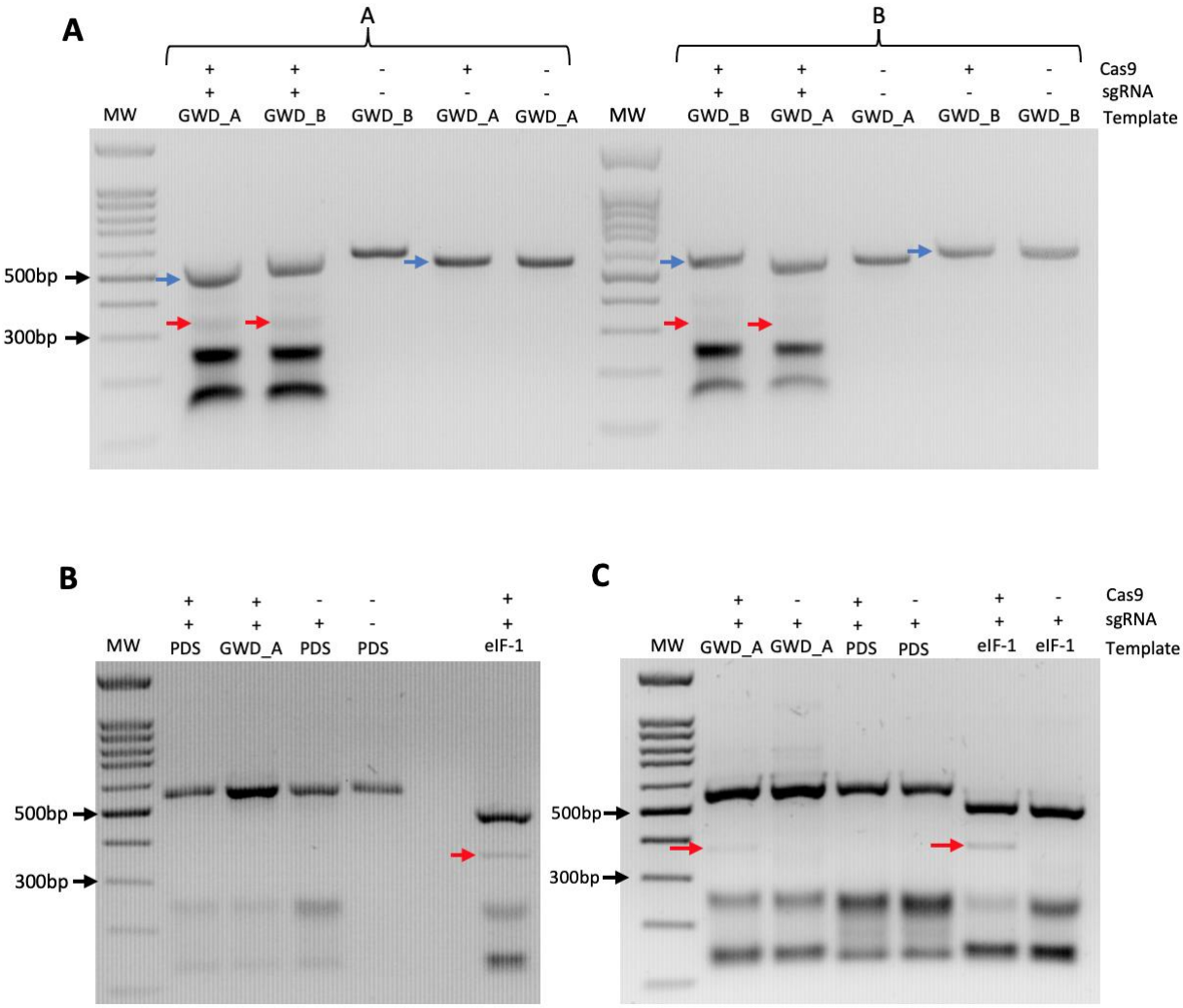

Figure 3.3. *In vitro* CRISPR/Cas9 reactions of the *Solanum tuberosum* single guide RNPs. RNPs targeting **(A)** *GWD1_A* and *GWD1_B* **(B)** *PDS* **(C)** *GWD1_A, PDS* and *eIF4E-1* separated on 1.5 % (w/v) agarose-Tris Borate EDTA gels by electrophoresis. **(A)** Red arrows indicating bands caused by sgRNA and blue arrows indicating shift in a particular target DNA fragment when sgRNA is included in the reaction. **(B + C)** Cleaved DNA fragments are indicated with red arrows. The inclusion or omission of each reaction component is denoted by a '+' or '-' respectively and displayed above each gel image. MW = 100 bp DNA ladder (GeneDireX).

The two other negative control reactions—either without sgRNA or sgRNA and Cas9—showed no cleavage. Single guide RNA transcript at the bottom of the gels would obscure the smaller of any cleaved fragment. Interestingly in some experiments when sgRNA is included in the reaction, the target DNA appears to migrate further in the agarose gel compared to reactions with no sgRNA (Figure 3.3A).

3.3.3 Protoplast isolation and micro-callus regeneration

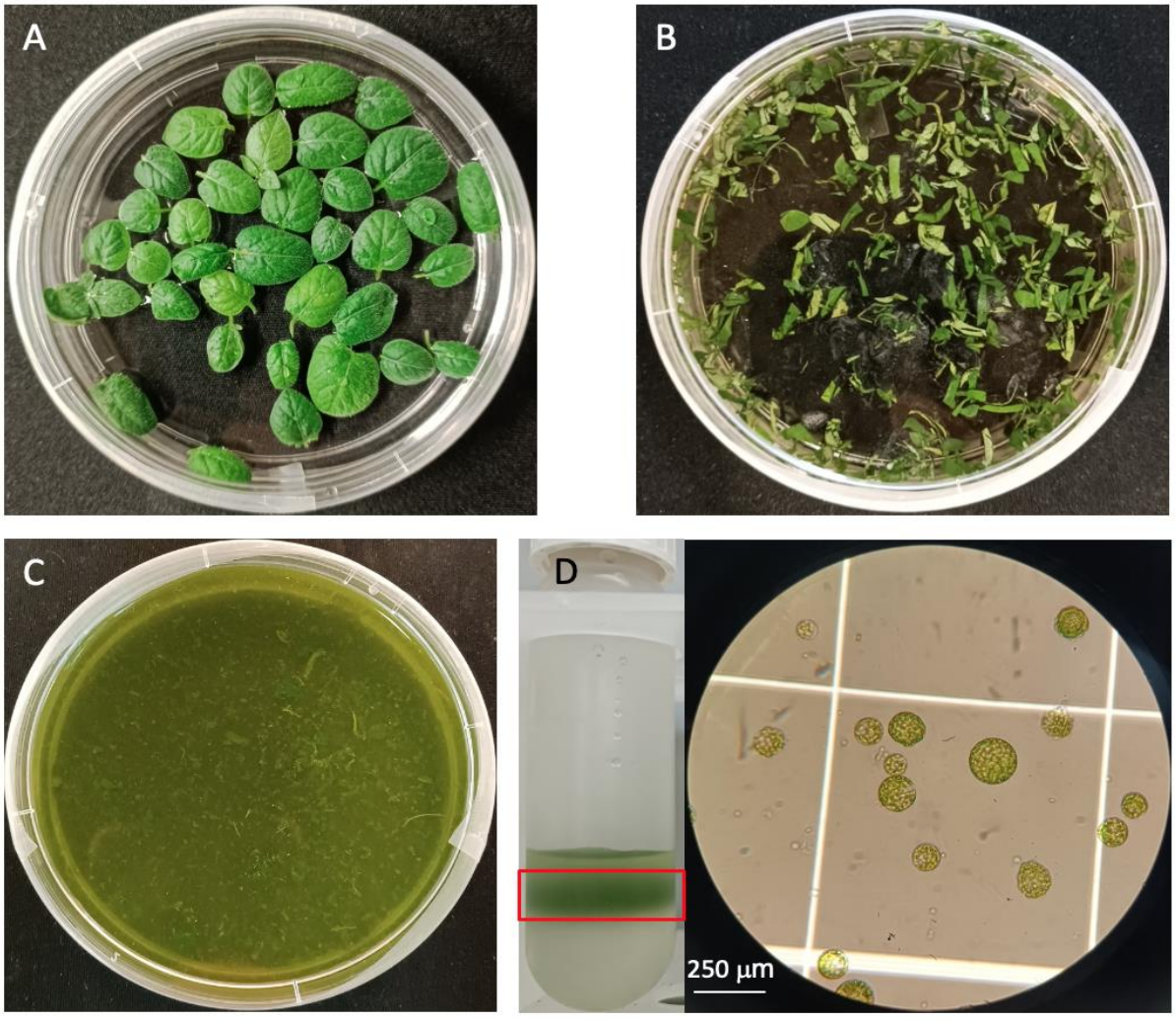

Figure 3.4. Isolation of potato protoplasts. (A) For the purpose of isolating protoplasts, leaves of tissue culture grown plants grown in tissue culture were harvested. **(B)** In preparation for an overnight enzymatic digestion, leaves were cut into 1-2 mm-wide strips. **(C)** By centrifuging on a sucrose-cushion, protoplasts were extracted from the digested solution. **(D)** Centrifugation on a sucrose-cushion enables for the separation of viable protoplasts from cell detritus.

Enzymatic digestion was used to successfully isolate protoplasts from the leaf tissue obtained from *S. tuberosum* cv. Désirée plants grown in tissue culture. Viable protoplasts were isolated from burst protoplasts and other cell detritus by sucrose gradient centrifugation (Figure 3.4). Across six protoplast isolation experiments, the average yield of viable protoplasts ranged from 1.3-2.7 x 10^6 protoplasts g^{-1} leaf tissue.

Solutions of viable protoplasts with concentrations of 1.6 x 10^6 protoplasts mL^{-1} were suspended in alginate lenses. The lenses were placed in growth medium after they had solidified, and the protoplasts developed into micro-calli that were visible after three weeks of cultivation (Figure 3.5). The micro-calli were left to develop into macro-calli for 8 weeks, but no further development was observed.

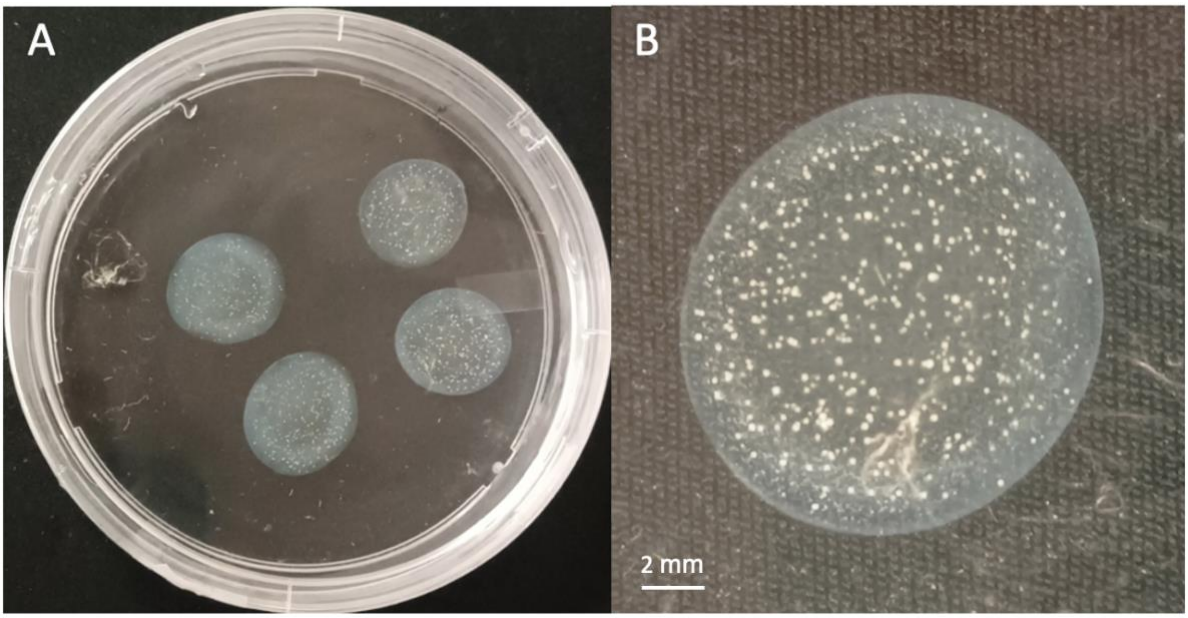

Figure 3.5. Development of potato callus from protoplasts. (A) Alginate lenses suspended in growth medium and displaying visible micro-calli growth after three weeks.**(B)** Micro-calli in an individual alginate lens.

3.4 Discussion

The aim of this experimental chapter was to create *StGWD1* gene knock-out mutations using the RNP CRISPR/Cas9 system. The RNP complex would be moved into potato protoplasts using polyethylene glycol to create double stranded breaks that would become improperly repaired. Plants containing the knock-out mutations should then produce tubers that are less susceptible to cold-induced sweetening.

The first step in targeting the mutation of a gene by RNPs is the identification of sequences that act as targets that can be used to design guides. In this study we aimed at identifying gene targets upstream of the region encoding the catalytically essential histidine that transfers phosphate to starch (Mikkelsen et al., 2004) as any premature stop, or missense mutation upstream of this would result in a protein that is unable to phosphorylate starch. In this study we identified two exons within *StGWD1* (exon 8 and 23, Figure 3.2A) that were predicted to contain suitable guide target regions. As StGWD1 acts upstream of StGWD3 (Baunsgaard et al., 2005; Kötting et al., 2005) mutating StGWD1 will eliminate incorporation of both C6 and C3 phosphate.

Successful editing of the potato *StGWD1* gene in exon 1, 24 and 25 has been achieved (Carlsen et al., 2022). That study targeted an area upstream of regions encoding both the catalytically essential histidine and a region thought to be required for intra- and inter-disulphide bond formation affecting redox-state regulation of StGWD1. In that study the guide RNAs were only tested in protoplasts and no plants were regenerated so there has been no report on the resulting phenotype. It is not clear, therefore, whether the resulting plants would display alterations in growth and/or a repression of cold induced sweetening. No effects on plant growth have previously been reported in *StGWD1* potato transgenics (Lorberth et al., 1998; Adegbaju, 2022), although repression or mutation of orthologous genes does affect growth in *Arabidopsis* (Pirone et al., 2017), wheat (*Triticum aestivum*; Bowerman et al., 2015) and cassava (*Manihot esculenta* Crantz; Zhou et al., 2017).

While the target site within a gene is a key component in sgRNA design, it is also crucial to take into account the sequence's expected suitability as a guide. All sequences in a query that come before a PAM site are considered potential guides by online sgRNA design platforms. Since this procedure is non-variable and non-discriminatory, the three design platforms used in this study identified the same number of regions in each of the exons as being potential guides. The number of guides were then reduced according to three criteria—the GC content, the guide's base-pairing score (Liang et al., 2016), and the possibility of the guide matching non-target sites within the host genome (Bae et al., 2014). This resulted in four suitable guides, and the two guides with the highest mean score across all three platforms were then selected for further use in this study (Table 3.3).

Due to significant variability between sgRNA design platforms, guides should first undergo an *in vitro* screening procedure to examine their capacity to guide Cas9 to putative

gene sequences for cleavage (Uniyal et al., 2019). Guide sequences predicted by sgRNA design programs can have varying ranges of efficiency *in vivo* (Bialk et al., 2016; Kieu et al., 2021; Carlsen et al., 2022), but those studies did not report *in vitro* screening assays to assess whether the guides could cleave their target sequence before being used *in vivo.* We decided to test this by forming RNPs containing transcribed sgRNAs with Cas9 and incubating them with target sequences to examine if they could cleave them. The StGWD1-1 RNP was shown to cleave, although neither StPDS (Bánfalvi et al., 2020) nor StGWD1-2 RNPs could cleave their target sequence. This provides evidence that StGWD1-1 may have an improved likelihood of cleaving target sequences *in vivo*. The *StPDS* guide has been demonstrated to cleave *in planta*, so its inability to cleave *in vitro* clearly does not demonstrate a lack of efficacy *in vivo*. The *in vitro* experiment therefore provides no clear evidence of guide efficacy *in vivo,* and both guide sequences will still need to be tested *in vivo* to validate efficiency. This may question the use of *in vitro* testing prior to *in vivo* work, and it may be faster and simpler to immediately analyse target sites from transformed protoplasts for cleavage and inaccurate repair. This could be achieved relatively easily using Tracking of Indels by Decomposition (TIDE) analysis, which allows identification of base pair differences in Sanger sequences within PCR amplicons.

In these *in vitro* experiments, the target-containing DNA fragments appear to migrate lower down the gel when sgRNA is included in the reaction compared with reactions containing no sgRNA. There's no obvious explanation for this, but because the amplicon incubated with the guide runs slightly lower indicating a lower molecular weight, this could potentially indicate cleavage by the guide alone. Additionally, the tertiary structure of the DNA may be altered by incubation with the guide, but further research is needed to explain this anomalous result.

The narrowness of the off-target activity screening is a drawback of this assay as only the DNA sequences that have been amplified were used to assess this. Previous research has indicated that guide efficiency can be maintained with up to two bp mismatches (Mali et al., 2013; Čermák et al., 2017). To gain better understanding of guide specificity in this study, the alternating StGWD1 target sequence was examined for each guide to see if it could be cleaved. In every instance, these controls showed no indication of off-target cleavage. Future experiments could look at designing sgRNAs containing both 1 or 2 bp mismatches to determine whether off-target cleavage occurs. Although *in silico* off-target screening was performed and no potential off targets were identified, *in planta* screening is required to

guarantee that off-target activity does not occur. This could be assessed for example by next generation sequencing of genomic DNA (Kim et al., 2015; Tsai et al., 2015; Kim et al., 2019).

Regeneration of protoplasts to form callus and then mature plants must first be established before utilizing these guides to create mutated plants. Even though potato protoplast regeneration procedures have been published, establishing such a system can still be challenging and requires significant tissue culture expertise (Reed and Bargmann, 2021). The average protoplast yields in this study were similar to those in literature (Nicolia et al., 2015), although the maximum number of protoplasts isolated was 2.7 x 10^6 mL^{-1}, which exceeds the average obtained from Nicolia et al., 2015 by 42 %. This protocol clearly allows the successful isolation of protoplasts, which can then be used to try regenerate callus.

The first step towards regenerating mature plantlets is the production of micro-calli from protoplasts, which was successfully accomplished. Unfortunately these did not then develop into larger macro-calli that would have allowed for root and shoot induction. According to Reed and Bargmann, (2021), protoplast cultivation protocols are highly species- and cultivar-specific. The protocol used in this study was created using the Desirée cultivar which was also the cultivar used by Nicolia et al., 2015. Other research groups have since improved that protocol using both Desirée and Kuras cultivars, demonstrating the necessity for laboratory-specific optimisation (Andersson et al., 2018; Moon et al., 2021). Factors that might impede callus development need to be evaluated on their own in order to progress this project. Three factors have been found to consistently affect the formation of callus after regeneration from protoplasts (Andreasson et al., 2022). These are the density of the protoplasts, the volume of the tissue culture vessel, and the composition of the hormones in the culture medium. In this study, micro-calli were grown in a medium that contained 1.77 μM of the cytokinin 6-Benzylaminopurine and 5.37 μM of the auxin 1-Naphthaleneacetic acid. For callus culture, cytokinins and auxins are typically utilized in a 1:1 molar ratio (Skoog and Miller, 1957). While we were able to generate calli using a 0.3:1 ratio as described by Nicolia et al., 2015, it may be advantageous to investigate whether raising the cytokinin concentration could improve callus regeneration. The final two factors are both associated with how quickly protoplasts can condition the regeneration media. According to Stuart and Street (1971), plant cells release conditioning factors (CFs) that promote the growth of cultured cells. Higher cell densities typically results in a more successful cell culture since CFs build up more quickly. For the current study protoplasts were suspended in alginate lenses,

which were then immersed in liquid media. While the external liquid medium can be replaced with fresh media, the cell density within the alginate lens remains constant. The alginate lenses and the liquid medium that surrounds them will both be adjusted by CFs released from protoplasts. While Nicolia et al. (2015) recommended a concentration of 5 x 10^4 protoplasts mL^{-1}, this was later adjusted to 8 x 10^4 protoplasts mL^{-1} by the same group (Nicolia et al., 2021). The rate at which the protoplasts condition the liquid media would be improved by the increase in cell density. However, while optimizing the Nicolia et al. (2015) methodology to increase protoplast yield and callus regeneration, Moon et al. (2021) reduced the protoplast concentration to 4 x 10^3 protoplasts mL^{-1}. They claimed that a decreased cell density in the alginate lenses provided more room for the micro-calli to form, resulting in healthier calli for inducing shoot and root growth. Future investigations should test all three concentrations as both hypotheses are credible. The volume of the tissue culture vessel in which the alginate lenses are inserted is another factor that can impact the outcome of callus growth from protoplasts. A lower volume would enable the accumulation of CFs to reach ideal levels sooner, but a vessel that is too small could deprive the cells of enough hormones and nutrients necessary for growth. Although the original methodology demonstrates success when the lenses are inserted into 20 mL of regeneration medium in a standard Petri dish (Nicolia et al., 2015), other studies show improved proliferation when the lenses are inserted into 6-well tissue culture plates containing 4 mL of regeneration medium (Andreasson et al., 2022). Future studies should compare protoplast culture in Petri dishes as well as in 6-well and 12-well plates to ascertain which one induces micro-calli with the greatest efficiency.

In conclusion, in order to evaluate on-target effectiveness, two guide RNAs targeting the *StGWD1* gene have been created *in silico* and tested *in vitro*. Only one of these guides displayed successful *in vitro* cleavage of the target region (Figure 3.3C). The StPDS guide had previously been confirmed to successfully cleave the target region (Bánfalvi et al., 2020). If successful, mutant plants with disrupted StGWD1 protein activity may show a phenotype that is resistant to cold-induced sweetening during refrigerated storage, where starch is no longer broken down into reducing sugars. Continuation of this work in a non-transgenic manner is, however, currently limited by the establishment of callus growth. Each of the variables that were described above that may enhance the current protoplast culture procedures should be further examined. If successfully established in the future, RNP transformation of protoplasts is a highly advantageous approach of introducing the CRISPR/Cas9 genome editing to plants.

The protoplast regeneration procedure in this study never extended beyond producing micro-calli; therefore, the non-transgenic CRISPR RNP method could not be used to produce gene-edited plants. The production of macro-calli needs to be optimised in order to efficiently pursue non-transgenic genome editing. To continue experimentation in targeting *StGWD1*, a transgenic approach was adopted and is discussed in the next research chapter.

3.5 References

Adegbaju MS (2022) Analysis of interactions between glucan, water dikinase and either isoamylase or starch branching enzymes in determination of starch structure. https://tinyurl.com/bde7utj7

Allen D, Rosenberg M, Hendel A (2020) Using synthetically engineered guide RNAs to enhance CRISPR genome editing systems in mammalian cells. Front Genome Ed **2**: 1–16

Amrein TM, Bachmann S, Noti A, Biedermann M, Barbosa MF, Biedermann-Brem S, Grob K, Keiser A, Realini P, Escher F, Amadó R (2003) Potential of acrylamide formation, sugars, and free asparagine in potatoes: a comparison of cultivars and farming systems. J Agric Food Chem **51**: 5556–5560

Andersson M, Turesson H, Olsson N, Fält AS, Ohlsson P, Gonzalez MN, Samuelsson M, Hofvander P (2018) Genome editing in potato via CRISPR-Cas9 ribonucleoprotein delivery. Physiol Plant **164**: 378–384

Andreasson E, Kieu NP, Zahid MA, Carlsen FM, Marit L, Sandgrind S, Peterson BL, Zhu LH (2022) Utilization of protoplasts to facilitate gene editing in plants: schemes for *in vitro* shoot regeneration from tissues and protoplasts of potato and rapeseed: implications of bioengineering such as gene editing of broad-leaved plants. Front Genome Ed **4**: 780004

Andrivon D (2017) Potato facing global challenges: how, how much, how well? Potato Res **60**: 389–400

Bánfalvi Z, Csákvári E, Villánya V, Kondrák M (2020) Generation of transgene-free PDS mutants in potato by *Agrobacterium*-mediated transformation. BMC biotechnol **20**: 25

Bae S, Park J, Kim JS (2014) Cas-OFFinder: a fast and versatile algorithm that searches for potential off-target sites of Cas9 RNA-guided endonucleases. Bioinformatics **30**: 1473–1475

Baunsgaard L, Lütken H, Mikkelsen R, Glaring MA, Pham TT, Blennow A (2005) A novel isoform of glucan, water dikinase phosphorylates pre-phosphorylated α-glucans and is involved in starch degradation in *Arabidopsis*. Plant J **41**: 595–605

Bhaskar PB, Wu L, Busse JS, Whitty BR, Hamernik AJ, Jansky SH, Buell CR, Bethke PC, Jiang J (2010) Suppression of the vacuolar invertase gene prevents cold-induced sweetening in potato. Plant Physiol **154**: 939–948

Bialk P, Sansbury B, Rivera-Torres N, Bloh K, Man D, Kmiec EB (2016) Analyses of point mutation repair and allelic heterogeneity generated by CRISPR/Cas9 and single-stranded DNA oligonucleotides. Sci Rep **6**: 1–9

Blancke S, Grunewald W, De Jaeger G (2017) De-problematizing 'GMOs': suggestions for communicating about genetic engineering. Trends Biotechnol **35**: 185–186

Bowerman AF, Newberry M, Dielen AS, Whan A, Larroque O, Pritchard J, Gubler F, Howitt CA, Pogson BJ, Morell MK, Ral JP (2016) Suppression of glucan, water dikinase in the endosperm alters wheat grain properties, germination and coleoptile growth. Plant Biotechnol J **14**: 398–408

Carlsen FM, Johansen IE, Yang Z, Liu Y, Westberg IN, Kieu NP, Jørgensen B, Lenman M, Andreasson E, Nielsen KL, Blennow A, Petersen BL (2022) Strategies for efficient gene editing in protoplasts of *Solanum tuberosum* theme: determining gRNA efficiency design by utilizing protoplast (Research). Front Genome Ed **3**: 1–12

Čermák T, Curtin SJ, Gil-Humanes J, Čegan R, Kono TJY, Konečná E, Belanto JJ, Starker CG, Mathre JW, Greenstein RL, Voytas DF (2017) A multipurpose toolkit to enable advanced genome engineering in plants. Plant Cell **29**: 1196–1217

Chakraborty S, Chakraborty N, Agrawal L, Ghosh S, Narula K, Shekhar S, Naik PS, Pande PC, Chakrborti SK, Datta A (2010) Next-generation protein-rich potato expressing the seed protein gene *AmA1* is a result of proteome rebalancing in transgenic tuber. Proc Natl Acad Sci **107**: 17533–17538

Clasen BM, Stoddard TJ, Luo S, Demorest ZL, Li J, Cedrone F, Tibebu R, Davison S, Ray EE, Daulhac A, Coffman A, Yabandith A, Retterath A, Haun W, Baltes NJ, Mathis L, Voytas DF, Zhang F (2016) Improving cold storage and processing traits in potato through targeted gene knockout. Plant Biotechnol J **14**: 169–176

Concordet JP, Haeussler M (2018) CRISPOR: intuitive guide selection for CRISPR/Cas9 genome editing experiments and screens. Nucleic Acids Res **46**: W242–W245

Dolničar P (2021) Importance of potato as a crop and practical approaches to potato breeding. Methods Mol Biol **2354**: 3–20

Doyle JJ, Doyle JL (1987) A rapid DNA isolation procedure for small quantities of fresh leaf tissue. Phytochem Bull **19**: 11–15

Ghogare R, Ludwig Y, Bueno GM, Slamet-Loedin IH, Dhingra A (2021) Genome editing reagent delivery in plants. Transgenic Res **30**: 321–335

Glaring MA, Baumann MJ, Hachem MA, Nakai H, Nakai N, Santelia D, Sigurskjold BW, Zeeman SC, Blennow A, Svensson B (2011) Starch-binding domains in the CBM45 family

– low-affinity domains from glucan, water dikinase and α-amylase involved in plastidial starch metabolism. FEBS Journal **278**: 1175–1185

Green J, Wang D, Lilley CJ, Urwin PE, Atkinson HJ (2012) Transgenic potatoes for potato cyst nematode control can replace pesticide use without impact on soil quality. PLoS One **7**: e30973

Hameed A, Tahir MN, Asad S, Bilal R, Van Eck J, Jander G, Mansoor S (2017) RNAi-mediated simultaneous resistance against three RNA viruses in potato. Mol Biotechnol **59**: 73–83

Hameed A, Bilal R, Latif F, Van Eck J, Jander G, Mansoor S (2018) RNAi-mediated silencing of endogenous *Vlnv* gene confers stable reduction of cold-induced sweetening in potato (*Solanum tuberosum* L. cv. Désirée). Plant Biotechnol Rep **12**: 175–185

Hameed A, Mehmood MA, Shahid M, Fatma S, Khan A, Ali S (2020) Prospects for potato genome editing to engineer resistance against viruses and cold-induced sweetening. GM Crops Food **11**: 185–205

He Y, Zhao Y (2019) Technological breakthroughs in generating transgene-free and genetically stable CRISPR-edited plants. aBIOTECH **1**: 88–96

Hurst RJ (2022) An investigation of the potato *eIF4E* isoforms as targets for non-transgenic CRISPR/Cas9 genome editing for viral resistance. https://tinyurl.com/y6nc4dpf

Inoue H, Nojima H, 0kayama H (1990) High efficiency transformation of *Escherichia coli* with plasmids. Gene **96**: 23–28

Kieu NP, Lenman M, Wang ES, Petersen BL, Andreasson E (2021) Mutations introduced in susceptibility genes through CRISPR/Cas9 genome editing confer increased late blight resistance in potatoes. Sci Rep **11**: 4487

Kim D, Bae S, Park J, Kim E, Kim S, Yu HR, Hwang J, Kim JI, Kim JS (2015) Digenome-seq: genome-wide profiling of CRISPR-Cas9 off-target effects in human cells. Nat Methods **12**: 237–243

Kim D, Luk K, Wolfe SA, Kim JS (2019) Evaluating and enhancing target specificity of gene-editing nucleases and deaminases. Annu Rev Biochem **88**: 191–220

Konstantakos V, Nentidis A, Krithara A, Paliouras G (2022) CRISPR-Cas9 gRNA efficiency prediction: an overview of predictive tools and the role of deep learning. Nucleic Acids Res **50**: 3616–3637

Kötting O, Pusch K, Tiessen A, Geigenberger P, Steup M, Ritte G (2005) Identification of a novel enzyme required for starch metabolism in *Arabidopsis* leaves. The phosphoglucan, water dikinase. Plant Physiol **137**: 242–252

Lei Y, Lu L, Liu HY, Li S, Xing F, Chen LL (2014) CRISPR-P: a web tool for synthetic single-guide RNA design of CRISPR-system in plants. Mol Plant **7**: 1494–1496

Li C, Chu W, Gill RA, Sang S, Shi Y, Hu X, Yang Y, Zaman QU, Zhang B (2023) Computational tools and resources for CRISPR/Cas genome editing. Genomics Proteomics and Bioinformatics. **21**: 108–126

Liang G, Zhang H, Lou D, Yu D (2016) Selection of highly efficient sgRNAs for CRISPR/Cas9-based plant genome editing. Sci Rep **6**: 1–8

Lorberth R, Ritte G, Willmitzer L, Kossmann J (1998) Inhibition of a starch-granule-bound protein leads to modified starch and repression of cold sweetening. Nat Biotechnol **16**: 473–477

Mali P, Aach J, Stranges PB, Esvelt KM, Moosburner M, Kosuri S, Yang L, Church GM (2013) Cas9 transcriptional activators for target specificity screening and paired nickases for cooperative genome engineering. Nat Biotechnol **31**: 833–838

Mikkelsen R, Baunsgaard L, Blennow A (2004) Functional characterization of α-glucan,water dikinase, the starch phosphorylating enzyme. Biochem J **377**: 525–532

Mikkelsen R, Blennow A (2005) Functional domain organization of the potato α-glucan, water dikinase (GWD): evidence for separate site catalysis as revealed by limited proteolysis and deletion mutants. Biochem J **385**: 355–361

Mikkelsen R, Mutenda KE, Mant A, Schü Rmann P, Blennow A (2005) Glucan, water dikinase (GWD): a plastidic enzyme with redox-regulated and coordinated catalytic activity and binding affinity. PNAS **102**: 1785–1790

Moon K, Park J, Park S, Lee H, Cho H, Min S, Park Y, Jeon J, Kim H (2021) A more accessible, time-saving, and efficient method for *in vitro* plant regeneration from potato protoplasts. Plants **10**: 781

Müller-Thurgau (1882) Through the accumulation of sugar in parts of the plant, lower in a row temperature. Agricultural yearbook of Switzerland **11**: 751–828

Nicolia A, Proux-Wéra E, Åhman I, Onkokesung N, Andersson M, Andreasson E, Zhu L (2015) Targeted gene mutation in tetraploid potato through transient TALEN expression in protoplasts. J Biotechnol **204**: 17–24

Nicolia A, Fält A, Hofvander P, Andersson A (2021) Protoplast-based method for genome editing in triploid potato. Methods Mol Biol **2264**: 177–186

Park J, Bae S, Kim JS (2015) Cas-Designer: a web-based tool for choice of CRISPR-Cas9 target sites. Bioinformatics **31**: 4014–4016

Pirone C, Gurrieri L, Gaiba I, Adamiano A, Valle F, Trost P, Sparla F (2017) The analysis of the different functions of starch-phosphorylating enzymes during the development of *Arabidopsis thaliana* plants discloses an unexpected role for the cytosolic isoform GWD2. Physiologia Plantarum **160**: 447–457

Pfister B, Zeeman SC (2016) Formation of starch in plant cells. Cell Mol Life Sci **73**: 2781–2807

Reed KM, Bargmann BOR (2021) Protoplast regeneration and its use in new plant breeding technologies. Front Genome Ed **3**: 734951

Ritte G, Lloyd JR, Eckermann N, Rottmann A, Kossmann J, Steup M (2002) The starch-related R1 protein is an alpha -glucan, water dikinase. Proc Natl Acad Sci USA **99**: 7166–7171

Ritte G, Heydenreich M, Mahlow S, Haebel S, Kotting O, Steup M (2006) Phosphorylation of C6- and C3-positions of glucosyl residues in starch is catalysed by distinct dikinases. FEBS Lett **580**: 4872–4876

Rivero M, Furman N, Mencacci N, Picca P, Toum L, Lentz E, Bravo-Almonacid F, Mentaberry A (2012) Stacking of antimicrobial genes in potato transgenic plants confers increased resistance to bacterial and fungal pathogens. J Biotechnol **157**: 334–343

Sandhya D, Jogam P, Allini VR, Abbagani S, Alok A (2020) The present and potential future methods for delivering CRISPR/Cas9 components in plants. J Genet Eng Biotechnol **18**: 25

Skoog F, Miller CO (1957) Chemical regulation of growth and organ formation in plant tissues cultured *in vitro*. Symp Soc Exp Biol **11**: 118–130

Smyth SJ (2017) Genetically modified crops, regulatory delays, and international trade. Food Energy Secur **6**: 78–86

Stuart R, Street HE (1971) Studies on the growth in culture of plant cells: further studies on the conditioning of culture media by suspension of *Acer pseudoplantanus* L. cells. J Exp Biol **22**: 96–106

Tavazza R, Ancora G (1986) Plant regeneration from mesophyll protoplasts in commercial potato cultivars (Primura, Kennebec, Spunta, Desirée). Plant Cell Rep **5**: 243–246

Tabata S, Hizukuri S (1971) Studies on starch phosphate: part 2. Isolation of glucose 3-phosphate and maltose phosphate by acid hydrolysis of potato starch. Starch **23**: 267–272

Tsai SQ, Zheng Z, Nguyen NT, Liebers M, Topkar VV, Thapar V, Wyvekens N, Khayter C, Iafrate AJ, Le LP, Aryee MJ, Joung JK (2015) GUIDE-seq enables genome-wide profiling of off-target cleavage by CRISPR-Cas nucleases. Nat Biotechnol **33**: 187–197

Uitdewilligen JGAML, Wolters AMA, van Eck HJ, Visser RGF (2022) Allelic variation for alpha-glucan water dikinase is associated with starch phosphate content in tetraploid potato. Plant Mol Biol **108**: 469–480

Uniyal AP, Mansotra K, Yadav SK, Kumar V (2019) An overview of designing and selection of sgRNAs for precise genome editing by the CRISPR-Cas9 system in plants. 3 Biotech **9**: 223

Viksø-Nielsen A, Blennow A, Jorgensen K, Kristensen KH, Jensen A, Moller BL (2001) Structural, physicochemical and pasting properties of starches from potato plants with repressed *r1*-gene. Biomacromolecules **2**: 836–843

Woo JW, Kim J, Kwon SI, Corvalan C, Cho SW, Kim H, Kim S-G, Kim S-T, Choe S, Kim JS (2015) DNA-free genome editing in plants with preassembled CRISPR-Cas9 ribonucleoproteins. Nat Biotechnol **33**: 1162–1164

Xu X, Pan S, Cheng S, Zhang B, Mu D, Ni P, Zhang G, Yang S, Li R, Wang J, Orjeda G, Guzman F, Torres M, Lozano R, Ponce O, Martinez D, De la Cruz G, Chakrabarti SK, Patil VU, Skryabin KG, Kuznetsov BB, Ravin NV, Kolganova TV, Beletsky AV, Mardanov AV, Di Genova A, Bolser DM, Martin DM, Li G, Yang Y, Kuang H, Hu Q, Xiong X, Bishop GJ, Sagredo B, Mejía N, Zagorski W, Gromadka R, Gawor J, Szczesny P, Huang S, Zhang Z, Liang C, He J, Li Y, He Y, Xu J, Zhang Y, Xie B, Du Y, Qu D, Bonierbale M, Ghislain M, Herrera Mdel R, Giuliano G, Pietrella M, Perrotta G, Facella P, O'Brien K, Feingold SE, Barreiro LE, Massa GA, Diambra L, Whitty BR, Vaillancourt B, Lin H, Massa AN, Geoffroy M, Lundback S, DellaPenna D, Buell CR, Sharma SK, Marshall DF, Waugh R, Bryan GJ, Destefanis M, Nagy I, Milbourne D, Thomson SJ, Fiers M, Jacobs JM, Nielsen KL, Sønderkær M, Iovene M, Torres GA, Jiang J, Veilleux RE, Bachem CW, de Boer J, Borm T, Kloosterman B, van Eck H, Datema E, Hekkert Bt, Goverse A, van Ham RC, Visser RG (2011) Genome sequence and analysis of the tuber crop potato. Nature **475**: 189–195

Zhou W, He S, Naconsie M, Ma Q, Zeeman SC, Gruissem W, Zhang P (2017) Alpha-glucan, water dikinase 1 affects starch metabolism and storage root growth in cassava (*Manihot esculenta* Crantz). Sci Rep **7**: 9863

Addendum 1

Macronutrient stock

Component	Concentration
KNO_3	74.0 g L^{-1}
$MgSO_4 \cdot 7H_2O$	49.2 g L^{-1}
KH_2PO_4	3.4 g L^{-1}

Micronutrient stock

Component	Concentration
H_3BO_3	1.5 g L^{-1}
$MnSO_4 \cdot H_2O$	5.0 g L^{-1}
$ZnSO_4 \cdot 7H_2O$	1.0 g L^{-1}
$Na_2MoO_4 \cdot 2H_2O$	1.2 g L^{-1}
$CuSO4 \cdot 5H_2O$	12.0 mg L^{-1}
$CoCl_2 \cdot 6H_2O$	12.0 mg L^{-1}
KI	380.0 mg L^{-1}

Iron stock

Component	Concentration
Na_2EDTA	1.4 g L^{-1}
$FeSO_4 \cdot 7H_2O$	1.9 g L^{-1}

Sugars stock

Component	Concentration
Sorbitol	6.25 g L^{-1}
Sucrose	6.25 g L^{-1}
D(-)Fructose	6.25 g L^{-1}
D(-)Ribose	6.25 g L^{-1}
D(+)Xylose	6.25 g L^{-1}
D(+)Mannose	6.25 g L^{-1}
L(+)Rhamnose monohydrate	6.25 g L^{-1}
D(+)Cellobiose	6.25 g L^{-1}
Myo-Inositol	2.50 g L^{-1}

Wash solution pH 5.6 (KOH)

Component	Concentration
Macronutrient stock	10.00 mL L^{-1}
Micronutrient stock	1.00 mL L^{-1}
Iron stock	10.00 mL L^{-1}
$CaCl_2$ stock (2 M)	3.00 mL L^{-1}
NaCl	14.03 g L^{-1}
NAA stock (2g L^{-1})	1.00 mL L^{-1}
BAP stock (1g L^{-1})	500.00 µL L^{-1}

Medium B pH 5.6 (KOH)

Component	Concentration
Murashige and Skoog basal medium	2.7 g L^{-1}
Casein hydrolysate	100.0 mg L^{-1}
NAA stock (2g L^{-1})	1.0 mL L^{-1}
BAB stock (1g L^{-1})	500.0 µL L^{-1}

Medium E pH 5.6 (KOH)

Component	Concentration
Macronutrient stock	10.00 mL L^{-1}
Micronutrient stock	1.00 mL L^{-1}
Iron stock	10.00 mL L^{-1}
Sugars stock	20.00 mL L^{-1}
Organic acids stock	10.00 mL L^{-1}
$CaCl_2$ stock (2 M)	1.25 mL L^{-1}
Casein hydrolysate	500.00 mg L^{-1}
Glucose	33.70 g L^{-1}
Mannitol	30.92 g L^{-1}
Bovine serum albumin	1.00 g L^{-1}
NAA stock (2g L^{-1})	500.00 µL L^{-1}
BAP stock (1g L^{-1})	400.00 µL L^{-1}

Medium C pH 5.6 (KOH)

Component	Concentration
Macronutrient stock	10.00 mL L^{-1}
Micronutrient stock	1.00 mL L^{-1}
Iron stock	10.00 mL L^{-1}
Sugars stock	20.00 mL L^{-1}
Organic acids stock	10.00 mL L^{-1}
Casein hydrolysate	500.00 mg L^{-1}
Glucose	36.95 g L^{-1}
Mannitol	37.35 g L^{-1}
PVP 10	20.00 g L^{-1}
NAA stock (2g L^{-1})	500.00 µL L^{-1}
BAP stock (1g L^{-1})	400.00 µL L^{-1}
Macerozyme	2.00 g L^{-1}
Cellulase RS	10.00 g L^{-1}
$CaCl_2$ stock (2 M)	3.00 mL L^{-1}

Chapter 4: Transgenic genome editing of *GWD1* in *Solanum tuberosum*

4.1 Introduction

During this study, a protoplast isolation and regeneration system was attempted (Chapter 3) that could be used for genome editing. Unfortunately the protoplasts only produced micro-calli and could not be regenerated into plants. We decided, therefore, to use a transgenic approach which has been used previously to edit plant genomes (Altpeter et al., 2005).

A vector series has been developed (Čermák et al., 2017) for production of plasmids allowing transgenic genome editing. These have been optimised for fast, modular assembly using the Golden Gate cloning system. One advantage of using Golden Gate cloning is that vectors can be constructed which express multiple guide RNA sequences that can modify several DNA loci simultaneously in a method known as multiplex genome editing (Kabadi et al., 2014). In this system, DNA fragments containing guide sequences with type IIS restriction enzyme sites at each end are aligned together in a specified linear order using a one-pot assembly method and ligated into a vector suitable for transformation of the chosen plant species.

The current research chapter uses the *pDIRECT_22C* vector system designed by Čermák et al., 2017. This vector already contains *Cas9* endonuclease and a Csy-type (CRISPR system yersinia) ribonuclease 4 (*Csy4*) RNase of *Pseudomonas aeruginosa* (Haurwitz et al., 2010; Čermák et al., 2017). The presence of *Csy4* in the vector allows guides linked together by Csy4 sites to be cleaved into individual guides post transcriptionally (Tsai et al., 2014). The Csy4 sites contain 5 bp complementary sequences that form a stem-loop which is cleaved by the Csy4 endoribonuclease (Haurwitz et al., 2010). This vector series has been used successfully in genome editing experiments in tobacco (*Nicotiana tabacum*), Arabidopsis (*Arabidopsis thaliana*), wheat (*Triticum aestivum*), tomato (*Solanum lycopersicum*), potato (*Solanum tuberosum*) barley (*Hordeum vulgare*) and *Medicago truncatula* (Čermák et al., 2017; Liu et al., 2019; Kieu et al., 2021). In this research chapter a transgenic approach to mutate *StGWD1* was attempted.

4.2 Materials and Methods

4.2.1 Plant material and growth conditions

Wild type *Solanum tuberosum* cv. Désirée plants were propagated as described in Section 3.2.2.

4.2.2 Production of gene editing plant transformation constructs by Golden Gate cloning

Three guide sequences aimed at mutating *StGWD1* (StGWD1-1, StGWD1-2 and StGWD1-3) and one for *StPDS* were designed. Three of these guides were identical to the ones described in chapter 3 (StGWD1-1, StGWD1-2 and StPDS). An additional guide sequence (StGWD1-3; 5'-TCAGTGGTAAGTACAGCATG-3') which has been demonstrated to mutate *StGWD1 in planta* (Carlsen et al., 2022) was also used. Golden Gate cloning was used to manufacture constructs containing the guide sequences, which were driven by the *CmYLCV* constitutive promoter. Some constructs contained only one guide (StPDS and StGWD1-3), while one other contained the StGWD1-1 and StGWD1-2 guides interspaced by *Csy4* repeats. Primer pairs to enable this (Table 4.1) were designed using the Voytas Lab Plant Genome Engineering Toolkit (http://crispr-multiplex.cbs.umn.edu; Čermák et al., 2017). Sequences encoding *Esp3I* or *SapI* restriction sites were incorporated into the primers allowing the amplification of guides and the promoter that could then be ligated together in a specific order within *pDIRECT_22C* (Figure 4.1).

To amplify each gRNA cassette for Golden Gate cloning, PCR reactions were set up using the Phusion proofreading DNA polymerase (Thermo Fischer Scientific) and primers described in Table 4.1. Each PCR reaction used *pDIRECT_22C* vector as template. The reactions proceeded in a thermocycler according to manufacturer's instructions for the Phusion DNA polymerase (Thermo Fischer Scientific).

Amplicons were separated on a 1.5 % (w/v) agarose-Tris borate EDTA gel containing 0.005% (v/v) ethidium bromide and visualised under ultraviolet light using a GelDoc imaging system (Thermo Fischer Scientific). Amplicons were purified from the agarose gel using the Wizard® SV Gel and PCR Clean-Up System (Promega Corp.) according to the manufacturer's instructions.

Table 4.1 Primer sequences used in this study to amplify desired regions of the vector cassette and integrate the sequences with restriction sites and the guide RNAs into *pDIRECT_22C*.

Gene	Primer Name	Sequence (5' – 3')	Amplicon length (bp)
Primer pairs for cloning			
StGWD1	Promoter_ *CmYLCV*	TGCTCTTCGCGCTGGCAGACATACTGTCCCAC	495
	CSY_GWD1-1	TCGTCTCCAGTGCAAGACGGCTGCCTATACGGCA GTGAAC	
	REP_GWD1-1	TCGTCTCACACTTGCAAGCAGTTTTAGAGCTAGA AATAGC	116
	CSY_GWD1-2	TCGTCTCCTGTCCTGTATGGCTGCCTATACGGCAG TGAAC	
	REP_GWD1-2	TCGTCTCAGACATTCGAGCAGTTTTAGAGCTAGA AATAGC	116
	CSY_term	TGCTCTTCTGACCTGCCTATACGGCAGTGAAC	
	Promoter_ *CmYLCV*	TGCTCTTCGCGCTGGCAGACATACTGTCCCAC	495
	CSY_GWD1-3	TCGTCTCCACTTACCACTGACTGCCTATACGGCAG TGAAC	
	REP_GWD1-3	TCGTCTCAAAGTACAGCATGGTTTTAGAGCTAGA AATAGC	116
	CSY_term	TGCTCTTCTGACCTGCCTATACGGCAGTGAAC	
StPDS	Promoter_ *CmYLCV*	TGCTCTTCGCGCTGGCAGACATACTGTCCCAC	495
	CSY_PDS	TCGTCTCCTGGCAAGAGTCCCTGCCTATACGGCA GTGAAC	
	REP_PDS	TCGTCTCAGCCAGCAATGCTGTTTTAGAGCTAGA AATAGC	116
	CSY_term	TGCTCTTCTGACCTGCCTATACGGCAGTGAAC	

The Golden Gate reaction was set up using "protocol 3A" described by Čermák et al., 2017. The following components were added to a PCR tube: 50 ng of the vector, 1-5 ng of each purified amplicon, 5 U SapI, 5 U Esp3I, 6 x 10^4 U T7 DNA ligase, 10 µl 2x T7 DNA ligase buffer and H_2O to a final volume of 20 µl. The reactions proceeded in a thermocycler as follows: 10 cycles of 37 ˚C for 5 min and 25 ˚C for 10 min, with a 4 °C hold. This led to the cloning of each guide into *pDIRECT_22C*, resulting in the plasmids *pDIRECT*:GWD1-1&2, *pDIRECT*:GWD1-3 and *pDIRECT*:PDS.

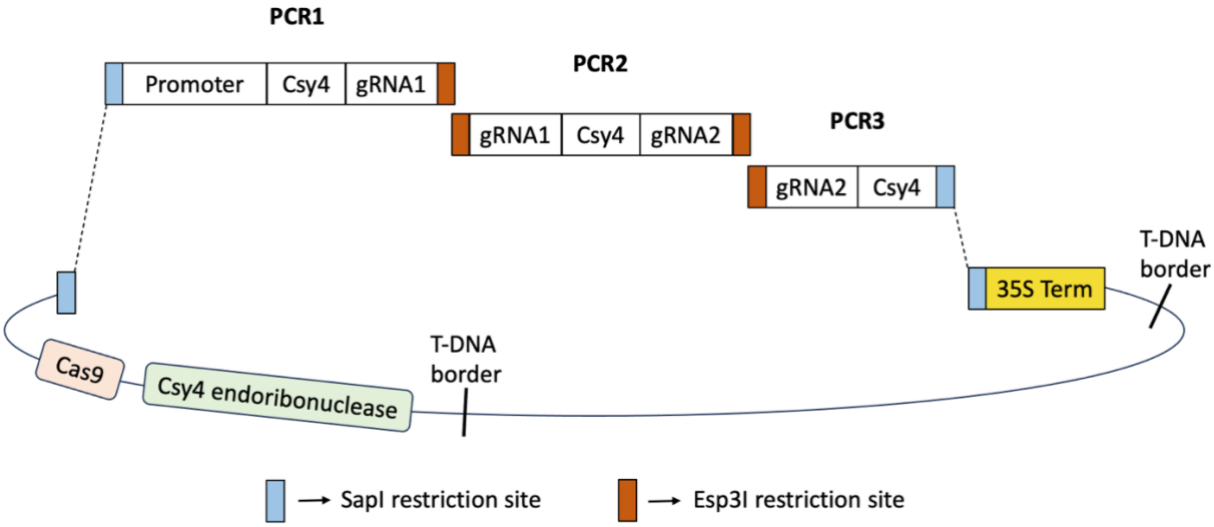

Figure 4.1. **Golden Gate cloning strategy**. PCR reactions required to amplify amplicons used in Golden Gate Cloning. Each 20 bp gRNA sequence was split between two primers that are used to create amplicons containing half the gRNA sequence. The first amplicon (PCR1) includes in the 5'-end the *SapI* restriction site, the *CmYLCV* promoter, *Csy4*, the first 12 nucleotides of the StGWD1-1 guide RNA, and an *Esp3I* restriction site in the 3'-end (Figure 4.1). The second amplicon (PCR2) also includes the *Esp3I* site, *Csy4* repeat, and the first 12 nucleotides of StGWD1-2 guide RNA in addition to the last 12 nucleotides of StGWD1-1 guide RNA. The final amplicon (PCR3) includes an *Esp3I* site, the final 12 nucleotides of StGWD1-2, a *Csy4* repeat and a *SapI* site. A similar set of amplicons were created for the StGWD1-3 and StPDS target sequences, with the exception of a *Csy4* repeat and a second target sequence.

4.2.3 Bacterial growth media

Bacteria were grown on sterile yeast extract peptone (YEP; 10 g L-1 yeast extract, 10 g L-1 peptone, 5 g L-1 NaCl, 12 g L-1 bacteriological agar), lysogeny broth agar (LBA; 10 g L-1 tryptone, 5 g L-1 yeast extract, 10 g L-1 NaCl and 15 g L-1 bacteriological agar) and liquid lysogeny broth (LB; 10 g L-1 tryptone, 5 g L-1 yeast extract, 10 g L-1 NaCl).

4.2.4 Transformation and confirmation of Golden Gate reaction into *Escherichia coli*

The Golden Gate reaction was transformed into DH5α *Escherichia coli* High Efficiency cells (New England Biolabs) according to the manufacturer's instructions. Colonies containing the inserts were confirmed by colony PCR and Sanger sequencing at the CAF sequencing

facilities using TC320 (5'-CTAGAAGTAGTCAAGGCGGC-3') and M13F (5'-GTAAAACGACGGCCAGT-3') primers (Čermák et al., 2017).

4.2.5 Preparation of *Agrobacterium tumefaciens* electro-competent cells

Agrobacterium tumefaciens strain GV2260 was plated on YEP media containing 50 mg mL^{-1} rifampicin. One colony was used to inoculate 5 mL liquid YEP containing 50 mg mL^{-1} rifampicin. The cultures were incubated for 16-18 h at 28 °C shaking at 150 rpm. This culture was used to inoculate 50 mL fresh liquid media and incubated until an OD_{600} of 0.5-0.7 was reached. The cultures were then placed on ice for 15 min before being centrifuged at 2350 x g for 10 min. The supernatant was discarded and the cells re-suspended in 50 mL of 10 % (v/v) glycerol. The previous two steps of centrifuging and re-suspending the cells were repeated. Aliquots of 100 µL from the re-suspended cells were inserted into 2 mL microcentrifuge tubes and snap-frozen in liquid N_2 for 10 min before being stored at -80 °C.

4.2.6 Transformation of *Agrobacterium tumefaciens*

All *pDIRECT*:gRNA vectors were transformed into *A. tumefaciens*. For electroporation, 100 µL of the ice cold suspension of electrocompetent cells were mixed with 150 ng plasmid DNA in a sterile microcentrifuge tube. This mixture was loaded into a chilled electroporation cuvette (gap = 2 mm) and shocked using the following parameters: 2.5 kV, 25 µF capacitance, and 200 Ohm resistance. One mL YEP medium was immediately added to the cuvette and the resulting bacterial suspension was transferred into a 2 mL microcentrifuge tube which was then incubated at 28 °C for 3 h shaking at 150 rpm. The cells were centrifuged at 4000 x g for 10 min before removing 700 µL of the supernatant and re-suspending the pellet in the remaining 300 µL. This was spread on YEP plates containing 50 µg mL^{-1} carbenicillin, 100 µg mL^{-1} rifampicin and 50 µg mL^{-1} kanamycin. The plates were incubated for 2 days at 28 °C.

4.2.7 *Solanum tuberosum* transformation with *Agrobacterium tumefaciens*

For plant transformation, the method outlined by Chetty et al., 2015 was used with a few minor modifications. Leaves from sterile tissue culture grown plants were sliced into approximately 1 cm^2 squares or approximately 5 mm long internodes and transferred onto sterile filter paper placed on 35 mL of clonal propagation medium (CPM; Table 4.2) in Petri

dishes. These were incubated for 48 h at 25 °C under a 16-h light and 8-h dark photoperiod (50 µmol photons m^2 s^{-1} of photosynthetically active radiation) under OrbitX Neptune LED 150W IP65 light emitting diode lights. A single colony of *Agrobacterium* was used to inoculate 2 mL of YEP containing 100 mg L^{-1} Rifampicin, 50 mg L^{-1} Kanamycin and Carbenicillin, and cultured with shaking at 150 rpm at 28°C for 48 h. After 48 h, 500 µL of the *Agrobacterium* culture was added to an additional 50 ml of YEP and incubated overnight while shaking at 150 rpm at 28 °C. The liquid cultures were then transferred to 50 mL tubes and centrifuged at 5150 x g for 10 min. The supernatant was discarded, and the pellet re-suspended in *Agrobacterium* infection media (AIM; Table 4.2) to an OD_{600} of 0.6 before acetosyringone was added to a final concentration of 2.5 mM in 30 mL of AIM-diluted *Agrobacterium* culture. Leaf explants were transferred into the *Agrobacterium* culture, and incubated with shaking for 20 min at 50 rpm. Explants were blot-dried using filter paper and transferred to Petri dishes containing filter paper placed on CIM. This was incubated for 48 h in the dark at 25 °C. After 48 h, the explants were blot-dried using filter paper and transferred to fresh CIM containing 500 mg L^{-1} carbenicillin, 100 mg L^{-1} kanamycin, and 250 mg L^{-1} cefotaxime. Any explants displaying *Agrobacterium* overgrowth after incubation in the

Table 4.2 Composition of *Agrobacterium* infection medium (AIM), Clonal propagation medium (CPM), Callus induction medium (CIM), shoot induction medium (SIM), root induction medium (RIM), all adjusted to pH 5.8. NAA = naphthalene acetic acid; MS = Murashige and Skoog salts with vitamins; GA_3 = Gibberellic acid.

Media components	**AIM**	**CPM**	**CIM**	**SIM**	**RIM**
MS salts with vitamins (g L^{-1})	4.3	4.3	4.3	4.3	4.3
Sucrose (g L^{-1})	30	30	20	20	20
Myoinositol (mg L^{-1})		100	100	100	100
NAA (mg L^{-1})		0.03	0.2	0.02	0.02
Zeatin riboside (mg L^{-1})			2.5	2	
GA_3 (mg L^{-1})			0.02	0.02	
Gelrite (g L^{-1})		2.23	2.23	2.23	

dark were rinsed four times in sterile H_2O, and rinsed again for 30 min with sterile H_2O containing 250 mg L^{-1} of cefotaxime. Explants were maintained in a growth room at 25 °C with

a 16/8-h light/dark photoperiod, and transferred to fresh CIM every two weeks until callus developed.

4.2.8 Confirmation of plant transformation

To confirm the insertion of each construct into the potato genome, PCR was used to analyse the putative transgenic lines. This was performed using a 2 mm^2 callus slice as DNA template and the Phire Plant Direct PCR Master Mix (Thermo Fischer Scientific., TC320 and M13F primers or *Cas9* primers (kind gift from Mr. Rudolph Bosman, Department of Genetics, Stellenbosch University (Table 4.3)). The reactions proceeded in a thermocycler according to Phire Plant Direct PCR Master Mix manufacturer's instructions (Thermo Fischer Scientific).

Table 4.3 Primer sequences used to amplify a *Cas9* fragment in *pDIRECT_22C* vector, and genomic DNA fragment from *Solanum tuberosum* containing sgRNA listed by Carlsen et al., 2022.

Gene	**Primer Name**	**Sequence (5' – 3')**	**Amplicon length (bp)**	**Annealing temperature (°C)**
Cas9	Cas9_F	ACTAAGGCTGAGAGGGGAGG	470	62
	Cas9_R	GATCTCACCGTTAGCGAGGG		
StGWD1-3	GWD1-3_F	CGTCCCATACAGGACATTCGAGCA	501	54
	GWD1-3_R	AAACTGCTCGAATGTCCTGTATGG		

4.2.9 Analysis of genome editing of *StGWD1* and *StPDS*

StGWD1 and St*PDS* target regions were amplified using Phire Plant Direct PCR Master Mix (Thermo Fischer Scientific) from putative transgenic callus and wild-type Désirée using Primers described in Table 3.1 (Chapter 3), and *StGWD1-3* primers described in Table 4.3. Amplicons were purified using the Wizard® SV Gel and PCR Clean-Up System (Promega Corp.) according to the manufacturer's instructions, and were sequenced at the Central Analytical Facility at Stellenbosch University.

4.3 Results

4.3.1 Amplifying guide RNA sequences for Golden Gate cloning

In order to mutate *StGWD1* in potato, two *pDIRECT_22C* vectors were designed containing three different guides. One of these vectors contained two guides previously designed for use in a non-transgenic approach (Chapter 3), and the other vector contained a guide from a recently published paper (Carlsen et al., 2022). A previously designed guide sequence by Bánfalvi et al., 2020 targeting *StPDS* was used to act as a positive control.

Polymerase chain reaction products containing *SapI* and *Esp3I* on the 5'- and 3'-ends respectively, along with the gRNA sequences were amplified. One of the primers for the first PCR amplicon (PCR1) binds at 2 places in the vector, meaning that two amplicons of 495 bp and 610 bp are synthesised (Figure 4.2A). The 495 bp amplicon containing only one *Csy4* repeat and the first half of the first guide were purified from PCR1 (Figure 4.2B, C, PCR1). The PCR reactions containing the remaining guide RNA segments and *Csy4* repeats are 116 bp in length (Table 4.1) as they only amplify one 20 bp *Csy4* repeat and a 76 bp spacer sequence.

4.3.2 CRISPR/Cas9 T-DNA Vector Assembly

For Golden Gate cloning, the StGWD1-1 and StGWD1-2 target sequences were ligated together into the *pDIRECT_22C* vector, whereas StGWD1-3 and StPDS target sequences were ligated individually (Figure 4.3). Three primer pairs were created to amplify targeted sections of the vector cassette for StGWD1-1 and StGWD1-2 (Table 4.1). A similar procedure was followed for the StPDS and StGWD1-3 target sequences, but which required only two primer pairs (Table 4.1). After *pDIRECT*:gRNA plasmid construction, and transformation into *E.coli,* the plasmids were isolated and sequenced. The results from this were then compared to the predicted plasmid sequence listed by Voytas Lab Plant Genome Engineering Toolkit (http://crispr-multiplex.cbs.umn.edu/assembly.php; Čermák et al., 2017), and successful insertion of the guide RNAs into *pDIRECT_22C* was confirmed. The *pDIRECT*:gRNAs vectors were then transformed into *A. tumefaciens* before being used to transform leaf explants.

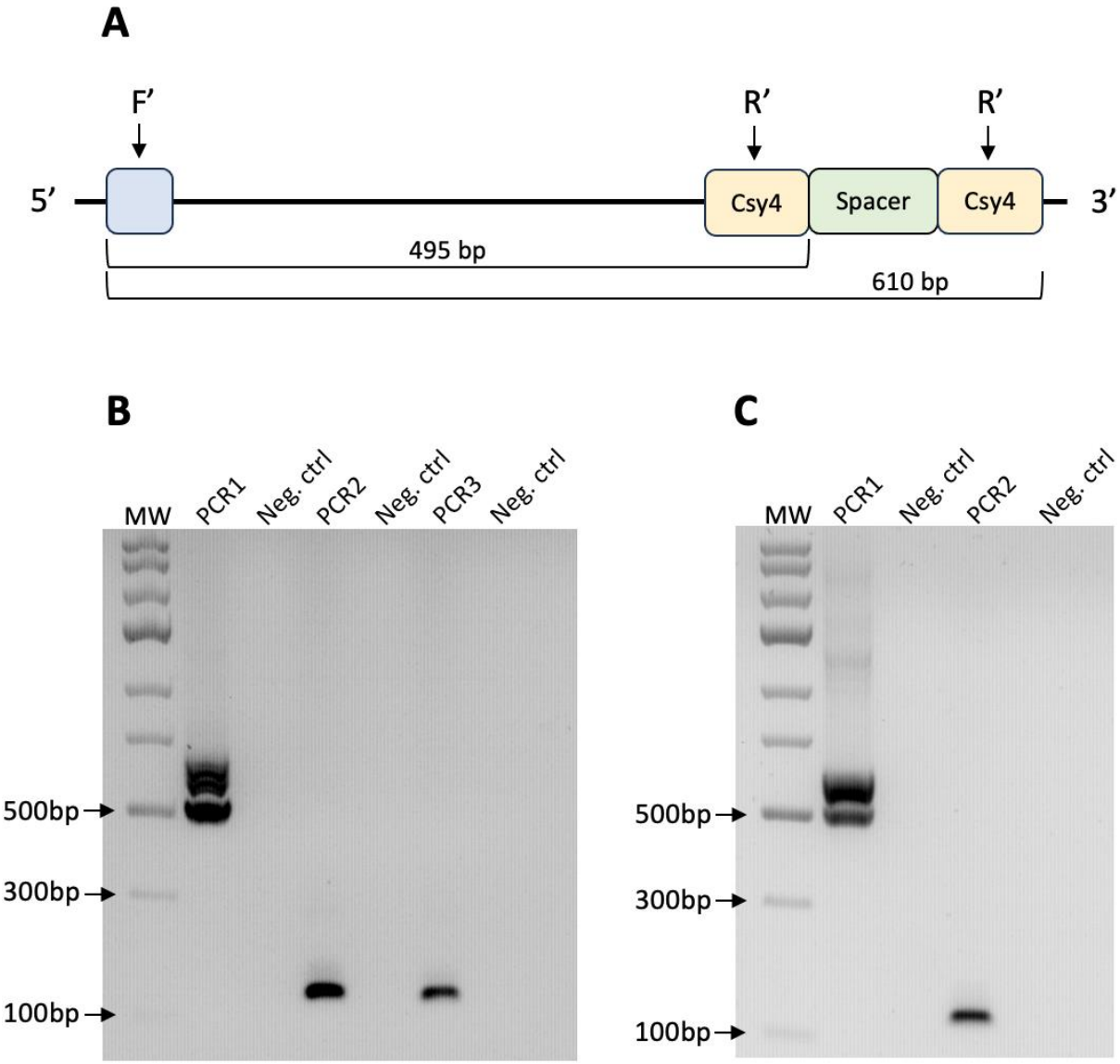

Figure 4.2. **Amplification of guide RNAs for Golden Gate assembly into *pDIRECT_22C*.** **(A)** Two products can be amplified in PCR1 (when amplifying the fragment containing the promoter) since the template vector has two Csy4 repeats, and the reverse primer binds to either sequence. **(B)** Three PCR reactions are required to amplify two guide RNA sequences (StGWD1-1 and StGWD1-2), and a control reaction without DNA template was included for each PCR reaction. PCR1 contains the promoter sequence and the first half of the first guide. Due to the presence of two *Csy4* repeats within the template vector, PCR1 amplifies two amplicons containing either one or two *Csy4* repeats, and the shorter band containing one *Csy4* repeat is used in Golden Gate assembly. **(C)** Two PCR reactions are required to amplify the guide RNA fragments, spacers and promoter required for the insertion of one guide RNA into *pDIRECT_22C* (StGWD1-3 and/or StPDS). MW = GeneRuler Express DNA ladder (Thermo Fischer Scientific).

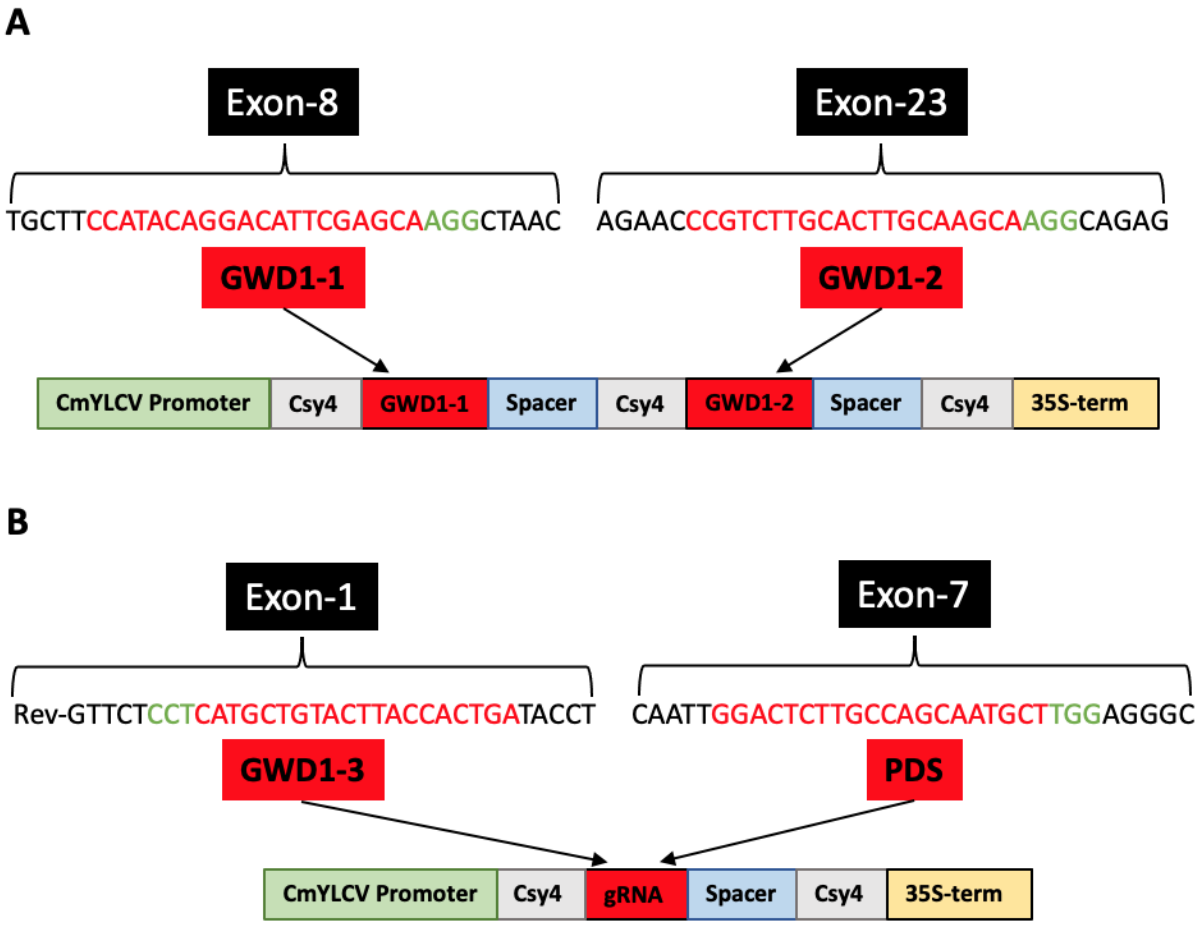

Figure 4.3. **Diagram of the Cas9/sgRNA *pDIRECT_22C* vector and target site selection in the *StGWD1* and *StPDS* genes.** **(A)** Guide sequences from exon 8 (StGWD1-1) and 23 (StGWD1-2) in Désirée were combined into one construct. The sequence of the guide RNAs are indicated in red, with the PAM (AGG) sequence indicated in green. The structure of the final pDIRECT:GWD1-1&2 vector cassette is represented with a *CmYLCV* promoter, the two cloned sgRNAs, Csy4 sequences, the spacer sequences, and a 35S terminator. **(B)** The same structure is indicated for the StGWD1-3 and StPDS guides that were independently cloned into separate pDIRECT_22C vectors.

4.3.3 *Solanum tuberosum* transformation

Solanum tuberosum, cv Désirée, leaf discs and petiole segments were employed as explants for transformation by *A. tumefaciens* GV2260 carrying *pDIRECT*:gRNAs. After slicing the leaves into approximately 1 cm^2 squares, the leaf discs and petioles were infected for each *pDIRECT*:gRNA plasmid (*pDIRECT*:GWD1-1&2; *pDIRECT*:GWD1-3; *pDIRECT*:PDS; Figure 4.4A). About 5-10% of *pDIRECT*:gRNA transformed explants generated antibiotic resistant callus

after 8 weeks on CIM (Figure 4.4B). *A. tumefaciens* containing no binary vector was used as a negative control and no calli regenerated from these transformation experiments (Table 4.4).

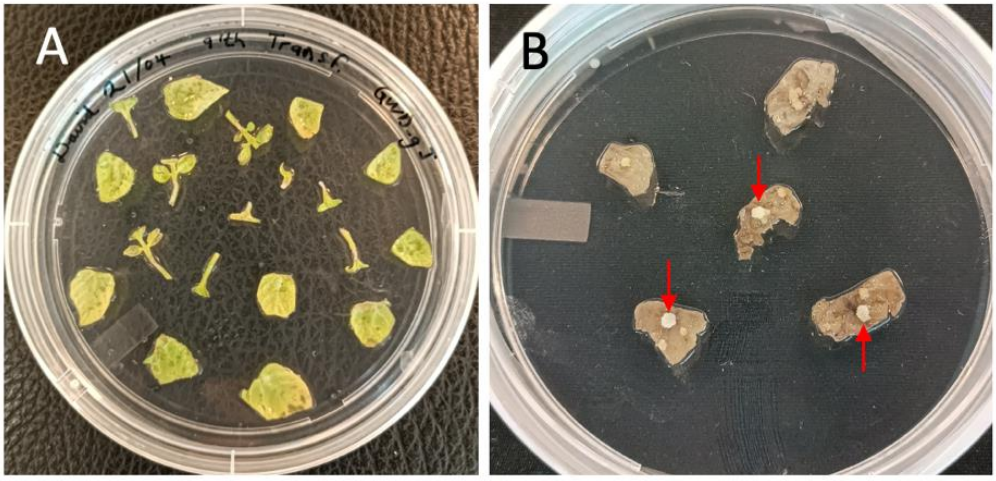

Figure 4.4. ***S. tuberosum*** **explants after co-cultivation with** ***A. tumefaciens*** **containing** ***pDIRECT*****:gRNAs**. **(A)** Leaf discs placed on CIM directly after infection with *A. tumefaciens*. **(B)** Antibiotic resistant calli appearing on leaf explants (indicated with red arrows) after 8-9 weeks.

Table 4.4 Summary of *S. tuberosum* transformation.

Vector	No. of Leaf Discs	No. of Petioles	Antibiotic-Resistant Calli		No. of Tested Calli
			No. of Leaf Discs	No. of Petioles	
pDIRECT:GWD1-1&2	100	80	8	3	10
pDIRECT:GWD1-3	100	80	5	2	7
pDIRECT:PDS	100	80	7	3	8
A. tumefaciens without vector	100	80	0	0	0

4.3.4 Analysis of trans DNA integration

Analysis of T-DNA integration was performed on putative transgenic calli (Table 4.4) by PCR using gDNA as template. TC320 and M13F primers were used to amplify the sgRNA cassette, and Cas9 primers (Table 4.3) to amplify a section of *Cas9*. Integration of the sgRNA cassette was confirmed for five out of ten calli transformed for StGWD1-1 and StGWD1-2, five out of seven for StGWD1-3 and five out of eight for StPDS (Figure 4.5A, B). All calli containing guides also contained the *Cas9* encoding gene (Figure 4.5C).

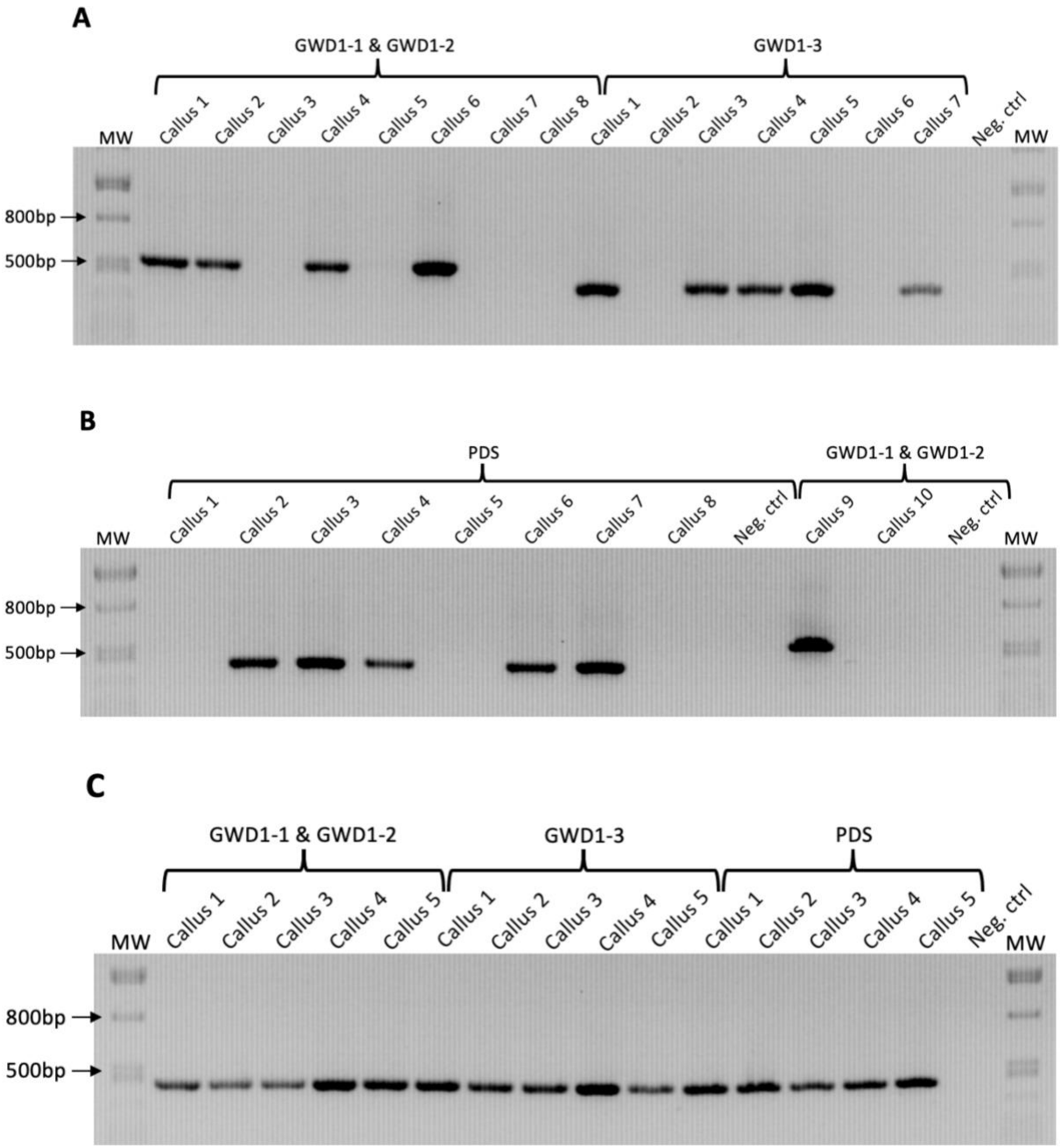

Figure 4.5. **<u>The detection of transgene integration into the genome of Désirée potato calli using PCR</u>**. **(A)** integration of StGWD1-1, StGWD1-2, and StGWD1-3. **(B)** Integration of the StPDS guide in eight tested calli, and integration of StGWD1-1 and StGWD1-2 in an additional two calli. **(C)** Integration of *Cas9*. MW = λ DNA digested with *PstI*, and Neg. ctrl is the same PCR reaction but without DNA template. The full images are in the supplementary information section and labelled Figure S4.1.

4.3.5 Analysis of CRISPR/Cas gene-editing

For each of the confirmed transgenic calli, amplicons representing the target were amplified from gDNA and sequenced. The same fragments were also amplified from gDNA isolated from untransformed plants and sequenced. Sequencing results were analysed using Tracking of Indels by DEcomposition (TIDE) analysis (http://shinyapps.datacurators.nl/tide/; Brinkman et al., 2014). In all samples, *in silico* analyses of the DNA sequences did not exhibit any editing or nucleotide modifications in the expected positions at the guide targets, and the DNA sequences matched that of the wild-type Désirée sequence.

4.4 Discussion

Ensuring both the quantity and quality of food supply will be necessary to meet the increasing global population. Potatoes are the fourth most important staple crop after maize, rice and wheat. When compared to other prospective food crops such as rice, wheat and maize, potato can deliver more carbohydrates, proteins, minerals, and vitamins per unit of time and land (https://www.fao.org/3/i0500e/i0500e.pdf).

When potato tubers are stored at temperatures below 6 °C, starch is catabolised to produce reducing sugars in a process called cold induced sweetening (CIS). These reducing sugars produce acrylamide when heated to high temperatures, which is a potential carcinogen, but which also demonstrates neurotoxicity and genotoxicity in animal models (Exon, 2006; Yang et al. 2016; Benford et al., 2022). Consuming potato goods that contain acrylamide has raised cancer concerns (Zaheer and Akhtar, 2016) and residue limits for acrylamide in potato chips has been set by the European Commission at 750 μg kg^{-1} (Powers et al., 2017). A survey by the European Food Safety Authority has demonstrated that the average acrylamide content in fried products can be as high as 1 mg kg^{-1} (Panel, 2015), but it is impractical to measure the acrylamide content in home-prepared potato products (Matthäus and Haase, 2014) and so lowering reducing sugar amounts in cold stored tubers is the preferred method of maintaining food safety. Since acrylamide was identified as a probable human carcinogen by the International Agency for Research on Cancer (IARC) in 1994, food scientists have worked to reduce acrylamide in heated meals while preserving desired colour and flavour attributes (El-Sayed et al., 2023). Reverse genetic methods have demonstrated the functionality of enzymes involved in starch degradation during CIS,

including α-glucan, water dikinase 1 (GWD1; Lorberth et al., 1998; Rommens et al., 2006; Xiao et al., 2018).

The improvement of potato traits has been achieved through the use of various breeding and molecular approaches. Traditional potato breeding methods aim to improve production, processing, and storage quality (Halterman et al., 2016). Although targeted trait improvement with less intraspecific variability has been accomplished through traditional breeding, the progress is generally slow and restricted (Hameed et al., 2018). As potatoes are complex tetraploids, more than one allele may need to be successfully modified in order for a trait to be expressed (Nadakuduti et al. 2018). Previous attempts to reduce CIS using traditional breeding techniques have met with limited success (Hameed et al., 2018); however, Xiao et al. (2018) were able to identify a quantitative trait loci for CIS on chromosome 5 that contains *GWD1* as well as QTL's on 2 other chromosomes.

New breeding techniques, such as Clustered Regularly Interspaced Short Palindromic Repeats/CRISPR Associated 9 (CRISPR/Cas9), offer an efficient method for crop plant trait enhancement as well as a platform for accurate and reliable plant genome editing (Jinek et al., 2012). Studies using CRISPR/Cas9 in potatoes have led to enhanced tuber starch quality (Andersson et al., 2017; Kusano et al., 2018) carotenoid biosynthesis (Khromov et al., 2018; Bánfalvi et al., 2020) and stress resistance (Hou et al., 2023) but have yet to reduce CIS.

The research described in this chapter focused on creating knockout mutations in the *StGWD1* gene through the application of the CRISPR/Cas9 system in potato. Mutation of *StGWD1* is expected to lead to plants that are less susceptible to CIS as this gene has been demonstrated to be involved in this process (Lorberth et al., 1998; Adegbaju, 2022). For this study we utilised the CRISPR/Cas9 system using the vector *pDIRECT_22C* (Čermák et al., 2017) that is especially useful for multiplexed gene editing. Previous studies have provided no clear evidence whether editing with a single gRNA is more efficient than when two or more are expressed simultaneously (Čermák et al., 2017; Carlsen et al., 2022); however, there is no decrease in efficiency when using multiple gRNAs (Kim et al., 2021) and this decreases the number of transformants required. In this study we designed two sgRNAs that targeted the exons 8 and 23 of *StGWD1* (Chapter 3). In addition, as positive controls we also used a gRNA that has recently been demonstrated to introduce indels in exon 1 of *StGWD1* (Carlsen et al., 2022) and a gRNA demonstrated to mutate *StPDS* (Bánfalvi et al., 2020) *in vivo*. The vector that was used already contains *Cas9* driven by a 35S promoter, and we chose the constitutive

CmYLCV promoter to drive expression of the gRNA cassette. This promoter was chosen due to its ability to drive gene expression in Solanaceous species in many different tissue types – including callus – at higher levels compared to other strong constitutive promoters (Stavolone et al., 2003). The *Csy4* post-transcriptional processing system was used to separate single guides from a multiple guide RNA transcript (Figure 4.1). An endoribonuclease also present within the T-DNA borders of pDIRECT-22C recognises and cleaves RNA-Stem loops created by *Csy4* elements between gRNA sequences (Haurwitz et al., 2010). This processing system has been successfully used in the past to produce multiple gRNAs from one transcript in other Solanaceous species (Čermák et al., 2017).

Several calli developed from the potato explants that had been transformed using *Agrobacterium* containing one of the vectors, but none of these regenerated into plants. Leaf discs were also transformed with *Agrobacterium* lacking *pDIRECT_22C* plasmid, and these did not regenerate on kanamycin, indicating that the selection system is effective. All the calli which formed contained the expected gRNA and Cas9 sequences within their genomes (Figure 4.5) demonstrating that they were transgenic.

Regions surrounding the target sites of transgenic calli were amplified and sequenced before being analysed using TIDE (Brinkman et al., 2014). This allows examination of mutation events which can be complicated in polyploid genomes – such as potato – where multiple alleles exist. The analysis enables examination of individual allelic sequences in complex Sanger sequencing data, which would show a multitude of nucleotide peaks at or around the location of double-stranded break repairs if editing of one or more allele has occurred. This analysis revealed that none of the chosen guides had created site-specific mutations despite them being designed in accordance with the best guidelines using CRISPR-RGEN, CRISPR P and CRISPOR programs (Chapter 3). All four guides used in this study contained a GC content ≥ 45 % which is correlated to editing efficiency (Bortesi et al., 2016; Malik et al., 2021), and the designed gRNAs had the highest mean score across the three *in silico* guide design platforms (Chapter 3, Section 3.3.1). The application of a multiplex system using 2 guides was intended to increase the likelihood of a disruptive mutation by increasing the chance of the construct being efficacious *in vivo*, however, this did not lead to any editing. Two guides that have previously been demonstrated to function well (Bánfalvi et al., 2020, Carlsen et al., 2022) were used as controls, and also did not lead to any editing. Research has indicated that guide editing efficiency can range from 0 % up to 52 % for sgRNAs (Bialk et al., 2016; Kieu et al.,

2021; Carlsen et al., 2022); identifying mutation events may therefore require testing a large number of samples to increase the likelihood of identifying gene-edited plants.

It has recently been discovered that the capacity of Cas9 to locate the PAM sequence and bind to DNA in the gRNA region is significantly impacted by local chromatin structure (Wu et al., 2014; Kuscu et al., 2014). There is still a lack of knowledge regarding the Cas9 protein's target recognition and target specificity mechanisms (Cong et al., 2013; Hsu et al., 2013; Cho et al. 2014). Even with the best design guidelines, it has been suggested that cellular and sequence characteristics may make it challenging to effectively target some genes with CRISPR/Cas technology (Doench et al., 2014). The editing activity of CRISPR/Cas has been demonstrated to vary greatly because of both gRNA structure and the target region (Sansbury et al., 2019), which may be attributed to chromatin structure and active promoter regions. Another study that targeted disease susceptibility genes in potato used the same vector as in this one and designed two sgRNAs per gene in separate vectors, one targeting *MLO1* and the other targeting *HDS* susceptibility genes (Kieu et al., 2021). After transformation of both vectors into Désirée, tetra-allelic mutants were only found in 0-13 % of plants. Plants that only demonstrated mutations in some of the alleles ranged from 14-20 %.

One of the major limitations of *Agrobacterium*-mediated transformations is the stability and variability of transgene expression. Independent transgenic events produced by the same *Agrobacterium* strain frequently exhibit transgene expression ranging from none to very high (Harpster et al., 1988; Ni et al., 1995; Kieu et al., 2021). The most likely explanation for the lack of genome editing in callus within this study is that more plants need to be regenerated. As has been demonstrated previously, mutation rates vary from 0-20 % (Kieu et al., 2021), and there can be many reasons for this. The degree of transgene expression has been attributed to T-DNA integration characteristics such as inverted head-to-head repeats that occur often and are frequently linked to transgene silencing (Mishiba et al., 2005) as well as chromosome position, copy number and methylation (Nagaya et al., 2005; Regulski et al., 2013; Tsuchiya and Eulgem, 2013). Only 15 calli were produced and sequenced during this study, and as mutation rates can greatly vary it would be ideal to regenerate ≥100 putative transgenics per construct in future studies to identify mutants.

In conclusion, three gRNA sequences were used in this study to target the *StGWD1* gene and one gRNA sequence was used to target *StPDS*. The *pDIRECT_22C* vector system was used by *A. tumefaciens* to integrate gRNAs into the host genome, but none of the regenerated

callus demonstrated imperfect repair at putative cleavage sites. This may be due to a lack of T-DNA expression, inefficiency of the gRNAs chosen to target the genes, or the total editing efficiency was too low in this sample range to be detected. Although the *CmYLCV* promoter is known to lead strong expression in callus, this was not examined in this study due to lack of material and should be assessed in future experiments. Future research will also need to look at potentially optimising the *Agrobacterium* transformation protocol to improve the regeneration efficiency, allowing for a more efficient screening method of putative transgenic plants. As the degree of editing efficiency is variable, it would be ideal to grow many regenerants that can be screened to improve the likelihood of identifying mutants.

4.5 References

Adegbaju MS (2022) Analysis of interactions between glucan, water dikinase and either isoamylase or starch branching enzymes in determination of starch structure. https://tinyurl.com/bde7utj7

Altpeter F, Baisakh N, Beachy R, Bock R, Capell T, Christou P, Daniell H, Datta K, Datta S, Dix PJ, Fauquet C, Huang N, Kohli A, Mooibroek H, Nicholson L, Nguyen TT, Nugent G, Raemakers K, Romano A, Visser R (2005) Particle bombardment and the genetic enhancement of crops: Myths and realities. Mol Breed **15**: 305–327

Andersson M, Turesson H, Nicolia A, Fält AS, Samuelsson M, Hofvander P (2017) Efficient targeted multiallelic mutagenesis in tetraploid Potato (*Solanum tuberosum*) by transient crispr-cas9 expression in protoplasts. Plant Cel Rep **36**: 117–128

Bánfalvi Z, Csákvári E, VillányaV, Kondrák M (2020) Generation of transgene-free PDS mutants in potato by *Agrobacterium*-mediated transformation. BMC biotechnol **20**: 25

Benford D, Bignami M, Chipman JK, Ramos Bordajandi L (2022) Assessment of the genotoxicity of acrylamide. EFSA J **20**: e07293

Bialk P, Sansbury B, Rivera-Torres N, Bloh K, Man D, Kmiec EB (2016) Analyses of point mutation repair and allelic heterogeneity generated by CRISPR/Cas9 and single-stranded DNA oligonucleotides. Sci Rep **6**: 1-9

Bortesi L, Zhu C, Zischewski J, Perez L, Bassié L, Nadi R, Forni G, Lade SB, Soto E, Jin X, Medina V, Villorbina G, Muñoz P, Farré G, Fischer R, Twyman RM, Capell T, Christou P, Schillberg S (2016) Patterns of CRISPR/Cas9 activity in plants, animals and microbes. Plant Biotechnol J **14**: 2203-2216

Brinkman EK, Chen T, Amendola M, van Steensel B (2014) Easy quantitative assessment of genome editing by sequence trace decomposition. Nucleic Acids Res **42**: 22

Carlsen FM, Johansen IE, Yang Z, Liu Y, Westberg IN, Kieu NP, Jørgensen B, Lenman M, Andreasson E, Nielsen KL, Blennow A, Petersen BL (2022) Strategies for efficient gene editing in protoplasts of *Solanum tuberosum* theme: determining gRNA efficiency design by utilizing protoplast (Research). Front Genome Ed **3**: 1–12

Čermák T, Curtin SJ, Gil-Humanes J, Čegan R, Kono TJY, Konečná E, Belanto JJ, Starker CG, Mathre JW, Greenstein RL, Voytas DF (2017) A multipurpose toolkit to enable advanced genome engineering in plants. Plant Cell **29**: 1196–1217

Chetty VJ, Narváez-Vásquez J, Orozco-Cárdenas ML (2015) Potato (*Solanum tuberosum* L.). *Agrobacterium* protocols. Methods Mol Biol **1224**: 85–96

Cho SW, Kim S, Kim Y, Kweon J, Kim HS, Bae S, Kim JS (2014) Analysis of off-target effects of CRISPR/Cas-derived RNA-guided endonucleases and nickases. Genome Res **24**: 132–141

Cong L, Ran FA, Cox D, Lin S, Barretto R, Habib N, Hsu PD, Wu X, Jiang W, Marraffini LA, Zhang F (2013) Multiplex genome engineering using CRISPR/Cas systems. Science **339**: 819–823

Doench JG, Hartenian E, Graham DB, Tothova Z, Hegde M, Smith I, Sullender M, Ebert BL, Xavier RJ, Root DE (2014) Rational design of highly active sgRNAs for CRISPR-Cas9-mediated gene inactivation. Nat Biotechnol **32**: 1262–1267

Edner C, Li J, Albrecht T, Mahlow S, Hejazi M, Hussain H, Kaplan F, Guy C, Smith SM, Steup M, Ritte G (2007) Glucan, water dikinase activity stimulates breakdown of starch granules by plastidial β-amylases. Plant Physiol **145**: 17–28

El-Sayed AA, El-Maaty SMA, Abdelhady MM (2023) Acrylamide reduction in potato chips as functional food product via application of enzymes, baker's yeast, and green tea powder. Scientific African **20**: 2468-2276

Exon JH (2006) A review of the toxicology of acrylamide. J Toxicol Environ Health B Crit Rev **9**: 397–412

González MN, Massa GA, Andersson M, Turesson H, Olsson N, Fält AS, Storani L, Décima Oneto CA, Hofvander P, Feingold SE (2020) Reduced enzymatic browning in potato tubers by specific editing of a polyphenol oxidase gene via ribonucleoprotein complexes delivery of the CRISPR/Cas9 system. Front Plant Sci **10**: 1649

Halterman D, Guenthner J, Collinge S, Butler N, Douches D (2016) Biotech potatoes in the 21st century: 20 years since the first biotech potato. Am J Potato Res **93**: 1–20

Hameed A, Zaidi SS, Shakir S, Mansoor S (2018) Applications of new breeding technologies for potato improvement. Front Plant Sci **9**: 925

Harpster MH, Townsend JA, Jones JDG, Bedbrook J, Dunsmuir P (1988) Relative strengths of the 35S cauliflower mosaic virus, 1', 2', and nopaline synthase promoters in transformed tobacco sugarbeet and oilseed rape callus tissue. Mol Gen Genet **212**: 182–190

Haurwitz RE, Jinek M, Wiedenheft B, Zhou K, Doudna JA (2010) Sequence- and structure-specific RNA processing by a CRISPR endonuclease. Science **329**: 1355–1358

Hou X, Guo X, Zhang Y, Zhang Q (2023) CRISPR/Cas genome editing system and its application in potato. Front Genet **14**: 1017388

Hsu PD, Scott DA, Weinstein JA, Ran FA, Konermann S, Agarwala V, Li Y, Fine EJ, Wu X, Shalem O, Cradick TJ, Marraffini LA, Bao G, Zhang F (2013) DNA targeting specificity of RNA-guided Cas9 nucleases. Nat Biotechnol **31**: 827–832

Jinek M, Chylinski K, Fonfara I, Hauer M, Doudna JA, Charpentier E (2012) A programmable dual-RNA-guided DNA endonuclease in adaptive bacterial immunity. Science **337**: 816–821

Jung C, Capistrano-Gossmann G, Braatz J, Sashidhar N, Melzer S (2018) Recent developments in genome editing and applications in plant breeding. Plant Breed **137**: 1–9

Kabadi AM, Ousterout DG, Hilton IB, Gersbach CA (2014) Multiplex CRISPR/Cas9-based genome engineering from a single lentiviral vector. Nucleic Acids Res **42**: e147

Khromov AV, Gushchin VA, Timberbaev VI, Kalinina NO, Taliansky ME, Makarov VV (2018) Guide RNA design for CRISPR/Cas9-mediated potato genome editing. Dokl Biochem Biophys **479**: 90–94

Kieu NP, Lenman M, Wang ES, Petersen BL, Andreasson E (2021) Mutations introduced in susceptibility genes through CRISPR/Cas9 genome editing confer increased late blight resistance in potatoes. Sci Rep **11**: 4487

Kim WN, Kim HJ, Chung YS, Kim HU (2021) Construction of multiple guide RNAs in CRISPR/cas9 vector using stepwise or simultaneous golden gate cloning: case study for targeting the FAD2 and FATB multigene in soybean. Plants (Basel) **10**: 2542

Kusano H, Ohnuma M, Mutsuro-Aoki H, Asahi T, Ichinosawa D, Onodera H, Asano K, Noda T., Horie T, Fukumoto K, Kihira M, Teramura H, Yazaki K, Umemoto N, Muranaka T, Shimada H (2018) Establishment of a modified CRISPR/Cas9 system with increased mutagenesis frequency using the translational enhancer dMac3 and multiple guide RNAs in potato. Scientific Reports **8**: 13753

Kuscu C, Arslan S, Singh R, Thorpe J, Adli M (2014) Genome-wide analysis reveals characteristics of off-target sites bound by the Cas9 endonuclease. Nat Biotechnol **32**: 677–683

Li JF, Norville JE, Aach J, McCormack M, Zhang D, Bush J, Church GM, Sheen J (2013) Multiplex and homologous recombination-mediated genome editing in *Arabidopsis* and *Nicotiana benthamiana* using guide RNA and Cas9. Nat Biotechnol **31**: 688–691

Liu Y, Gao Y, Gao Y, Zhang Q (2019) Targeted deletion of floral development genes in *Arabidopsis* with CRISPR/Cas9 using the RNA endoribonuclease Csy4 processing system. Hortic Res **6**: 1–10

Lorberth R, Ritte G, Willmitzer L, and Kossmann J (1998) Inhibition of a starch-granule-bound protein leads to modified starch and repression of cold sweetening. Nat Biotechnol **16**: 473–477

Malik A, Gul A, Munir F, Amir R, Alipour H, Babar MM, Bakhtiar SM, Paracha RZ, Khalid Z, Hayat MQ (2021) Evaluating the cleavage efficacy of CRISPR-Cas9 sgRNAs targeting ineffective regions of *Arabidopsis thaliana* genome. PeerJ **21**: 9

Matthäus B, Haase NU (2014) Acrylamide - still a matter of concern for fried potato food? Eur J Lipid Sci **116**: 675–687

Mikkelsen R, Mutenda KE, Mant A, Schurmann P, Blennow A (2005) Alpha-glucan, water dikinase (GWD): a plastidic enzyme with redox-regulated and coordinated catalytic activity and binding affinity. Proc Natl Acad Sci USA **102**: 1785–1790

Mishiba K, Nishihara M, Nakatsuka T, Abe Y, Hirano H, Yokoi T, Kikuchi A, Yamamura S (2005) Consistent transcriptional silencing of 35S-driven transgenes in gentian. Plant J **44**: 541–556

Nadakuduti SS, Buell CR, Voytas DF, Starker CG, Douches DS (2018) Genome editing for crop improvement – applications in clonally propagated polyploids with a focus on potato (*Solanum tuberosum* L.). Front Plant Sci **871**: 1–11

Nagaya S, Kato K, Ninomiya Y, Horie R, Sekine M, Yoshida K, Shinmyo A (2005) Expression of randomly integrated single complete copy transgenes does not vary in *Arabidopsis thaliana*. Plant Cell Physiol **46**: 438–444

Ni M, Cui D, Einstein J, Narasimhulu S, Vergara CE, Gelvin SB (1995) Strength and tissue specificity of chimeric promoters derived from the octopine and mannopine synthase genes. Plant J **7**: 661–676

Panel (2015) Scientific Opinion on acrylamide in food. EFSA J **13**: 4104 10.2903/j.efsa.2015.4104

Powers SJ, Mottram DS, Curtis A, Halford NG (2017) Acrylamide levels in potato crisps in Europe from 2002 to 2016. Food Addit Contam Part A Chem Anal Control Expo Risk Assess **34**: 2085–2100

Regulski M, Lu Z, Kendall J, Donoghue MT, Reinders J, Llaca V, Deschamps S, Smith A, Levy D, McCombie WR, Tingey S, Rafalski A, Hicks J, Ware D, Martienssen RA (2013) The maize methylome influences mRNA splice sites and reveals widespread paramutation-like switches guided by small RNA. Genome Res **23**: 1651–1662

Rommens CM, Ye J, Richael C, Swords K (2006) Improving potato storage and processing characteristics through all-native DNA transformation. J Agric Food Chem **54**: 9882–9887

Sansbury BM, Hewes AM, Kmiec EB (2019) Understanding the diversity of genetic outcomes from CRISPR-Cas generated homology- directed repair. Commun Biol **2**: 458

Stavolone L, Kononova M, Pauli S, Ragozzino A, de Haan P, Milligan S, Lawton K, Hohn T (2003) Cestrum yellow leaf curling virus (CmYLCV) promoter: a new strong constitutive promoter for heterologous gene expression in a wide variety of crops. Plant Mol Biol **53**: 663–673

Tsai SQ, Wyvekens N, Khayter C, Foden JA, Thapar V, Reyon D, Goodwin MJ, Aryee MJ, Joung JK (2014) Dimeric CRISPR RNA-guided *FokI* nucleases for highly specific genome editing. Nat Biotechnol **32**: 569–576

Tsuchiya T, Eulgem T (2013) An alternative polyadenylation mechanism coopted to the *Arabidopsis RPP7* gene through intronic retrotransposon domestication. Proc Natl Acad Sci USA **110**: E3535–E3543.

Wu X, Scott DA, Kriz AJ, Chiu AC, Hsu PD, Dadon DB, Cheng AW, Trevino AE, Konermann S, Chen S, Jaenisch R, Zhang F, Sharp PA (2014) Genome-wide binding of the CRISPR endonuclease Cas9 in mammalian cells. Nat Biotechnol **32**: 670–676

Xiao G, Huang W, Cao H, Tu W, Wang H, Zheng X, Liu J, Song B, Xie C (2018) Genetic loci conferring reducing sugar accumulation and conversion of cold-stored potato tubers revealed by QTL analysis in a diploid population. Front Plant Sci **9**: 315

Yang Y, Achaerandio I, Pujolà M (2016) Influence of the frying process and potato cultivar on acrylamide formation in French fries. Food Control **62**: 216–223

Yano R, Nakamura M, Yoneyama T, Nishida I (2005) Starch-related α-glucan/water dikinase is involved in the cold-induced development of freezing tolerance in *Arabidopsis*. Plant Physiol **138**: 837–846

Zaheer K, Akhtar MH (2016) Potato production, usage, and nutrition—a review. Crit Rev Food Sci Nutr **56**: 711–721

Supplementary information

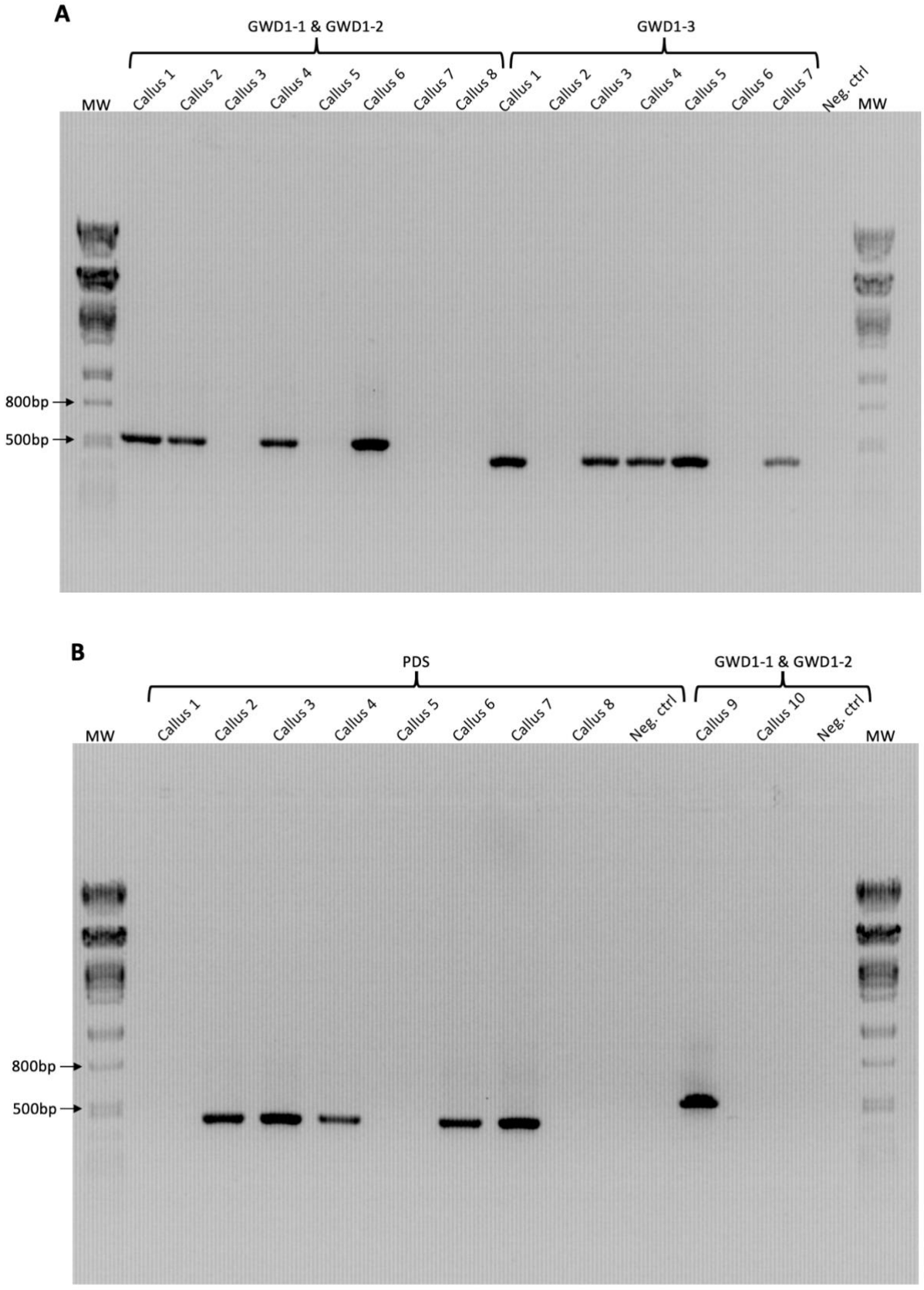

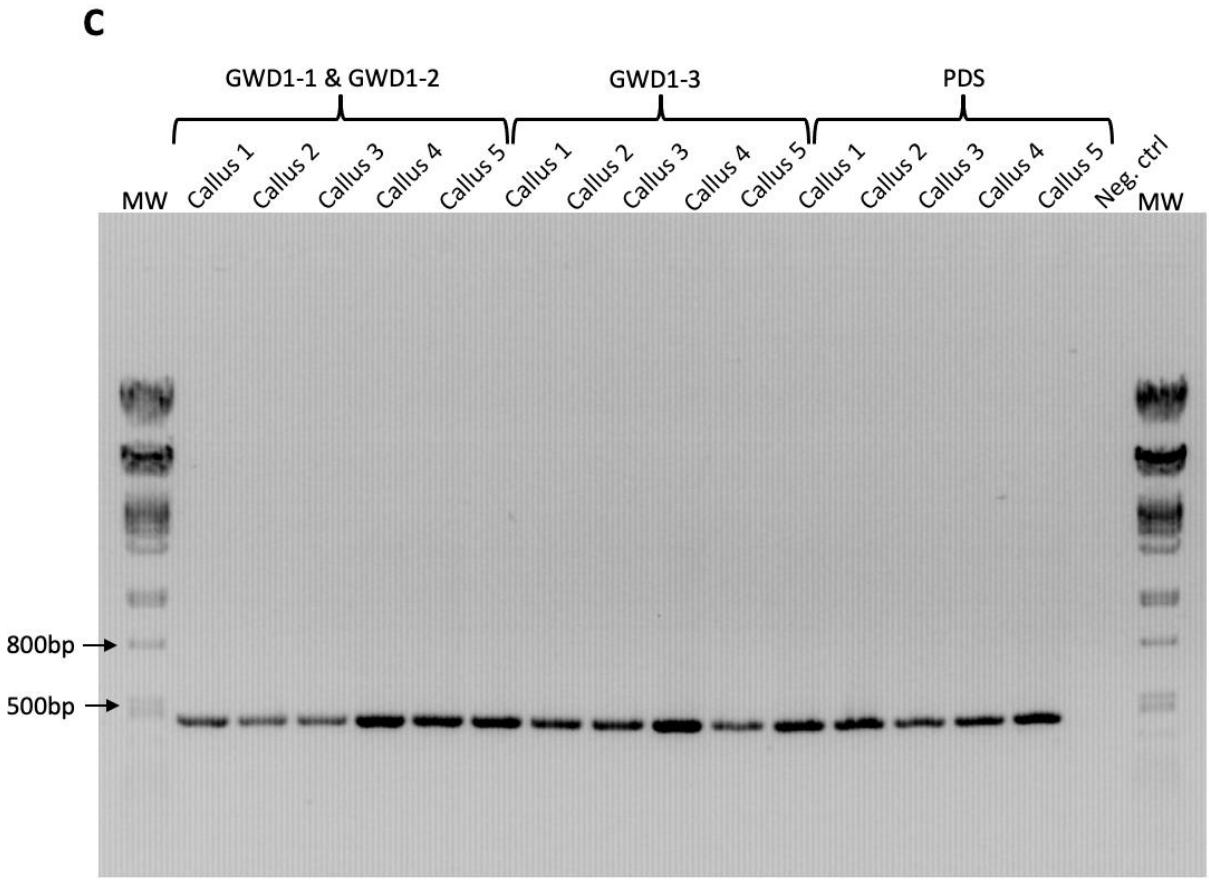

Figure S4.1. Agarose gel depicting PCR screening of gRNA and *Cas9* integration from *pDIRECT_22C* vector into host plant genome.

Chapter 5: Conclusion

5.1 Synopsis of this study

Genome editing offers an exciting and efficient way to improve future plant breeding efforts. In this study we aimed at targeting the α-glucan, water dikinase (*GWD1)* gene in *Solanum tuberosum* that encodes a starch phosphorylating protein. This gene has been shown to be involved in starch breakdown within tubers during cold storage leading to accumulation of reducing sugars (Lorberth et al., 1998; Rommens et al., 2006; Xiao et al., 2018) that form the neurotoxic and potentially carcinogenic compound acrylamide after exposure to high temperatures (Exon, 2006; Benford et al., 2022).

We started by trying to establish a transgene-free genome editing system using CRISPR/Cas ribonucleoproteins (RNPs) by isolating and regenerating potato protoplasts. After a successful isolation and regeneration system had been established, RNPs would be transformed into protoplasts. These RNPs can create double stranded DNA breaks and potentially produce mutations that will prevent GWD1 activity. Two single guide RNAs were designed to target *StGWD1* upstream of a region encoding a catalytically essential histidine (Table 3.3; Mikkelsen et al., 2004; Carlsen et al., 2022). Each of the guides' *in silico* analyses revealed low potential for off-target genome editing, and all the guides were transcribed *in vitro* to evaluate how well they cleaved amplified target sequences. On-target DNA cleavage was assessed *in vitro* for each RNP complex, and one of the guide RNAs demonstrated cleavage. Although this *in vitro* assay may provide supporting evidence for potential *in vivo* cleavage, it does not guarantee this. This is demonstrated by a guide RNA that was used as a positive control which functions efficiently *in vivo* (Bánfalvi et al., 2020), but which did not cleave its target *in vitro* (Figure 3.3B, C). This indicates that *in vitro* data is not necessarily a good predictor of *in vivo* activity. We then established and refined a method for separating viable potato protoplasts for RNP transformations (Figure 3.4). It proved very difficult to regenerate callus from protoplasts and we only managed to produce micro-calli (Figure 3.5). For this method to be effective, the entire protoplast culture process—from single cells to mature plants—must be accomplished.

As no plants were regenerated from protoplasts, we then progressed to using a transgenic approach. Guide RNAs were ligated into a transformation vector using Golden Gate

Cloning (Figure 4.3) and inserted into leaf explants using *Agrobacterium*-mediated transformation. From these explants we managed to obtain transgenic calli (Figure 4.5), but unfortunately that did not lead to editing of the desired gene.

5.2 Future prospects

The quality of processed goods is negatively impacted by cold-induced sweetening (CIS) in potatoes. After starch phosphorylation by GWD1 and GWD3, amylases are thought to be key enzymes involved in CIS by releasing soluble glucans from the starch molecule. Most research examining starch degradation has been performed in plant leaves, primarily using *Arabidopsis thaliana* where much, if not all of the pathway has been established. In that plant, two routes of starch degradation have been established, one where glucose is produced and one where maltose is formed. The route *via* maltose is more important as mutants effecting it have a much greater effect on starch degradation that mutants affecting the pathway *via* glucose. Although this pathway appears similar in potato leaves (Lorberth et al., 1998; Sitnicka D and Orzechowski, 2014; Van Harrselaar et al., 2017; Samodien et al., 2018; Orzechowski et al., 2021; Adegbaju, 2022) it is unclear if the same pathway is present in potato tubers (Sergeeva et al., 2022).

The underlying mechanism of starch degradation in leaves and tubers may differ as some proteins have been demonstrated to affect starch degradation in potato leaves, but not in tubers undergoing CIS (Lloyd et al., 2004; Hou et al., 2017; Samodien et al., 2018). The primary pathway of starch degradation in leaves includes the release of soluble glucans from starch granules which are catabolised to malto-oligosaccharides, maltose and glucose (Sergeeva et al., 2022). Less is known about this pathway during CIS. Repression of disproportionating enzyme 2 or the phosphatases SEX4 and LSF2 prevented starch degradation in potato leaves but not in tubers (Lloyd et al. 2004, Samodien et al., 2018). Starch degradation was decreased, however, in tubers after targeting *StAMY23*, *StBAM1*, *StBAM9* (Hou et al., 2017) or *StGWD1* (Lorberth et al., 1998) using RNAi technology. This could indicate that while degradation *via* the maltose pathway is important in leaves, the pathway is more plastic in tubers with functional redundancy between the glucose and maltose pathways. Alternatively, a different catabolic route may be being used in tubers. Starch phosphorylase is known to be present in plant tissues (Mori et al., 1991; Sonnewald et al., 1995) and could, in

principle, catalyse a phosphorolytic catabolic pathway. This enzyme plays only a small role in leaf starch degradation (Zeeman et al., 2004), whereas tubers could use this pathway primarily, or use both amylolytic and phosphorolytic pathways. Interestingly when expression of starch phosphorylase was down-regulated in combination with *StGWD1*, a reduction in CIS was observed (Rommens et al., 2006). This study did not, however, provide evidence that only starch phosphorylase affected CIS, and future research will need to determine this. A final alternative is that the 35S promoter used to repress DPE2, SEX4 or LSF2 (Lloyd et al. 2004, Samodien et al., 2018) may have been less effective in silencing in tubers than leaves. CRISPR/Cas9 could be used to overcome some of these issues and help unravel the starch degradation pathway in tubers.

For non-transgenic engineering of *StGWD1* to be successful, it is essential to generate potato protoplasts into callus and then plantlets. This step of the process is known to be difficult and can cause a bottleneck in the process due to the requirement for optimization. Based on research from additional studies requiring protoplast regeneration (Moon et al., 2021; Nicolia et al., 2021) potential modifications to the regeneration protocol outlined in chapter 3 are being investigated to determine the limiting factor. These include both increasing and decreasing protoplast cell densities during regeneration. Increasing cell density may facilitate the protoplasts conditioning the surrounding regeneration liquid medium, and decreasing cell density may provide more space for the protoplasts to divide within the alginate lenses. Additionally, the volume of the tissue culture vessel should be decreased which may promote conditioning factors released by protoplasts to achieve an optimum regeneration environment sooner.

After protoplast regeneration from wild-type plants has been successfully accomplished, each sgRNA-Cas9 complex created in this study can be used to edit cells. Potato leaves will then be harvested from *StGWD1* mutants and subjected to staining of starch by iodine. Leaves from edited plants are expected to stain blue because of their high starch contents (Lorberth et al., 1998). DNA isolated from plants demonstrating a starch excess phenotype can be sequenced and analysed using TIDE analysis to confirm gene editing. Starch and reducing sugar content of potato tubers can then be evaluated to determine whether CIS has decreased in plants where differing numbers of alleles are mutated. All regenerants will also be examined for unfavourable phenotypic alterations that might result from the gene knockouts or protoplast regeneration techniques.

Transgenic gene-editing techniques can also be used to create regenerants edited for *StGWD1*. A popular method of transgenesis in plants is *Agrobacterium*-mediated transformation. Although this would be less easy to commercialise than those plants produced by a non-transgenic method, for scientific studies it would be acceptable. Potato transformation takes several months, and it may be advantageous to test constructs for efficacy using other Solanaceous species that are transformed quicker. One potential plant that could be used is *Nicotiana tabacum* as it can produce transformed plants within several weeks and its genome demonstrates high sequence similarity to potato, meaning that the same guides can be used in both species. The use of this plant would provide evidence of *in vivo* guide efficiency before beginning the long and laborious task of protoplast transformation and regeneration, and should be the next step taken in this research study. It is exciting to consider the potential of new breeding techniques such as CRISPR/Cas and how they will be utilised to improve crop species in following years.

5.2 References

Adegbaju MS (2022) Analysis of interactions between glucan, water dikinase and either isoamylase or starch branching enzymes in determination of starch structure. https://tinyurl.com/bde7utj7

Benford D, Bignami M, Chipman JK, Ramos Bordajandi L (2022) Assessment of the genotoxicity of acrylamide. EFSA J **20**: e07293

Carlsen FM, Johansen IE, Yang Z, Liu Y, Westberg IN, Kieu NP, Jørgensen B, Lenman M, Andreasson E, Nielsen KL, Blennow A, Petersen BL (2022) Strategies for efficient gene editing in protoplasts of *Solanum tuberosum* theme: determining gRNA efficiency design by utilizing protoplast (Research). Front Genome Ed **3**: 1–12

Exon JH (2006) A review of the toxicology of acrylamide. J Toxicol Environ Health B Crit Rev **9**: 397–412

Hou J, Zhang H, Liu J, Reid S, Liu T, Xu S, Tian Z, Sonnewald U, Song B, Xie C (2017) Amylases StAmy23, StBAM1 and StBAM9 regulate cold-induced sweetening of potato tubers in distinct ways. J Exp Bot **68**: 2317–2331

Lloyd JR, Blennow A, Burhenne K, Kossmann J (2004) Repression of a novel isoform of disproportionating enzyme (StDPE2) in potato leads to inhibition of starch degradation in leaves but not tubers stored at low temperature. Plant Physiol **134**: 1347-1354

Lorberth R, Ritte G, Willmitzer L, Kossmann J (1998) Inhibition of a starch-granule-bound protein leads to modified starch and repression of cold sweetening. Nat Biotechnol **16**: 473–477

Mikkelsen R, Baunsgaard L, Blennow A (2004) Functional characterization of α-glucan,water dikinase, the starch phosphorylating enzyme. Biochem J **377**: 525–532

Moon K, Park J, Park S, Lee H, Cho H, Min S, Park Y, Jeon J, Kim H (2021) A more accessible, time-saving, and efficient method for *in vitro* plant regeneration from potato protoplasts. Plants **10**: 781

Mori H, Tanizawa K, Fukui T (1991) Potato tuber type H phosphorylase isozyme: molecular cloning, nucleotide sequence, and expression of a full-length cDNA in *Escherichia coli*. J Biol Chem **266**: 18446–18453

Nicolia A, Fält AS, Hofvander P, Andersson M (2021) Protoplast-based method for genome editing in tetraploid potato. Methods Mol Biol **2264**: 177–186

Orzechowski S, Sitnicka D, Grabowska A, Compart J, Fettke J, Zdunek-Zastocka E (2021) Effect of short-term cold treatment on carbohydrate metabolism in potato leaves. Int J Mol Sci **22**: 7203

Rommens CM, Ye J, Richael C, Swords K (2006) Improving potato storage and processing characteristics through all-native DNA transformation. J Agric Food Chem **54**: 9882–9887

Samodien E, Jewell JF, Loedolff B, Oberlander K, George GM, Zeeman SC, Damberger FF, van der Vyver C, Kossmann J, Lloyd JR (2018) Repression of *Sex4* and *Like Sex Four2* orthologs in potato increases tuber starch bound phosphate with concomitant alterations in starch physical properties. Front Plant Sci **9**: 1044

Sergeeva EM, Larichev KT, Salina EA, Kochetov AV (2022) Starch metabolism in potato *Solanum tuberosum* L. Vavilovskii Zhurnal Genetiki i Selektsii **26**: 250–263

Sitnicka D, Orzechowski S (2014) Cold-induced starch degradation in potato leaves — intercultivar differences in the gene expression and activity of key enzymes. Biologia Plantarum **58**: 659–666

Sonnewald U, Basner A, Greve B, Steup M (1995) A second L-type isozyme of potato glucan phosphorylase: cloning, antisense inhibition and expression analysis. Plant Mol Biol **27**: 567–576

Xiao G, Huang W, Cao H, Tu W, Wang H, Zheng X, Liu J, Song B, Xie C (2018) Genetic loci conferring reducing sugar accumulation and conversion of cold-stored potato tubers revealed by QTL analysis in a diploid population. Front Plant Sci **9**: 315

Zeeman SC, Thorneycroft D, Schupp N, Chapple A, Weck M, Dunstan H, Haldimann P, Bechtold N, Smith AM, Smith SM (2004) Plastidial α-glucan phosphorylase is not required for starch degradation in *Arabidopsis* leaves but has a role in the tolerance of abiotic stress. Plant Physiol **135**: 849–858